

NASA REPORT NO. CR-174832
1 APRIL, 1985

MULTI-HUNDRED KILOWATT ROLL RING ASSEMBLY FINAL REPORT

THIS WORK SPONSORED BY THE NATIONAL AERONAUTICS
AND SPACE ADMINISTRATION, LEWIS RESEARCH CENTER
UNDER CONTRACT NAS3-24264

SUBMITTED TO

NATIONAL AERONAUTICS AND SPACE ADMINISTRATION
LEWIS RESEARCH CENTER
POWER SYSTEMS BRANCH
21000 BROOKPARK ROAD
CLEVELAND, OHIO 44135

PREPARED BY

SPERRY CORPORATION
AEROSPACE & MARINE GROUP
SPACE SYSTEMS DIVISION
PHOENIX, ARIZONA 85032

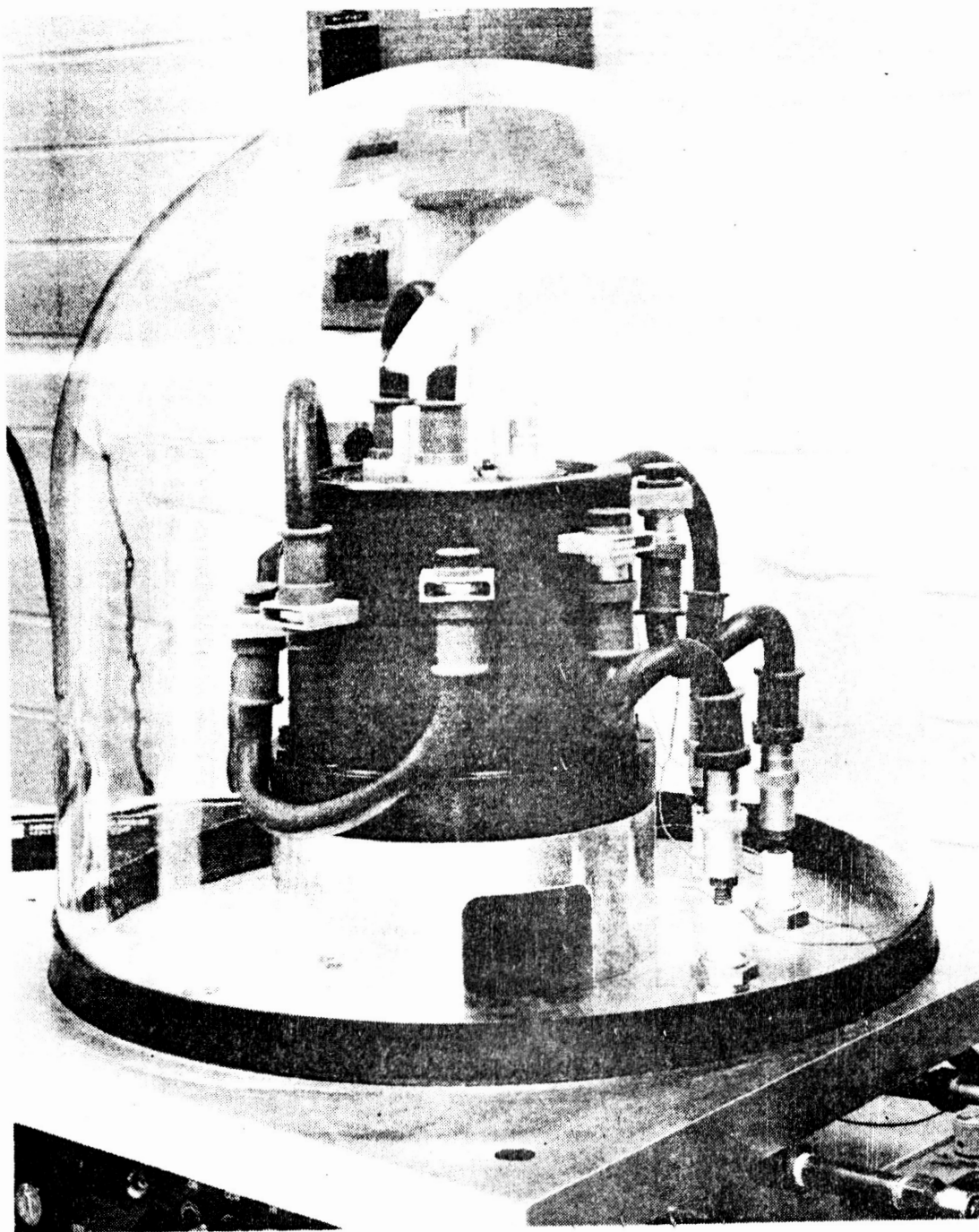
(NASA-CR-174832) MULTI-HUNDRED KILOWATT
ROLL RING ASSEMBLY Final Report (Sperry
Corp.) 122 p CSCL 09C

N89-15335

Unclas
G3/33 0185080

PUB. NO. S71-5240-1/2-0

ORIGINAL PAGE IS
OF POOR QUALITY



FORWARD

This document is the final report of the development effort of a multi-hundred kilowatt AC/DC power transfer device. This work was carried out by the Space Systems Division of the Aerospace & Marine Group of Sperry under contract Number NAS3-24264 for the National Aeronautics and Space Administration. The hardware was fabricated and tested by personnel from the Bearing/Sensor Laboratory at the Space Systems Division. This power transfer device was an extension of Sperrys Roll Ring technology. The hardware developed under this contract was an eight channel Roll Ring power transfer Evaluation Unit (EU) and an associated Test Fixture (TF). The latter provides an integral rotational drive as well as a vacuum chamber in a portable system. The contract included only short term testing of the EU since the long term full power testing will be conducted by the Lewis Research Center.

Mr David Renz was the NASA Program Monitor for this contract. Mr. Pete Jacobson was the Sperry Project Leader. Mr. Ryan Porter contributed to the design concept and various analyses and manufacturing techniques. Mr. Richard Wetnight directed the numerically controlled machining at Sperry while Messrs Richard Ajaski and Kent Gabbitas performed the many assembly/test operations. All plating of critical circuit components was performed by American Electroplating of Sommerville, Massachusetts under the direction of Mr. Gene Levy.

SUMMARY

This document describes the results of an intensive technical effort by Sperry personnel to produce an Evaluation Unit (EU) for the ultimate transfer of high voltage (up to 500 volts) high current (up to 200 amperes) power across a rotating interface in vacuum for ultimate utilization in space vehicles. Both AC and DC power can be transferred. The total unit power transfer capability has been increased from the original 4KW for a two circuit configuration to 800KW for an 8 circuit module. The base technology for this effort was a signal and power transfer device known as a Roll Ring developed by Sperry on previous programs. The Roll Ring is a device for conducting electrical energy across a rotating interface with rolling rather than sliding contacts.

Previous hardware development efforts on the Roll Ring had resulted in a two circuit, low voltage, configuration which was capable of transferring currents to 200 amperes. The performance on this initial unit demonstrated advantages over alternate devices such as rotary transformers at power levels of 2 KW. A subsequent advanced design introduced modifications to the original prototype which provided a number of refinements to the prototype design with additional potential performance improvements. It was from this background that the EU design and hardware was developed on the contract described in this report. This contract effort has demonstrated these important design improvements such as high voltage integrity, increased power transfer efficiency, improved circuit paths and terminations as well as multi-circuit capability. A patent has been applied for on these improvements.

A set of analyses were conducted at the outset of this effort related to key design parameters. A design layout was then executed for both the EU and the TF from which a set of manufacturing drawings were prepared. Fabrication tooling was then designed and fabricated followed by complete fabrication and/or procurement of all detail components of both the EU and the TF.

The EU was assembled first with only one circuit in a holding fixture to allow a static temperature map and transfer efficiency to be determined in both air and in vacuum with conducted currents of 50 to 200 amperes. These tests provided valuable heat transfer data for various thermal path design variations and formed a basis for optimization of the transfer in the final unit.

The full eight circuit EU was then assembled after making a few minor modifications which reflected the thermal mapping tests. The unit was assembled onto the TF and subjected to a set of static pre-tests. The unit was then subjected to both static and dynamic testing while conducting currents of 50 to 200 amperes at <10 volts both in air and in vacuum. All performance requirements were met with the exception of circuit capacitance a relatively unimportant design goal. A kinematic problem was discovered during this testing, however, which necessitated a minor design change and refurbishment of three of the EU components. The unit was subsequently refurbished and resubjected to test. A second set of test data was then compiled with essentially identical results with that of the previous build.

The initial configuration of the EU was wired to impose a worst case condition relative to voltage differential between adjacent circuits. During 500 volt testing at 2 amps an internal plasma occurred which short circuited two adjacent circuits. As a result the unit was refurbished, modified to eliminate this worst case test mode and subsequently passed all critical test requirements. The final transfer efficiency was determined to be 99.98 percent per circuit projected to a 100 Kw power level.

The EU and the TF have been shipped to the Lewis Research Center for full power testing at up to 100 KW per circuit. The primary objectives of this development contract have been met. The power transfer unit developed on this program is now available for power transfer evaluations at levels never before achieved for a vacuum compatible rotational interface. With further refinements, it is a prime candidate, therefore, for the initial Space Station applications and beyond.

Frontispiece
Foreward
Summary

Page No.

1. Introduction - - - - -	1
1-1 Background- - - - -	1
2. Discussion - - - - -	1
2-1 Design- - - - -	4
2-1.1 Flexure - - - - -	4
2-1.2 Flexure/Ring Groove Interface - - - - -	11
2-1.3 Circuit Path- - - - -	14
2-1.4 Thermal Path- - - - -	17
2-1.5 Design Details- - - - -	20
2-2 Fabrication - - - - -	23
2-2.1 Circuit Components- - - - -	23
2-2.2 Electrical Insulators - - - - -	24
2-2.3 Heat Transfer Members - - - - -	25
2-2.4 Housing Components- - - - -	28
2-2.5 Bearing System- - - - -	28
2-2.6 Assembly- - - - -	30
a. Cables - - - - -	30
b. Vacuum Bake- - - - -	30
c. Cleaning - - - - -	30
d. EU Assembly- - - - -	30
e. TF Assembly- - - - -	32
2-3 Testing - - - - -	32
2-3.1 Single Circuit Tests- - - - -	32
2-3.2 Multi Circuit Tests - - - - -	39
a. DC Low Current Resistance- - - - -	39
b. Insulation Resistance- - - - -	40
c. Capacitance- - - - -	40
d. Torque - - - - -	41
e. Low Voltage/High Current - - - - -	43
f. High Voltage/Low Current - - - - -	48
3. Conclusions and Recommendations- - - - -	50

List of Figures

1. Single Flexure Roll Ring Circuit.- - - - -	2
2. High Current Roll Ring Test Module - - - - -	3
3. Multiple Flexure/Idler Configuration - - - - -	6
4. Fatigue Characteristics of Berylco 172 Alloy - - - - -	8
5. Flexure/Ring Groove Geometrics - - - - -	10
6. Cross Section of Roll Ring Evaluation Unit - - - - -	15
7. Terminal-to-Terminal Circuit Path- - - - -	16

	<u>Page No.</u>
8. Collector Ring Heat Transfer Components - - - - -	18
9. Heat Transfer Optimization - - - - -	19
10. Inner and Outer Collector Ring Sets - - - - -	26,27
11. Close up of Evaluation Unit Components - - - - -	29
12. Eight Circuit Power Roll Ring Components - - - - -	31
13. Typical Power Transfer Component Layout - - - - -	33
14. Vacuum Base Heat Exchange Manifold - - - - -	34
15. Vacuum Base with Sealed Manifold - - - - -	35
16. High Power Roll Ring Test Fixture - - - - -	36
17. Test Fixture Base and Adapter - - - - -	37
18. Bottom View of Test Fixture - - - - -	38
19. Roll Ring Evaluation Unit Mounted on Test Fixture - - - - -	44
20. Roll Ring Evaluation Unit Set-up for Temperature Testing -	45
21. Plasma Onset Voltage Related to Chamber Pressure - - - - -	47
22. Power Transfer Efficiency for the Evaluation Unit - - - - -	48

LIST OF TABLES

I. Acceptable Idler/Guide Rail Configurations - - - - -	5
II. Flexure Design Parameters and Related Stress - - - - -	7
III. Flexure/Ring Interface Design Parameters - - - - -	11
IV. Flexure Dynamic Stability Terms - - - - -	13
V. Gold Plating Matrix for Circuit Components - - - - -	24
VI. Low Current Resistance - - - - -	39
VII. Insulation Integrity - - - - -	40
VIII. Capacitive Coupling - - - - -	41
IX. Resistance and Temperature Summary of Power Tests - - -	46
X. Summary of High Voltage Testing in Air at 5RPM - - - - -	49

LIST OF APPENDICIES

A. Flexure Bending Stress and Stiffness
B. Circuit Resistivity Analysis
C. Diaphragm Design Analysis
D. High Power Roll Ring Single Circuit Heat Transfer Optimization.
E. Cable Assembly Details
F. Bearing Preloading Procedure
G. Ring Set Assembly Procedure
H. High Power Roll Ring Evaluation Unit Test Fixture
I. Engineering Bulletin for the Set up and Test of High Power Roll Ring Evaluation Unit (EB 011451)

Nomenclature

A_C	=	Area of Flexure Contact, cm^2
A_S	=	Area of Spring Contact, cm^2
A_F	=	Flexure Section Area, cm
a	=	Contact Circumferential Footprint Half Length, mm (I = subscript for Inner Ring, etc.)
b	=	Contact Axial Footprint Half Length, mm (I = Subscript for Inner Ring, etc.)
c	=	Centroidal Distance to Stress Fiber, cm (I = Subscript for Inner Fiber, etc.)
E_1	=	Elastic Modulus of Flexure Material, Newton/cm^2
E_2	=	Elastic Modulus of Ring Material, Newton/cm^2
E	=	Source Potential, volts
e	=	Transfer Efficiency, Percent
F_T	=	Normal Clamping Force, Newtons
F_R	=	Radial Preload, Newtons
I	=	Flexure Section Second Moment about Neutral Axis, cm^4
I_{XX}	=	Flexure Section Second Moment about Radius Center, cm^4
I_C	=	Conducted Current, Amperes
K	=	Flexure Bending Stiffness, Newtons/Cm
L	=	Flexure Radius Center Axial Location, Cm
L_A	=	Flexure Radius Center Radial Location, Cm
L_R	=	Bending Moment, Newton Cm
M	=	Number of Flexures
n	=	Radial Clamping Pressure, Newtons/cm^2
P	=	Heat Transfer, Cal/Hr
Q	=	Conformity Ratio
R	=	Free Flexure Inside Radius, Cm
R_C	=	Major Radius of curvature of Ring Groove, Cm (I = Subscript for Inner Groove, etc.)
R_F	=	
R_G	=	

NOMENCLATURE (cont'd)

R_H = Thermal Resistivity, $\text{sec}^{\circ} \text{C cm}^2 / \text{cal cm}$
 R_S = Stability Ratio
 R_T = Terminal-to-Terminal Resistance, Ohms
 r_1 = Minor Radius of Curvature of Flexure, Cm
 r_2 = Minor Radius of Curvature of Ring Groove, Cm
 r = Radius to Neutral Axis of Flexure, Cm
 \bar{r} = Radial Distance to Centroid, Cm
 S_R = Stability Ratio
 T = Shim Thickness, Cm
 t = Flexure Wall Thickness, Cm
 W = Flexure Width, cm
 Y_R = Flexure Radial Deflection, Cm
 \bar{y} = Flexure Neutral Axis to Radius Center, Cm

α_I = Location Angle of Inner Arc, Degrees
 α_O = Location Angle of Outer Arc, Degrees
 β = Contact Straddle Angle, Degrees (β Subscript for Inner Ring, etc.)
 θ = Location Angle, Degrees ($\theta' = \text{Radians}$)
 ρ_B = Bending Stress, Newtons/Cm
 ρ_C = Current Density at Contact, Amp/cm^2
 ρ_F = Current Density of Flexure, Amp/cm^2

SECTION 1 INTRODUCTION

1-1 BACKGROUND

The purpose of Contract Number NAS3-24264 was to support the development of an eight circuit Roll Ring electrical power transfer device and associated Test Fixture (TF) and to conduct an initial short term performance evaluation of the device. Throughout this report this power transfer device will be referred to as the Evaluation Unit (EU). Previous to this contract a two circuit prototype power transfer module had been developed and evaluated which utilized the Roll Ring configuration. This initial unit, however, was not designed to accommodate an operating voltage as high as 500 volts nor was it designed to accommodate as many as eight circuits. The terminal-to-terminal resistance, a very important design parameter, was only 0.6 milli-ohms but not as low as potentially possible. External connections to this initial module were inefficient and inconsistent from a resistive standpoint and were difficult to interface with externally. A major task of this latest contract development was to overcome these and other limitations and to provide an EU with improved operating characteristics for long term testing in a simulated environment.

The reliable transfer of large currents at high voltage levels across a rotating interface in a hard vacuum for long periods of time is a difficult problem. Any sliding interfaces require the disciplines of Physics (friction), Metallurgy (wear), Chemistry (lubrication) and Thermodynamics (heat transfer). These problems are compounded in a vacuum environment. When an electrical current is passed through an interface of two components design guidelines are almost non-existent. When this interface is rolling even less is known relative to the design requirements.

A set of design guide lines were imposed at the outset of this development effort which were derived from previous Roll Ring development tests. These guide lines will be cited throughout this report without any attempt to support their authority with the exception of a few which will be backed up with a reference document or report. It should also be emphasized here that these guidelines are of a proprietary nature and should be handled accordingly.

The operating principles of the Roll Ring will not be described in this report since references are cited which cover that area thoroughly. The basic concept is covered in reference 1. The high current concept is covered in references 2 and 3. Figure 1 is a photograph of an early single Flexure Roll Ring circuit and Figure 2 is a photograph of a high current test module prototype taken from reference 3. The Figure also summarizes the test data taken on this unit.

2. DISCUSSION

This report will cover the various stages of the contracted development in the chronological order in which they occurred.

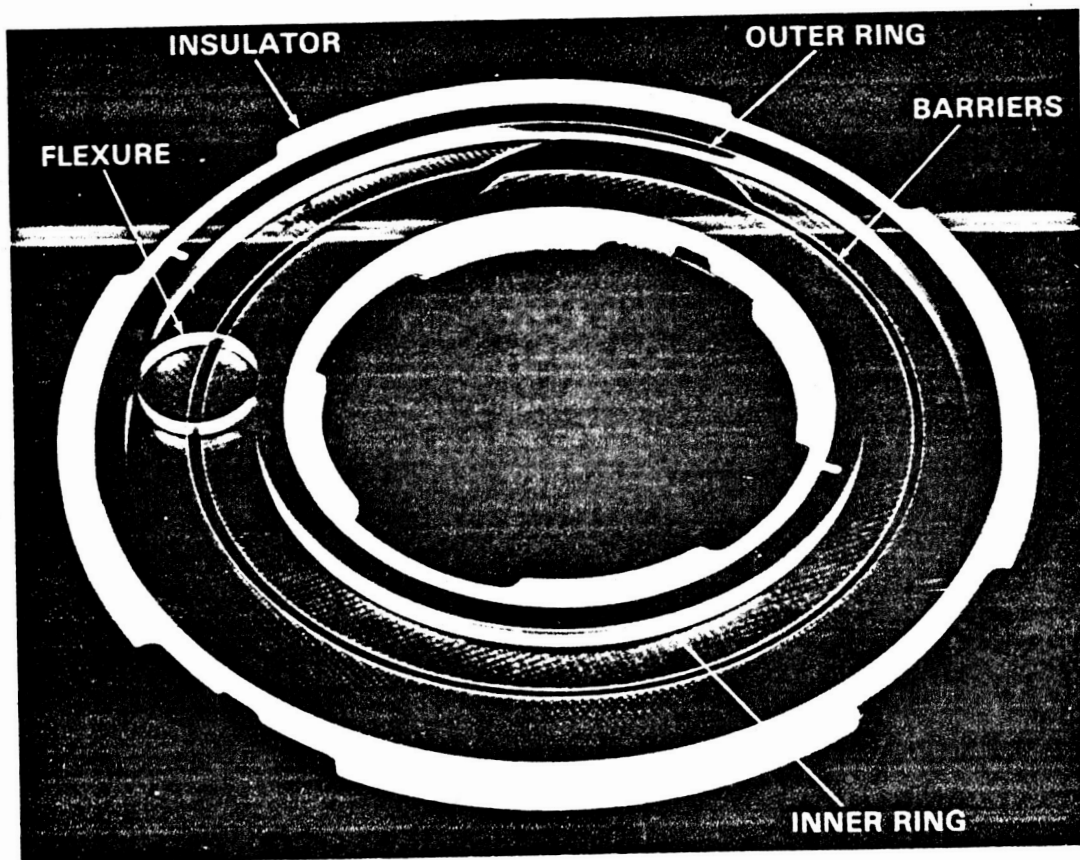


Figure 1

Single Roll Ring Signal Circuit

ORIGINAL PAGE IS
OF POOR QUALITY

● Test Matrix

- 185 amps at 10 volts for 12 hours at 10^{-3} torr
- No power at 10^{-3} torr for 300K revs
- No power at 10^{-3} torr with divided flexure for 400K revs
- 150 amps at 10 volts for 100K revs at 10^{-6} torr
- 200 amps at 10 volts at 10^{-6} torr (planned)

ORIGINAL PAGE IS
OF POOR QUALITY

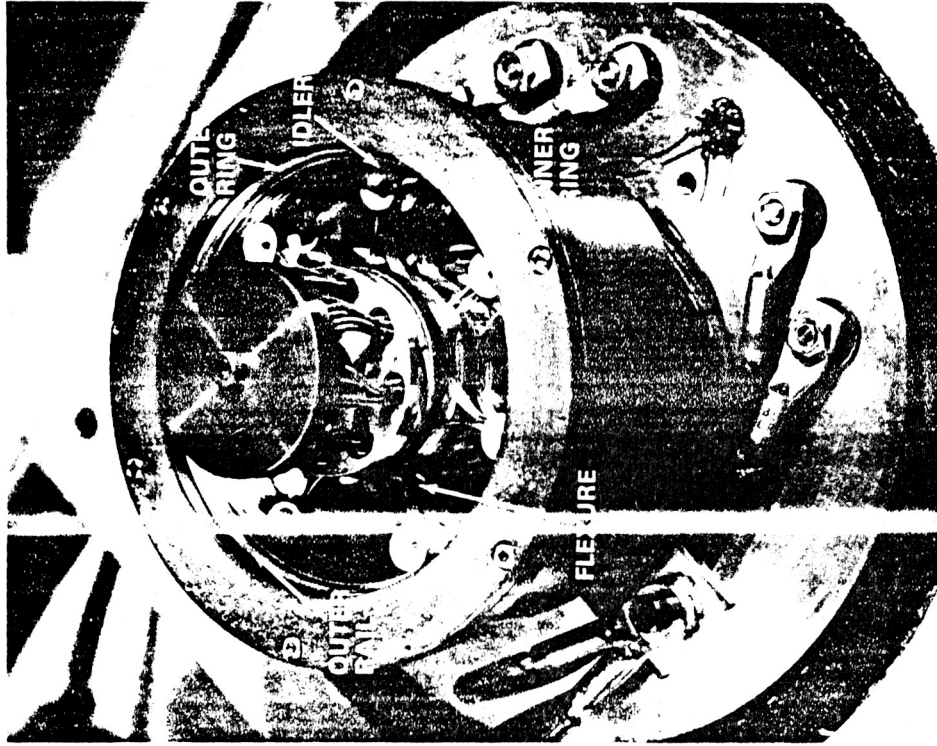


Figure 2

High Current Roll Ring Test Prototype

2-1 DESIGN

The actual design of the EU and TF components was preceded by a set of design analyses. These covered the most critical of the primary operating parameters. Each of these analyses and the related design parameter will be discussed.

2-1.1 Flexure - Multiple Flexures (see Figure 2) in a single ring set annulus are used to obtain a greater transfer current capacity since the Flexures are electrically connected in parallel. To prohibit sliding between adjacent flexures, an idler system is used which provides a rolling interface at every Flexure/Idler contact. The Idlers are piloted by a Guide Rail which is fixed to, and rotates with, the Inner current collection ring. To maintain Idler preloading a full complement of Idlers and Flexures is used. The size of the various rolling elements is so selected as to assure a negligible slip at each of the three interfaces.

Figure 3, taken from reference 3, is a mechanical schematic of these three interfaces and shows the various velocity vectors involved. A computer program was used to select this interface matching on the basis of zero sliding and provides a print out of all acceptable designs of the Idler and Guide Rail for a given set of Collector Ring radii and Flexure quantity. Table I is a compilation of all acceptable combinations with the final design identified on the table. An EU configuration with 10 Flexures was chosen. Small dimensional deviations from the ideal radii represent micro sliding at one or more interface and are not critical.

Another important design parameter of the Flexure is bending stress. The stress magnitude and distribution math model is given in Appendix A. Table II is a summary of the derived stress and stiffness of the Flexure designed into the EU. It is to be noted that the centroidal distance to the outer fiber of the Flexure is slightly larger than to the inner so that the maximum compressive stress is at the load (contact) points and the maximum tensile stress is slightly less at the same location. Fatigue, however, would propagate from a tensile stress point. Since the maximum tensile stress occurs at the Flexure inner wall at the free loop zones this area is the most important from a design standpoint.

The allowable fatigue stress was determined from a previous set of fatigue test data taken on actual plated rings. (Reference 5). These samples were fabricated from Beryllium Copper Alloy 172 in a manner identical to that used in flexure fabrication. The samples were solution annealed to remove residual stresses and for grain refinement, precipitation hardened and plated. The test data was used to determine the worst case (-3σ) scatter of the data as shown in Figure 4 (taken from reference 3) and is compared with published "sheet stock" data available at the time. The maximum ($+3\sigma$) predicted stress levels of the EU design are below the 20,000 Newton/Cm² endurance stress limit shown in Figure 4 even though the life cycles are less than the "knee"

INPUT PARAMETERS

o Inner Ring Major Radius (in) ----- 1.746
o Ring Minor Radi (in) ----- 0.218
o Outer Ring Major Radius (in) ----- 3.033
o Number of Flexures ----- 10

IDLER DESIGN		GUIDE DESIGN
OUTER ROLLER RADIUS (IN)	INNER ROLLER RADIUS (IN)	OUTER RING RIM RADIUS (IN)
.1636	.1103	2.6086
.1786	.1182	2.6586
.1956	.1270	2.7086
.2142	.1366	2.7586
.2343	.1467	2.8086
.2557	.1573	2.8586
.2783	.1683	2.9086
.3020	.1796	2.9586
.3268	.1910	3.0086
.3524	.2026	3.0586
.3788	.2143	3.1086
.4061	.2261	3.1586
.4341	.2379	3.2086
.4627	.2498	3.2586
.4920	.2615	3.3086
.5219	.2733	3.3586
.5523	.2850	3.4086
.5833	.2966	3.4586
.6148	.3082	3.5086
.6467	.3196	3.5586
.6791	.3310	3.6086
.7120	.3423	3.6586
.7452	.3534	3.7086
.7789	.3645	3.7586
.8129	.3754	3.8086
.8473	.3862	3.8586
.8820	.3969	3.9086
.9170	.4074	3.9586
.9524	.4179	4.0086
.9881	.4282	4.0586
1.0241	.4384	4.1086
1.0603	.4485	4.1586
1.0969	.4584	4.2086
1.1337	.4682	4.2586
1.1707	.4779	4.3086
1.2080	.4875	4.3586
1.2455	.4969	4.4086
1.2833	.5062	4.4586
1.3213	.5155	4.5086
1.3595	.5245	4.5586
1.3980	.5335	4.6086
1.4366	.5424	4.6586

*** SUBSEQUENT DESIGNS UNACCEPTABLE DUE TO ROLLER INTERFERENCE ***

NOTE:

1. Items in () represent final design.

ACCEPTABLE IDLER/GUIDE RAIL CONFIGURATIONS

Table I

MULTIPLE FLEXURE/IDLER KINEMATICS

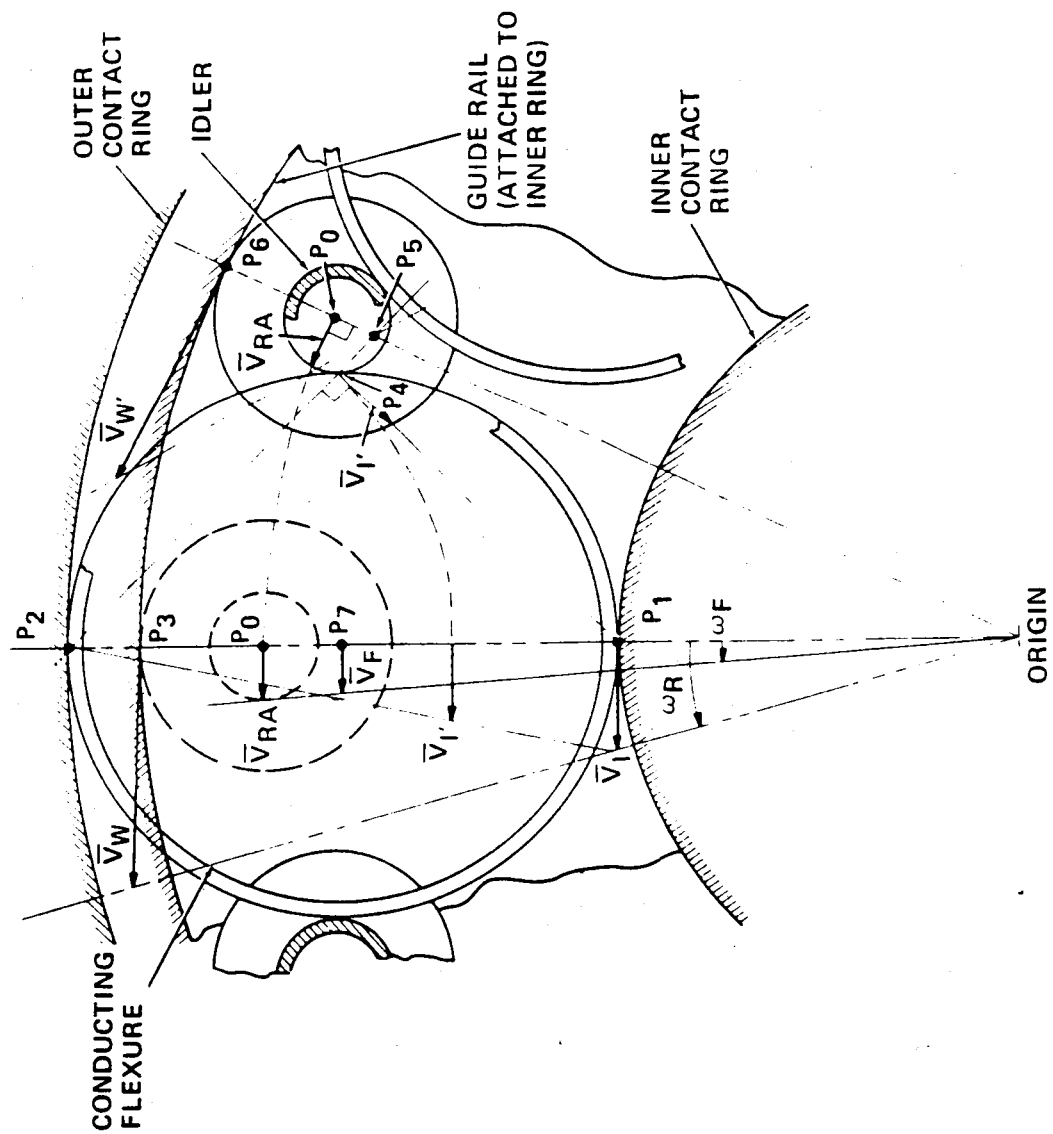
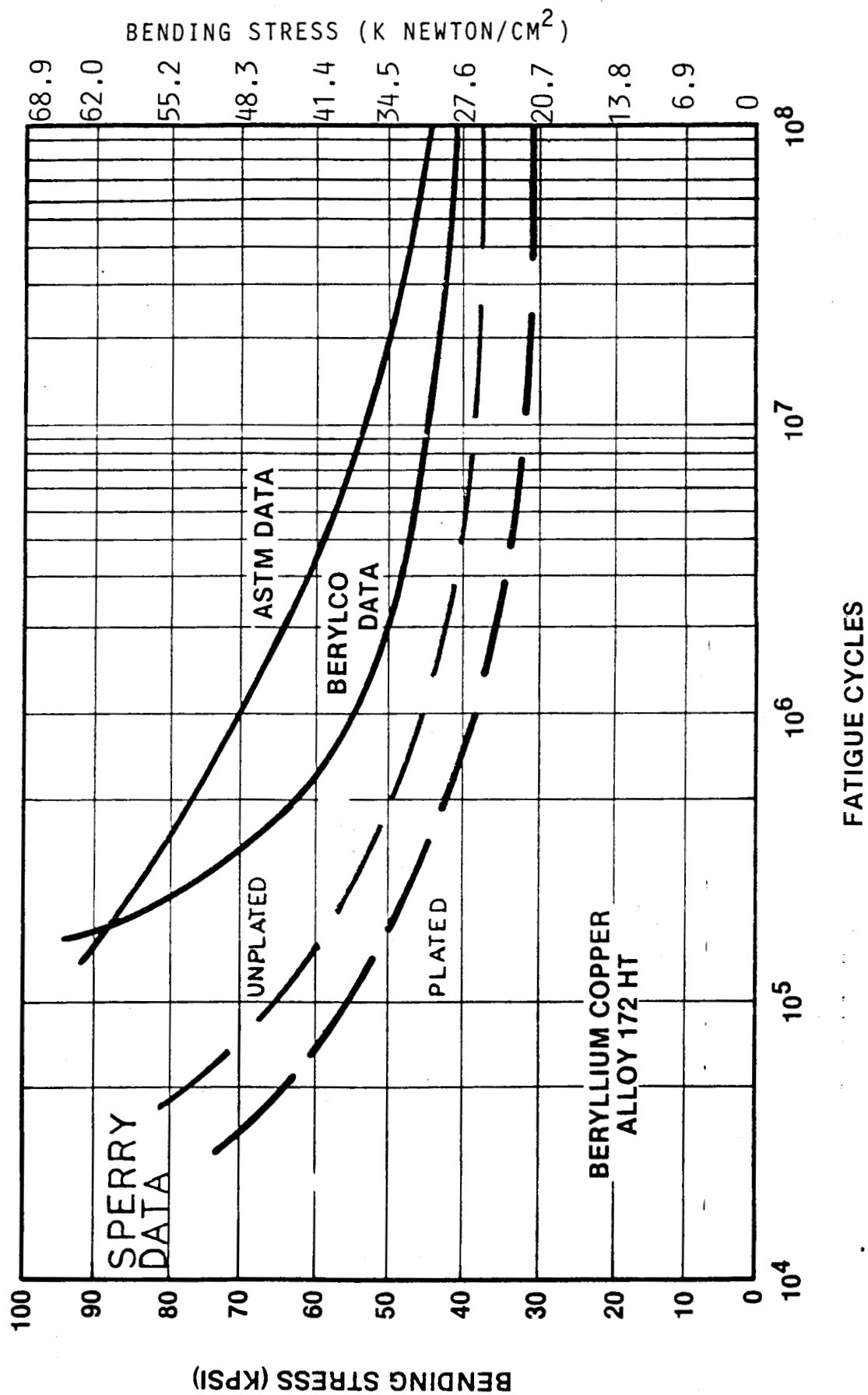


Figure 3

Inside Diameter, cm (in) -----	3.255	(1.2817)
Width, cm (in) -----	0.477	(0.188)
Thickness, mm (in) -----	0.353	(0.0139)
Elastic Modulus, Newton/cm ² (lb/in ²)-----	1.31 x 10 ⁷	(1.90 x 10 ⁷)
Nominal Preload, Newtons (lbs) -----	3.34	(0.75)
Cross Section Area, mm ² (in ²) -----	1.51	(2.34 x 10 ⁻³)
Deflection at Contact, mm (in) -----	1.04	(0.0409)
Free Loop Deflection, mm (in) -----	0.95	(0.0376)
Inner Fiber Stress at Contact, Newton/cm ² (lb/in ²)-----	-1.84 x 10 ⁴	(-2.67 x 10 ⁴)
Outer Fiber Stress at Contact, Newton/cm ² (lb/in ²)-----	2.13 x 10 ⁴	(3.09 x 10 ⁴)
Inner Fiber Stress at Free Loop, Newton/cm ² (lb/in ²)-----	1.05 x 10 ⁴	(1.53 x 10 ⁴)
Outer Fiber Stress at Free Loop, Newton/cm ² (lb/in ²)-----	-1.22 x 10 ⁴	(-1.77 x 10 ⁴)

FLEXURE DESIGN PARAMETERS AND RELATED STRESS
TABLE II



FATIGUE CHARACTERISTICS OF BERYLLIUM COPPER ALLOY 172

Figure 4

of the curve. The maximum anticipated tensile stress of the EU Flexures was derived using the model of Appendix A and is shown in Figure 4 as a dashed line. This level of stress should be low enough as to not impose any life limitation.

The flexure design determines the bending stiffness and the Flexure and Ring Groove designs determine the resultant preload. Refer to Figure 5 for the nomenclature involved. The bending stiffness, K , is calculated from the model given in Appendix A.

For the final EU design:

$$t = 0.35 \text{ mm (0.0139 in)}$$

$$w = 4.8 \text{ mm (0.188 in)}$$

$$E_1 = 1.31 \times 10^7 \text{ Newton/cm}^2 (1.9 \times 10^7 \text{ lb/in}^2)$$

and radial stiffness, K , is

$$K = 32.2 \text{ Newton/cm (18.4 lb/in)}$$

also for

$$R_F = 1.63 \text{ cm (0.6408 in)}$$

$$r_1 = 0.533 \text{ cm (0.210 in)}$$

$$r_2 = 0.554 \text{ cm (0.218 in)}$$

$$R_{GI} = 4.435 \text{ cm (1.746 in)}$$

$$R_{GO} = 7.704 \text{ cm (3.033 in)}$$

A model for the determination of deflection as related to the design parameters is given in reference 6.

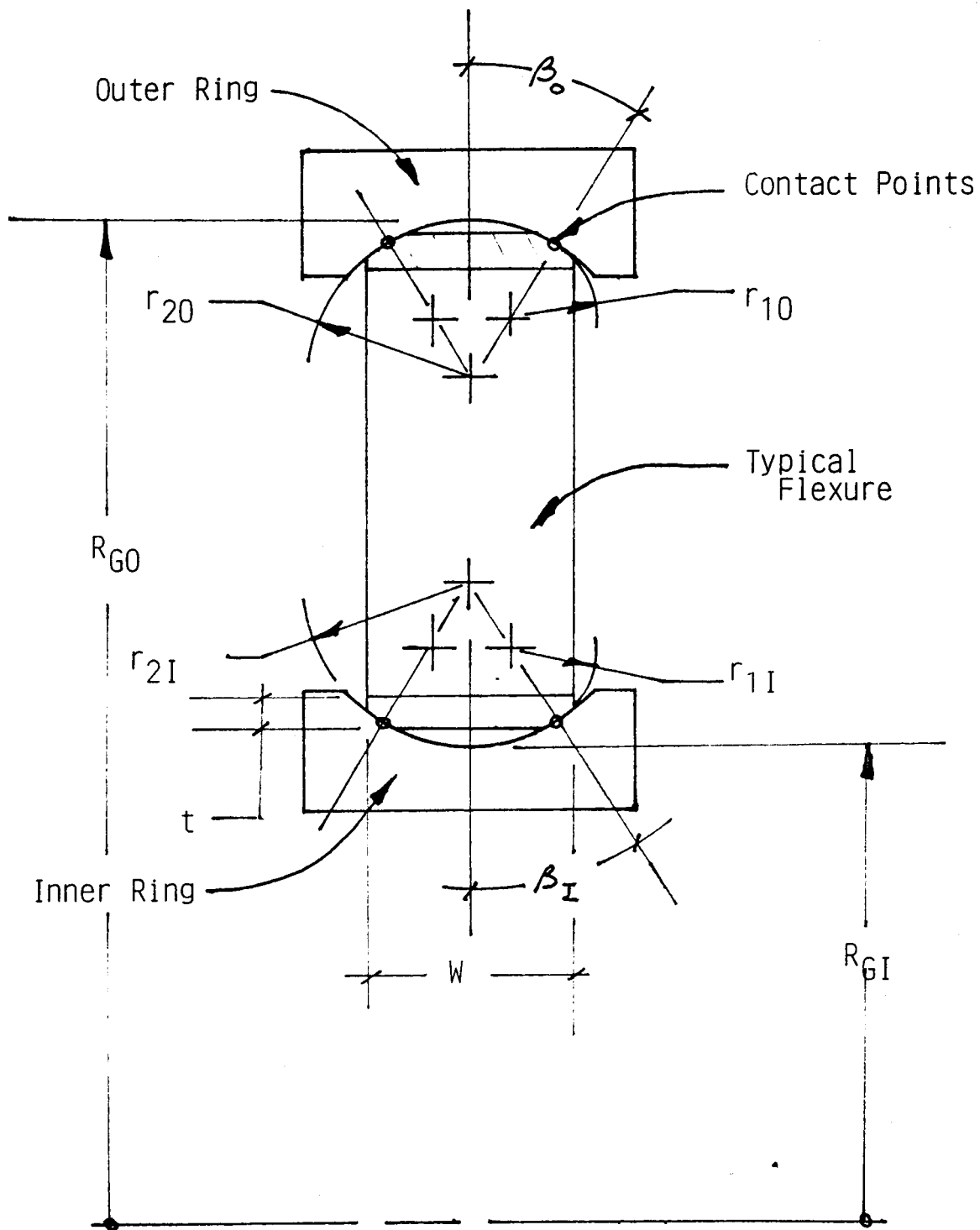
As based upon the reference:

$$2Y_R = 1.04 \text{ mm (0.041 in)}$$

therefore preload, F_R is

$$\begin{aligned} F_R &= 2Y_R K \\ &= 3.34 \text{ Newtons (0.75 lbs)} \end{aligned}$$

An electrical design parameter related to the Flexure is the current density. The cross sectional area of the Flexure may be derived by the model of Appendix A, equation A-13. since each Flexure provides two parallel current paths the current density of the flexure per circuit, ρ_F , is



FLEXURE/RING GROOVE GEOMETRICS

Figure 5

$$\rho_F = \frac{I_C}{2nA_F}$$

where n = number of Flexures per circuit.

For the final EU design

$$A_F = 0.015 \text{ cm}^2 (2.34 \times 10^{-3} \text{ in}^2)$$

$$n = 10$$

and for $I_C = 200$ amps

$$\rho_F = 0.67 \text{ K Amp/cm}^2 (4.27 \text{ K Amp/in}^2)$$

which is acceptable even at 200 amps. It is to be noted, here, that the measure of acceptability is steady state temperature. The heat developed in the Flexure due to its resistivity is conducted to the external sink by way of the interface foot prints. The Flexure absolute temperature in vacuum may be determined by a static test which also produces the highest value. It is assumed from previous Roll Ring testing that the Flexure steady state temperature may be as high as 150°C without affecting life or reliability. Refer to section 2-3 of this report for actual test data.

2-1.2 Flexure/Ring Groove Interfaces - The Flexure/Ring Groove interfaces are important for several reasons. One of these reasons is contact footprint size as pointed out previously since as the size increases the current density and resultant self-heating decrease and the heat transfer resistivity decreases as well, resulting in reduced Flexure temperature. Each of these parameters will be discussed.

	<u>INNER</u> <u>RING</u>	<u>OUTER</u> <u>RING</u>
Normal Load, Newtons (Lbs)	1.71 (0.38)	1.71 (0.38)
Mean Contact Stress, Newtons/cm ² (Lbs/in ²)	4709 (6830)	3695 (5360)
Contact Ellipse, mm x mm (in x in)	1.29 x 0.03 (0.0507 x 0.0011)	1.45 x 0.03 (0.0573 x 0.0013)
Effective Area / Contact, mm ² (in ²)	0.030 4.4 x 10 ⁻⁵	0.034 5.9 x 10 ⁻⁵

FLEXURE/RING INTERFACE DESIGN PARAMETERS

TABLE III

The contact current density, ρ_c , is determined using the model used for ball bearing interfaces. This model which is based upon the background established by A.B. Jones and A.E.H. Love is too extensive to include in this report. It is the basis, however, of a computer program in the Sperry Bearing/Sensor Laboratory and was used to derive the Flexure/Ring interfaces of the EU. Table III identifies the resultant parameters of the EU design.

The contact current density, ρ_c , may be derived from the footprint dimensions (major and minor dimensions of the contact ellipse) and the current for a given number of Flexures, n , assuming two contacts per Flexure/Ring interface:

$$\rho_c = \frac{I_c}{2\pi abn}$$

since $A_c = \text{Area of contact}$
 $= \pi ab$

where $a = \text{Contact Ellipse Major Radius (In circumferential plane).}$

$b = \text{Contact Ellipse Minor Radius (Parallel to rotation axis).}$

The current density is strongly (and inversely) related to the conformity ratio, R_c , which is a function of the transverse contact radii. This ratio is related to the minor (or transverse) groove radii by

$$R_c = \frac{r_1}{r_2}$$

For the final EU design

$$E_2 = 9.6 \times 10^6 \text{ Newton/cm}^2 (1.4 \times 10^7 \text{ lb/in}^2)$$

$$a_I = 0.64 \text{ mm (0.025 in)}$$

$$b_I = 0.013 \text{ mm (0.0005 in)}$$

$$a_O = 0.71 \text{ mm (0.028 in)}$$

$$b_O = 0.015 \text{ mm (0.0006 in)}$$

$$n = 10$$

and at $I_c = 200$ amps the maximum contact current density, ρ_c , is

$$\rho_c = 38 \text{ K Amp/Cm}^2 (255 \text{ K Amp/In}^2)$$

which is acceptable even at 200 amps.

The measure of acceptability of this current density is the effective operating temperature as discussed previously. Tests have been con-

ducted in the Sperry Bearing/Sensor Laboratory, to contact current densities as high as 100 K Amps/Cm² (650 K Amp/in²) which indicate that this higher level is acceptable at least for short (50 hour) exposures at intermediate vacuum levels of 10⁻³ Torr.

Another important Flexure/Ring Groove interface parameter is the dynamic stability of the Flexure. This term relates to the ability of the Flexure to roll in the two capture grooves in the two rings and remain in a plane which lies normal to the rolling axis. This rolling stability which is important to assure that the Flexures will not contact the barriers is quantitatively related to the contact Straddle Angle, β , and the Stability Ratio, R_s and is improved by a reduced ratio and an increased angle respectively. The straddle angle is also indirectly related to the conformity ratio, R_c , which is a function of the contact radii. Previous testing in the Sperry Bearing/Sensor Laboratory has indicated that the straddle angle should be >10 degrees and the stability ratio <1.0 to provide proper Flexure rolling dynamics to the maximum test speed of approximately 10 rev/min. After testing the initial design, however, it was determined that these values were too lenient and a design change resulted. Table IV summarizes these various values for the two EU designs as well as the previous prototype unit.

The Straddle Angle is that shown in Figure 5. For all designs shown in Table IV the inner and outer angles were equal. As noted in the table the actual angle of the initial EU components was on either extreme of the two angles shown because of small plating thickness variations and the extremely tight conformity.

CONFIGURATION	CONFORMITY RATIO (R_c)	STRADDLE ANGLE (β) (deg)	STABILITY RATIO (R_s)
Initial prototype	0.69	17	0.27
Assumed guidelines	<1.00	>10	<1.0
Initial EU	0.99	13	0.51
Measured Range of Initial EU	0.98 to 1.02	8 ₁ to 18 ₂	0.5
Final EU	0.96	21	0.34

NOTES:

1. Resulted in unacceptable dynamics.
2. Resulted in acceptable dynamics.

FLEXURE DYNAMIC STABILITY TERMS
TABLE IV

The machining tolerances were adjusted in the initial EU design so as to result in this close conformity. The subsequent plating thickness variations, however, introduced a change to the conformity (and

straddle angle). Ironically the unacceptable conformity (>10) resulted in acceptable Straddle Angles (18 deg) and acceptable Flexure dynamics. The design was changed slightly as shown in Table IV to always result in acceptable values for both parameters.

The Stability Ratio, R_S , relates to the "fit" of the Flexure in the Ring grooves. The ratio is related to the groove radii by:

$$R_S = \frac{r_{2I} + r_{2O}}{R_{GO} - R_{GI}}$$

The interplay between the three terms shown in Table IV as related to Flexure stability is not known but assumed to be unimportant.

Last, but certainly not least, is the relationship the Flexure/Ring groove interface has upon Contact resistivity. As the Conformity Ratio, R_C , approaches a unity ratio (where conformity is perfect) the contact electrical resistance approaches that of the bulk material. A complete terminal-to-terminal circuit resistance assessment has been made and is included in this report as Appendix B. The contact resistance is included in this analysis as R_4 and R_6 for the outer and the inner contacts respectively. The sum of these two terms represents only 3 percent of the total resistance of the EU.

2-1.3 Circuit Path - After the initial design analyses were completed the EU layout was made. Figure 6 is an isometric cut-away of the design which shows the key components. The most important design features are identified in the figure. The terminal-to-terminal mechanical circuit path of the EU is shown in Figure 7. The numerical call-outs correspond with those shown in Figure 8-1 of Appendix B.

After the initial layout and associated detail drawings were completed the initial resistivity analysis was made. The results revealed excessive internal resistance at various locations especially that associated with the tie bolt and its related hardware. The initial layout was then modified and the resistivity assessment updated as it now appears in Appendix B. The total resistance, R_T , is calculated to be approximately 0.22 milli-ohms.

The design is such as to eliminate as many of the internal interfaces as possible to reduce the total circuit resistance. The most resistive of the path elements is the Flexure which represents 60 percent of the total. The material selected for the Flexure is Berylco Alloy 172 which provides an acceptable compromise between allowable stress, elastic modulus, electrical conductivity and thermal resistance.

The terminal-to-terminal circuit path design eliminates all solder connections and cables. All interfaces (other than Flexure/Ring groove) are high pressure threaded with gold/gold abating surfaces. The difference between the calculated and the measured (under current) circuit resistance is approximately 1:2 (measured greater) and is probably related to a less-than-total effective area at each interface. To minimize this influence all interfaces were lapped and matched prior to plating.

ORIGINAL PAGE IS
OF POOR QUALITY

CROSS SECTION OF ROLL RING EVALUATION UNIT

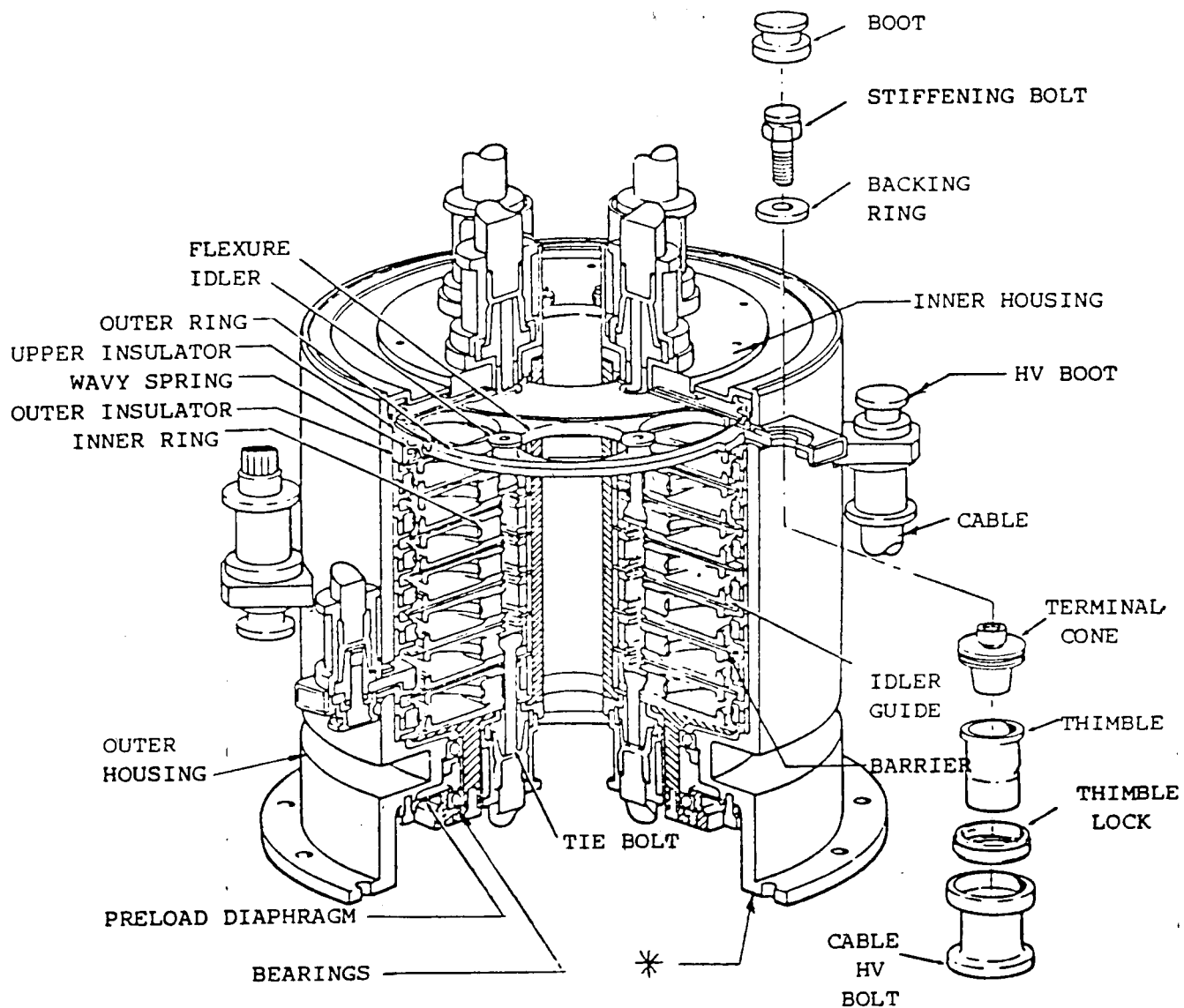
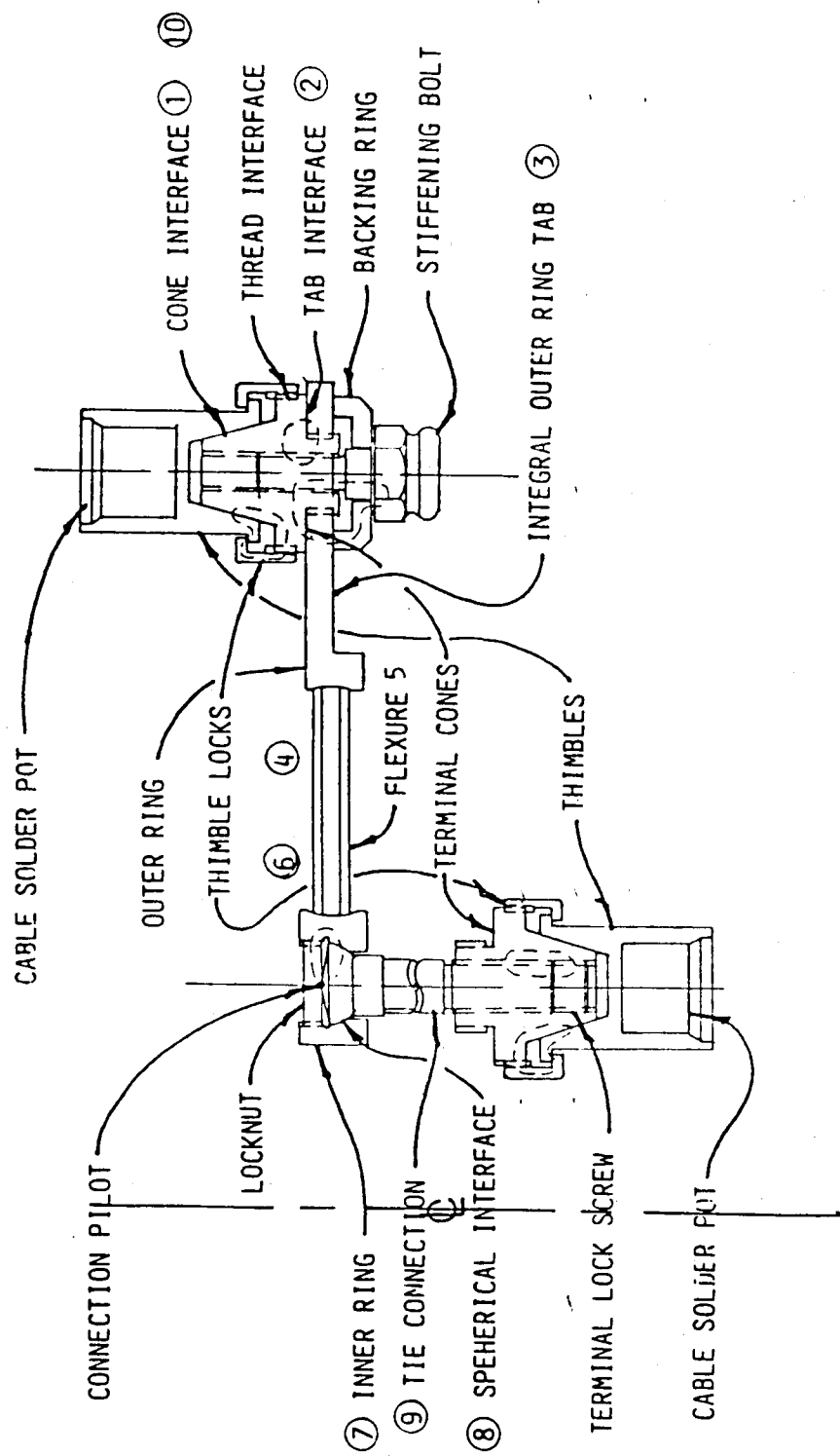


FIGURE 6



TERMINAL-TO-TERMINAL CIRCUIT PATH

FIGURE 7

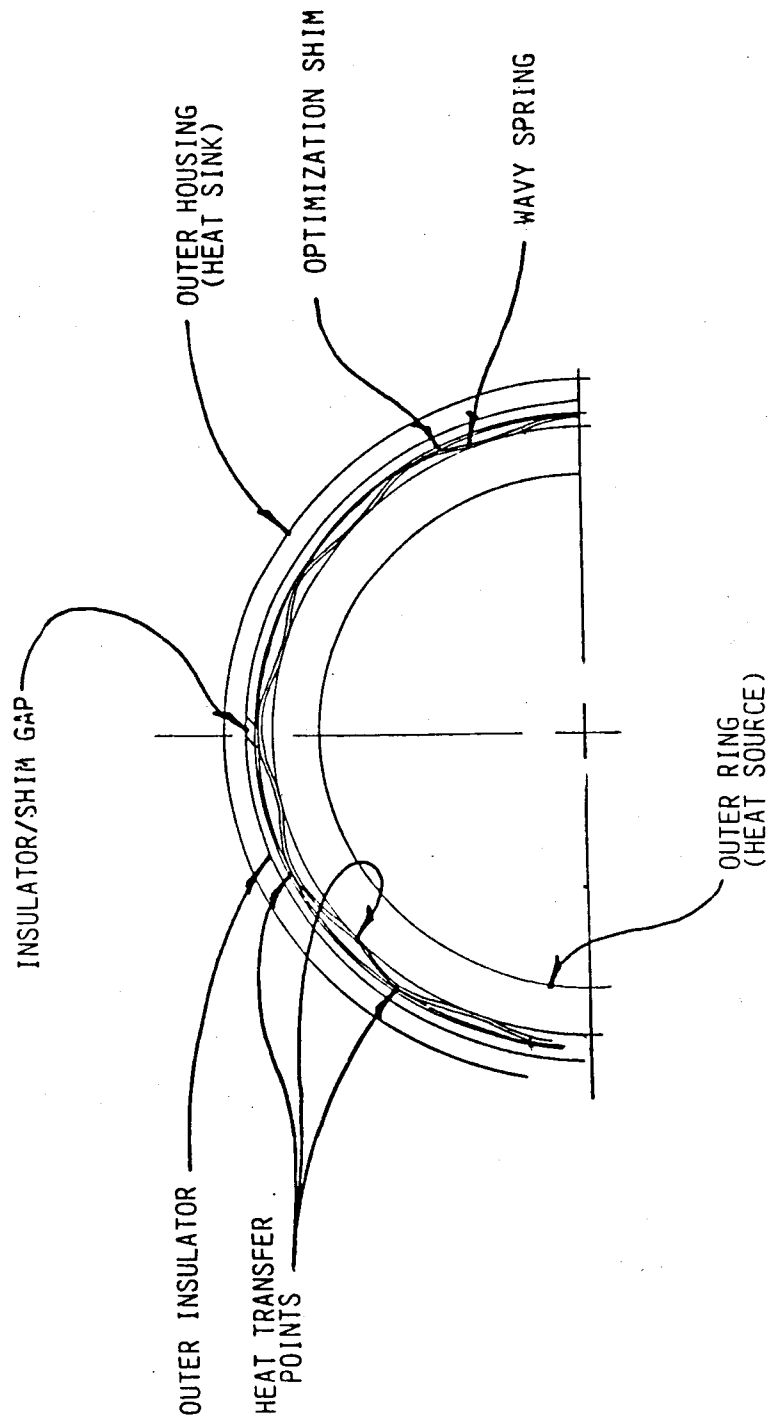
2-1.4 Thermal Path - All " $I_c^2 R_T$ " losses of the EU are converted to heat within the EU. This heat is transferred predominantly by conduction in vacuum from each of the resistive circuit elements to the Inner and the Outer Housing and on to the space craft through the two mechanical mounting faces. These two faces are denoted with an asterisks in Figure 6. The Inner and Outer Housings are the heat sinks to which it is desired to transfer the heat for eventual transfer to the space craft or other collecting points.

Figure 8 is a half section of a partial (Outer Ring) circuit taken in a plane normal to the rotational axis of the EU. This section drawing shows the means of transferring the heat radially by conduction from the Outer Collector Ring (in this case) to the Outer Housing. The Wavy Spring shown in the figure is a convoluted strip in the free state which is compressed and inserted into the annulus space between the Collector Ring and the Outer Insulator. This technique provides a multiple point, and uniformly spaced, transfer of heat.

A heat transfer analysis was performed to determine the steady state temperature at key locations of the EU. Unfortunately, this analysis did not predict realistic assessments of these temperatures since the effective resistivity of each interface was not known for the materials involved. The assumption of perfect (no resistance) interfaces resulted in unrealistically low temperature predictions. It was determined by test that there is an optimum Spring compression from the standpoint of heat transfer (as indicated by the temperature drop) across the annulus. This optimization of heat transfer was accomplished on the EU by actual test with a single static circuit. The design characteristics and technique is discussed in the following paragraphs. Reference is made to Figure 8.

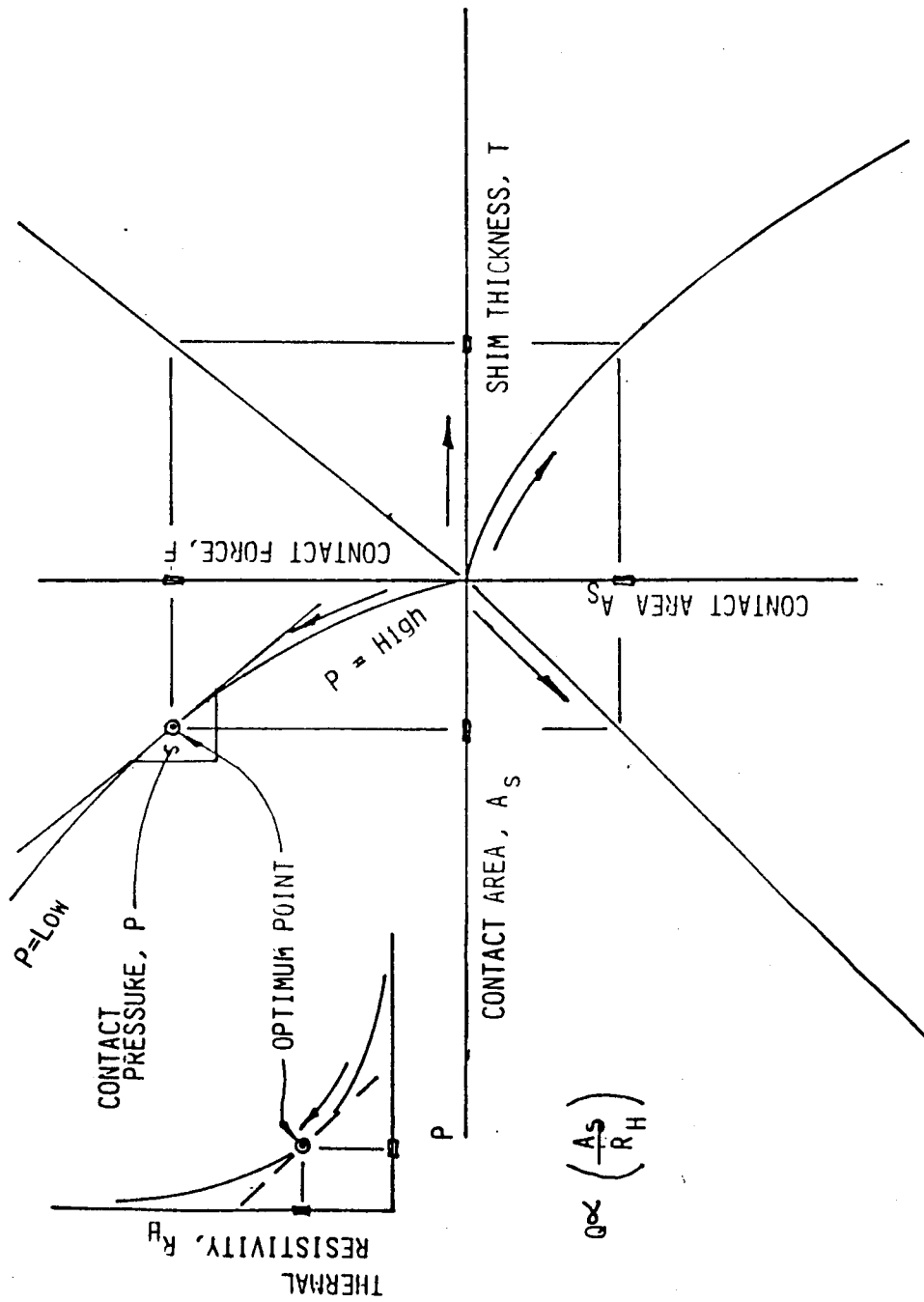
The Wavy Spring inserted between the Collector Ring and the Insulator applies multiple radial forces between the Ring in one direction and the Insulator and Housing in the other. The Insulator is provided with a gap which allows the walls of the Insulator to be forced into intimate contact with the wall of the Housing by action of the Wavy Spring. Various thickness optimization Shims are inserted between the Spring and the Housing until maximum heat conduction is effected. The Shim thickness, which results in minimum temperature differential between the Ring and the Housing for a given heat source at the Ring, is that which provides optimum heat transfer efficiency.

The explanation of this effect is as follows. The thermal transfer between two clamped members is related to the effective thermal resistivity at the interface. Figure 9 shows the qualitative relationship between this resistivity and the clamping pressure, P , in the upper left quadrant of the figure. Unfortunately, the quantitative relationship for the materials involved was not available. This dictated, therefore, that the heat transfer characteristics be determined empirically. Data was collected relative to the steady state temperature differential between the Ring and the Housing for various Shim thicknesses, " T ". Referring again to Figure 9 as the Shim thickness was varied the deflection of the Wavy Spring was changed and the normal contact force " F " at the Insulator and the Housing inner wall was also changed as shown in the plot. In addition, the contact area " A_s " of



COLLECTOR RING HEAT TRANSFER COMPONENTS
(HALF SECTION THROUGH OUTER CIRCUIT)

FIGURE 8



HEAT TRANSFER OPTIMIZATION

FIGURE 9

the Wavy Spring at the Ring and at the Insulator was also effected by the various Shim thicknesses. Since both normal force "F" and area "A" are being influenced, but not equally, the ratio of the two, normal pressure, "P" was also changed with Shim thickness. The heat transfer was effected by the thermal resistivity, " R_H " and the area of contact " A_S ".

Starting at the optimum point shown in Figure 9 as the Shim thickness, "T", increases contact force "F" and contact area " A_S " increase, contact pressure "P" decreases and resistivity, " R_H " increases. Since resistivity is increasing faster than area " A_S " is, the heat transfer, "Q" decreases. Conversely as the Shim thickness, "S", decreases contact force "F" and contact area " A_S " decrease, contact pressure "P" increases and resistivity " R_H " decreases. Since area " A_S " is decreasing faster than resistivity is the heat transfer "Q" decreases. Thus it can be seen that an optimum heat transfer can be effected by a unique Shim thickness. The Shim thickness selected for the EU was 0.040 inches thick.

2-1.5 Design Details - This section covers some of the more important design details of the EU components taken in a random order.

Referring to Figures 6 and 7 the external connecting Thimble is attached to the cables by means of conventional solder pots in the Thimbles. The Thimble is configured with a tapered cone which engages the Terminal Cone and is held securely in place with the Thimble Lock by means of a threaded interface. The Terminal Cone is firmly engaged with a ring tab which is an integral part of the Outer-Ring. The Stiffening Bolt assures a positive terminal Cone-to-Ring Tab interface by means of the Backing Ring which assures full contact even when external cable induced mechanical load strains on the external connection bend and twist the Ring tab. This type of loading is a common source of resistance changes on more conventional existing connecting means such as spring loaded pins and plugs and even the bolted connections used on spade lugs commonly used on welding cables.

Continuing on through the circuit the Outer Ring transfers the current through multiple paths through multiple Flexures (as described in reference 2) and hence to the Inner Ring. Connection at the Inner Ring to the Terminal on that ring is made by the Tie connection. The latter connection is configured with a spherical interface which engages with a like interface in the Inner Ring. The center of the radius of the spherical interface is located at a connection pilot which is at the outer extremity of the connection. The Locknut engages the connection radius center at a pilot thereby avoiding any movements within the spherical interface when the Locknut clamps the connection. The Locknut is not secured until the Terminal Cone on the Inner Ring is secured into position in the rest of the assembly. This assures that no mechanical strain is developed in any of the current transfer components which could relieve after the unit is in service resulting in a changed interface resistance. In addition, the self aligning feature of the spherical interface eliminates the possible effects of manufacturing and assembly variations. A Terminal Lock Screw is used to secure the Terminal Cone to the Tie connection in a manner similar to the Lock Nut engagement in the Ring against the other end of the Tie

Connection. This preloading arrangement insures that temperature excursions and mechanical loading of circuit components after the module is placed into service do not result in resistance changes at any of these interfaces since the preload loops are short. These and other preload loops are shown by dashed lines in Figure 7.

All of the circuit components are plated with a matrix which assures long term servicability. The base or matrix item is first plated with a copper strike to assure adhesion. An intermediate nickel layer is plated on to provide a hard base for the subsequent surface plating and to inhibit copper migration into the gold. The outer most layer is gold which provides a low resistance, non-tarnishing, conductive surface.

All of the smaller non-flexing circuit components are fabricated from Tellurium Copper alloy C14500 which provides both high thermal and electrical conductivity and good machinability. The large collector Rings are fabricated of free machining brass.

The material for the electrical insulators which must conduct heat was selected as Glass Fabric Melamine, (MIL-P-15037). This material provides a low thermal resistance while exhibiting excellent electrical insulation properties. The material for all other insulators was selected to be Glass Fabric Epoxy (MIL-P-18177) . The design of the EU provides mechanical barriers between circuits as well as double insulation. The latter insulation pair is comprised of two different materials to assure that a given environment which might degrade one insulator does not degrade the other. These two insulation materials were Melamine and hard anodized aluminum.

The external Terminal Cones and their associated attaching hardware on the Outer Housing are designed to allow the Terminals to be reversed during an actual application to facilitate a given configuration. In addition, the layout of the Terminals is such as to provide maximum accessibility by both axial and circumferential staggering of the Terminals into a stair step pattern.

The Thimble Locks on the connecting cables provide positive cone interface clamping action of the Thimble/Cable assemblies. The Terminals are backed up mechanically on each of the Outer Ring connections with a Backing Ring and a Stiffening Bolt. This configuration assures that the Terminal/Ring tab interface will remain unchanged even under the influence of bending moments resulting from external movements of the stiff cables. All preload loops throughout the EU are short and within metallic members only as shown by dashed lines in Figure 7. This negates the effects of time and temperature on the various preloaded components.

Molded silicone Boots are provided for the external connection to assure that no line-of-sight conditions exist either between circuits or from a given circuit to ground.

The Inner Housing assembly is rigidly supported within the Outer Housing with a "DB" bearing arrangement using two thin line bearings and a preloading diaphragm. This diaphragm provides radial stiffness

and axial compliance such that a precise preload is effected and maintained. In this arrangement all four bearing rings are precisely clamped thereby avoiding mechanical shifts during use with associated torque and alignment changes. The "DB" preloading is accomplished by loading the bearings axially through the inner rings against an internal Spacer which has been lapped to provide a given diaphragm deflection. The design assessment of the diaphragm is given in Appendix C. The axial spring rate is 3.7×10^3 Newton/Cm (2.1K lb/in). At an axial deflection of 0.25 mm (0.010 inches) the preload is 93 Newtons (21 lbs.)

2-2 FABRICATION

After all of the detail drawings were completed, the fabrication of the TF and EU components was initiated. This section of the report will provide an overview of the most significant details of the fabrication process.

2-2.1 Circuit Components - The most critical detail parts were the circuit components. Of these components the Flexures as well as the Inner and Outer Rings were fabricated by computer control. This technique was selected to assure that the contact tracks were uniform and to accommodate the large number of Flexures required. The machining was performed in its entirety on these three components using a Monarch tape controlled lathe with a Bendix System 5 Command unit for the Flexures and a Bostomatic 312 Tape Controlled Mill with a CNC Command Unit. Special tooling was required to eliminate distortions in the Outer Ring roundness.

After all of the machining operations were complete on the circuit components they were coded and assigned to specific circuits. The identification technique selected was to engrave the circuit number (1 through 8) on non-functional surfaces of each part. The interfaces of each mating part were then lap fitted with Time Saver Products 60 grit compound and thoroughly cleaned to remove all lapping grit. This matching and lapping procedure included the cable terminal fittings. All threads were fabricated as a class 2 fit to assure acceptable fit up after plating.

The Flexures were fixture heat treated to prevent distortion by mounting on an arbor with a 1.4 mm (0.056 inch) total clearance. This represents 4 percent of the mean diameter. The arbor was fabricated of the same material as that of the Flexure Beryllium Copper Alloy 172. The heat treating was performed in a vacuum oven although an inert gas oven is an acceptable alternate. The resultant distortion of the Flexure roundness was less than 0.15 percent. The heat treat process consisted of precipitation hardening for 3.0 hours at 600 $\pm 10^{\circ}$ F followed by an air cool.

All of the circuit components were electroplated at American Electroplating in Somerville, Mass. This firm was selected to do the plating because of their vast experience in electroplating critical space components. Although previous testing has proven that the Roll Ring components do not require near perfect plating, the platers experience was critical for this program in that only a limited quantity of spare parts were available for plating parameter testing and fallout. As it turned out 100 percent of the components produced by American Electroplating were acceptable. Quality control tests which were performed on the plated components included adhesion, surface texture and thickness.

The gold plating used for these components was selected from two types, Orosene 999 cobalt/gold ("hard") and Pur-a-gold ("soft"). Experience has shown that the moving interfaces exhibit the longest trouble free life if they are of different gold alloys. This is especially true if the interface is one that is either constantly or even intermittently changing. Table V lists the gold alloys chosen for the circuit comp-

onents. The detail parts are listed in mechanical order from the outer (stator) terminal to the inner (rotor) terminal. The interfaces shown in the table are of the three types "fixed" (assembled and not disturbed in use), "connector" (occasionally disturbed) and "rolling" (constantly disturbed). The plating matrix consisted of a copper flash of approximately 1.25 microns (50 microinches), sulfamate nickel 3.1 \pm 1.2 micron (125 \pm 50 microinches) thick followed by the gold (or gold alloy) 3.1 \pm 1.2 micron (125 \pm 50 microinches) thick. Previous testing has indicated that this matrix is optimum for long wear free life.

DETAIL NAME	PART NUMBER	INTERFACE TYPE			GOLD PLATING	
		FIXED	CONNECTOR	ROLLING	SOFT	HARD
Thimble Terminal	5240-050442					X
			X			
Contact Cone	5240-050741				X	
		X				
Outer Ring	5240-011841				X	
				X		
Flexure	5240-010951					X
				X		
Inner Ring	5240-011842				X	
		X				
Connecting Rod	5240-050448					X
		X				
Contact Cone	5240-050741				X	
			X			
Thimble Terminal	5240-050442					X

GOLD PLATING MATRIX FOR CIRCUIT COMPONENTS

TABLE V

2-2.2 Electrical Insulators - The design of the EU is such as to utilize two electrical insulators between each pair of conducting components and between each component and the Housing ground members. The most critical of these components is the Outer Ring Insulator. Its design is such as to provide a location seat for the eight Outer Rings, to provide a uniform heat conduction path between the Ring and the Housing and to provide electrical insulation to the Housing. The latter insulation includes a box like structure which completely surrounds the terminal attachment tab on the Ring which protrudes through the various windows in the Housing.

The Outer Insulator was vendor machined on a tape controlled mill to assure that all of the manufacturing tolerances could be met and repeated. the Insulators were fabricated out of a Glass Fabric Melamine material which presented a hazardous working environment. As a result of this situation a difficult part of the fabrication process was to locate a suitable (and willing) machine shop with the proper capabil-

ity. An alternate material could have been selected with non-optimum heat transfer properties such as epoxy glass laminate but with less hazardous machining characteristics. After encountering the difficulty locating the machining vendor for the Melamine material a decision was made to utilize the material only where the heat transfer property (reduced thermal resistance) was important. This resulted in a specification of the Melamine material for the Inner and Outer Ring Insulators.

Figures 10a and 10b are photographs of the Inner and Outer Ring Sets. These figures show the various components discussed. Not shown in Figure 10a is the heat transfer Wave Spring as is shown for the Outer Ring in Figure 10b. The nylon Insulator for the Connecting Rod is also not shown in Figure 10a since the EU design was modified to change the design of this Insulator from a polyolefin shrink sleeve to the Nylon material shortly before shipping the unit. (See Test Section 2-3.2f for further details.)

The Idler Guides were fabricated from 6061-T6 aluminum alloy sheet stock. The sheets were roughed to size and finish machined on a vacuum chuck to prevent distortion. After the machining operations were complete the Guides were hard anodized to provide a wear resistant track where the Idlers roll against the Guide rail and to provide additional electrical insulation. The anodizing process was specified to have a 0.025 mm (0.001 inch) penetration and buildup. These influences on the final size were anticipated during the fabrication process.

A set of Insulator Barriers were fabricated from glass fabric reinforced phenolic sheet stock. These barriers provide the important task of separating each adjacent circuit, electrically, with a labyrinth path at the outer extremities. Details of this component as it is incorporated in the EU can be seen in Figure 6.

A single Insulator Cup was fabricated out of glass fabric phenolic bar stock which was subsequently assembled around the lower (circuit 1 through 4) Inner (rotating) Housing terminations. A set of four Insulator Cups was fabricated out of the same material for electrical insulation of the upper (circuits 5-8) Inner Housing terminations. Both of these insulator designs provide supplemental dielectric strength to the rotating cable terminations. Refer to Figure 6 for additional details of these insulators.

The Terminal/Cable Insulator Boots were gravity/vacuum molded out of Silicone Rubber molding compound General Electric RTV-60 (AMS 3366). After molding the Boots were cured at 25°C for 170 hours followed by 2 hours each at 120, 135, 150, 165 and 180°C to achieve optimum tear strength.

2-2.3 Heat Transfer Members - The key heat transfer component was the convoluted Wave Spring. This detail was fabricated from 0.25 mm (0.010 inch) thick Beryllium Copper Alloy 172 strip stock. Each Outer Ring Spring had 13 waves with a pitch of 3.8 cm (1.5 inches) and a wave height of 0.63 cm (0.25 inches). Each Inner Ring Spring had 4 waves of the same basic design. These Springs were fitted into a stainless

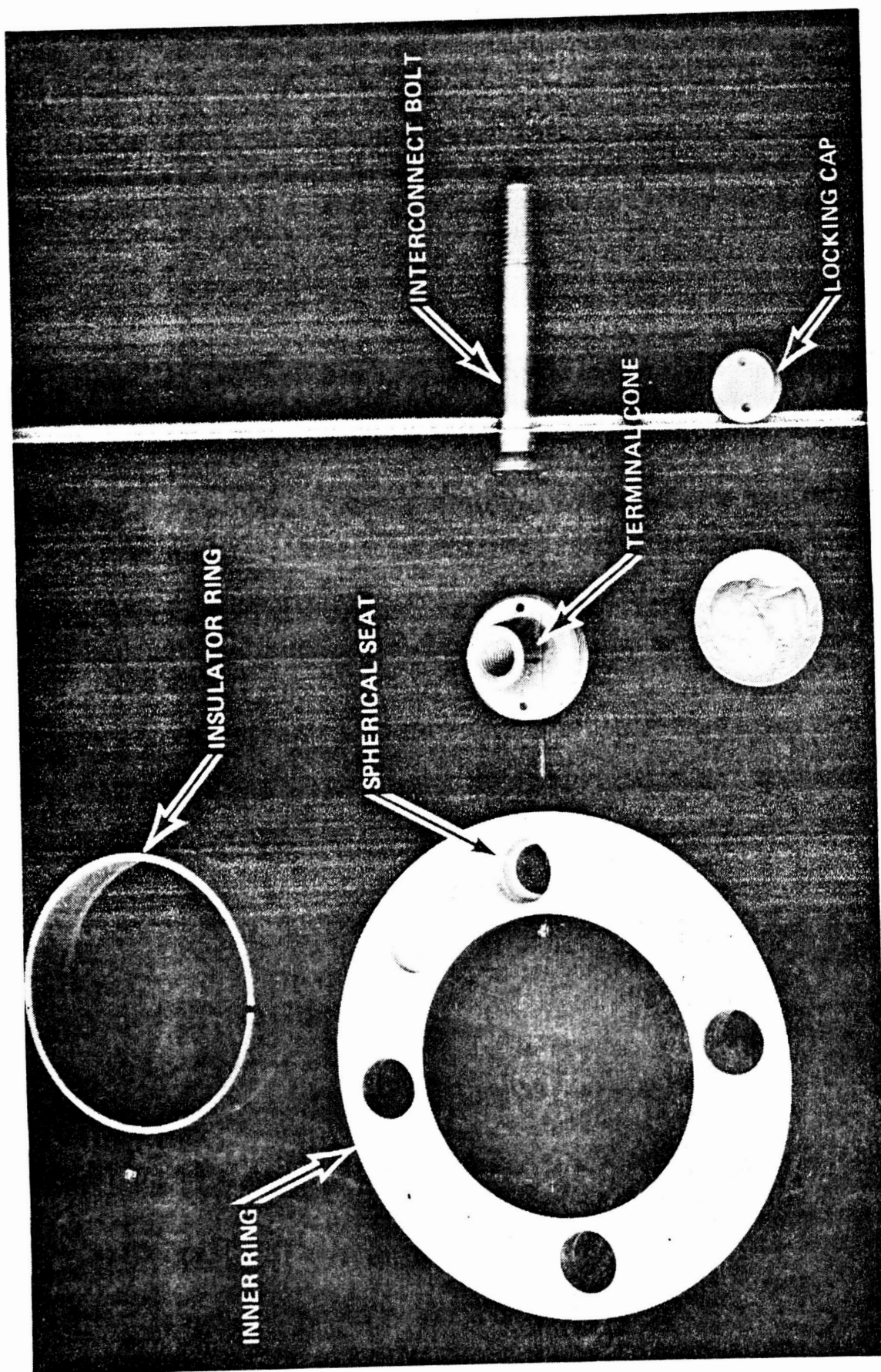


Figure 10a

High Power Roll Ring Inner Collector Ring Set

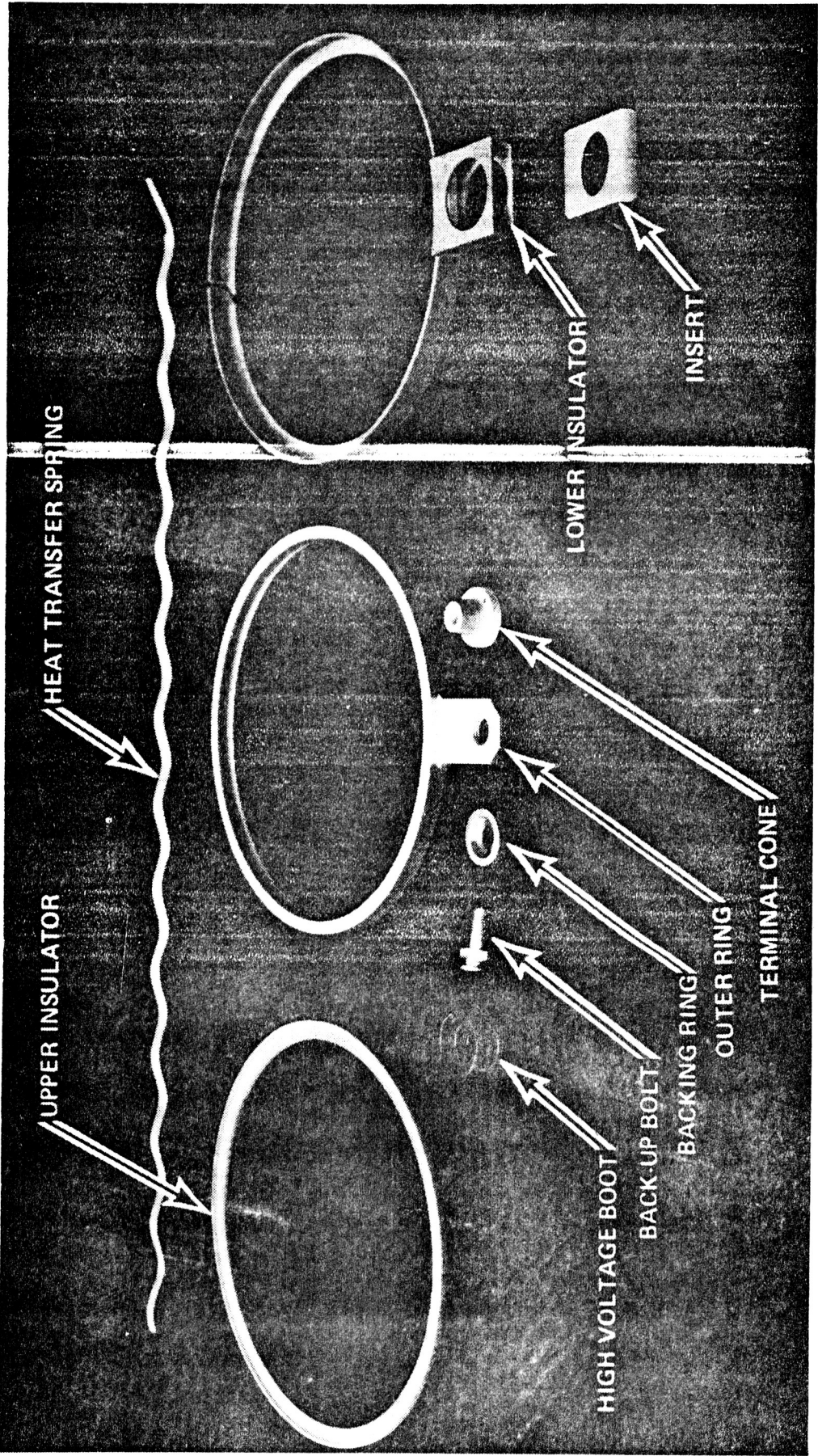


Figure 10b

High Power Roll Ring Outer Collector Ring Set

steel heat treat fixture which developed the required wave shape with 0.95 cm (0.375 inch) diameter pins. Heat treating was performed in a vacuum oven to achieve a minimum hardness of Rockwell 15N80. The Springs were plated with 0.025mm (0.001 inches) of Silver after heat treating to provide efficient heat transfer interfaces with the Rings and Insulators. A typical Outer Ring Wave Spring is shown in Figure 10. Note that the Spring is straight in the free state.

The heat transfer optimization Shims were fabricated out of aluminum alloy sheet by slitting the 1mm (0.040 inch) thick sheet stock and rolling to approximate size. Since the Wave Springs radially preload the Shims into intimate engagement with the Insulators the exact free diameter is not critical. It is important, however, that the Shims be free of any local undulations which would decrease the effective heat transfer area. For this reason the Shims were rolled with a roller diameter which was close to the finished size.

- 2-2.4 Housing Components - Both the Inner and the Outer Housings were fabricated out of 6061-T6 aluminum alloy bar stock. After all machining and finishing operations were complete the Housings were sent out for hard anodizing. This anodizing process provides electrical insulation of approximately 120K volts/cm (300K volts/inch). Superior alternate coatings are "Nituff" (Nimet Industries, Inc.) and "Hardtuff" (Tiodize). The coating results in a penetration and a buildup of 0.025 mm (0.001 inches). The original critical dimensions were adjusted during the fabrication process to accomodate the anodizing buildup. All threads and the bearing mounting surfaces were masked off during the anodizing process. Figure 11 is a close up photograph of the two completed Housings and other components of the EU.

A set of hardware was fabricated which was subsequently used to axially clamp the two ring sets after all assembly was complete. This hardware also provides an overlapping barrier to foreign debris. Refer to Figure 6 for details of this hardware.

- 2-2.5 Bearing System - A pair of Kaydon KB 45 "Reali-Slim" bearings were selected for the EU during the design stage. After procurement these bearings were cleaned and lubricated with approximately 50 mgm of KRYTOX AZ grease in each bearing. The original single piece bronze ball cage was used since speeds are low and dynamic/torque problems are improbable.

A Bearing Preloading Housing was rough machined from 440C stainless steel, fixture heat treated in an inert gas oven to R_c 56-60 and final ground to size. The heat treating fixture was such as to clamp both sides of the 0.5mm (0.020 inch) diaphragm to prevent distortion. After heat treat a reference face was ground on the Housing mounting face and the diaphragm was reduced by grinding to a 0.2 mm (0.008 inches) thickness. The bearing outer diameter mounting surface was also ground to size in the final finishing operations. Details of the Housing and the Bearing pair are visible in Figure 11.

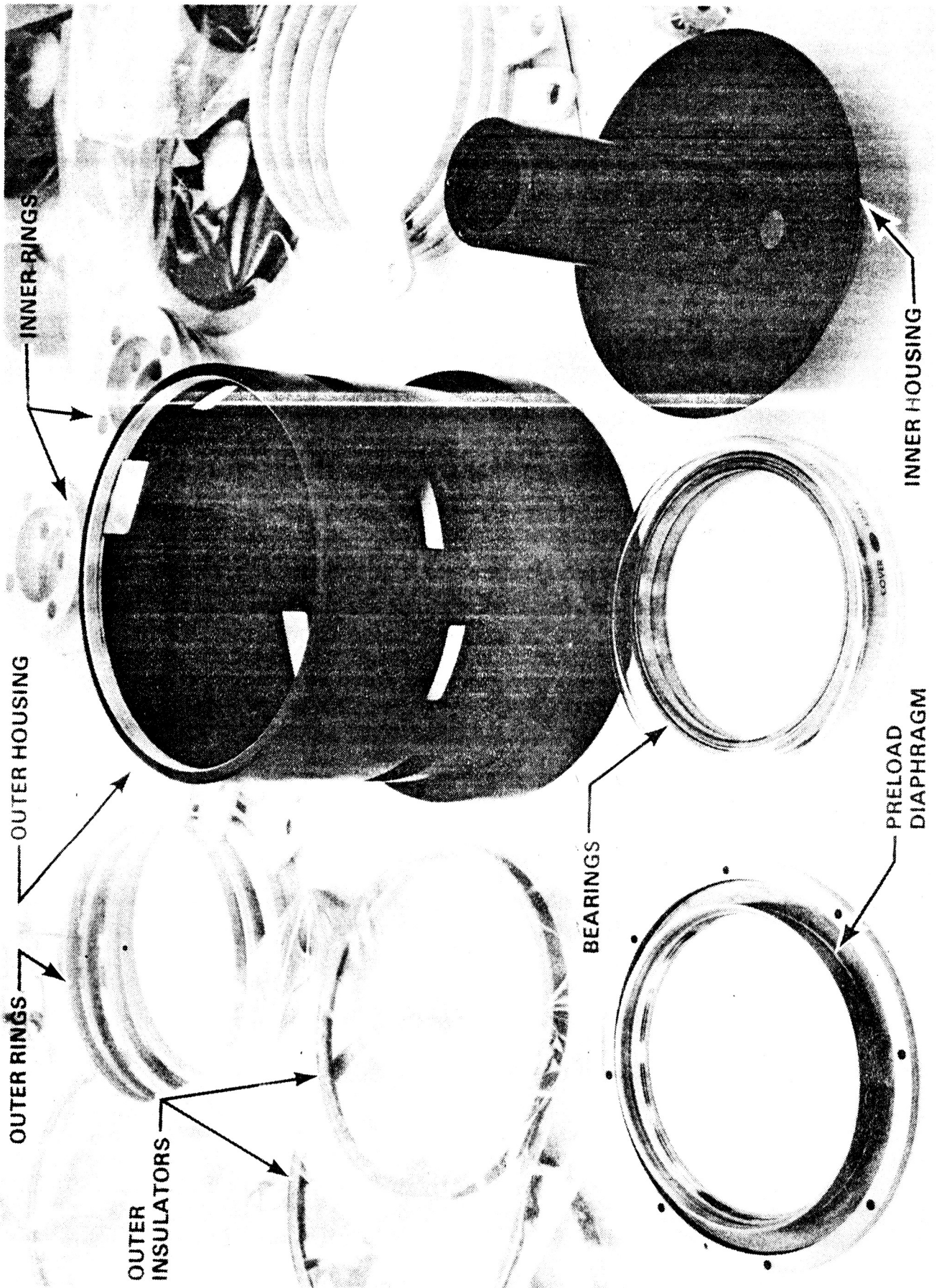


Figure 11

Close Up of Evaluation Unit Components

2-2.6 ASSEMBLY

- a. Cables - The Cable Assemblies were fabricated using a hot plate to maintain the Thimble cavities at $220 \pm 20^{\circ}\text{C}$. Appendix E provides sub-component and fabrication process details.
- b. Vacuum Bake - All non-metallic components were thoroughly vacuum baked in an oven at 100°C for 50 hours prior to final cleaning. Prior to this vacuum baking the components were cleaned in Freon Type TEC for 15 minutes. The Outer Ring Insulators exhibited a size change during this vacuum baking process which necessitated a shimming process during the assembly procedure. (Refer to Section 2-2.6d to follow.)
- c. Cleaning - After all machining and finishing operations are complete the EU components were cleaned by the following procedure:
 - o Ultrasonically clean parts for 3 minutes minimum in Freon TES. Care should be taken to avoid contact between parts.
 - o Remove the parts from the ultrasonic during agitation and blow dry with filtered dry nitrogen.
 - o Vapor degrease the parts in Freon TES until condensation ceases.
 - o Remove from the vapor degreaser and blow dry with filtered dry nitrogen.

All EU components were handled with clean non-talc finger cots throughout the cleaning and post-cleaning processes. No form of metallic instruments were allowed to contact any of the circuit components from the outset of the cleaning process. After the cleaning operations were completed the circuit components were either heat sealed (pill packed) in a 0.1mm minimum thickness polyethylene bag or carefully stored in pyrex dishes in a FED-STD-209 or better clean hoods.

After vacuum baking the non-metallic parts were given a secondary ultrasonic Freon TEC wash.

All tooling which was to be used in the EU assembly operations was thoroughly cleaned with Freon TA and acetone prior to usage.

- d. EU Assembly - The actual assembly of the EU was initiated after all sub-component cleaning and vacuum baking processes were completed. Figure 12 is a photograph of the complete set of detail parts of the EU ready for assembly. The assembly procedure was repeated four times during the first build and test of the EU because of a number of operational problems with the EU which had to be corrected. These problems are discussed elsewhere in this report.

The initial step of the assembly consisted of mounting and preloading the ball bearings. This procedure is included in this report as Appendix F.

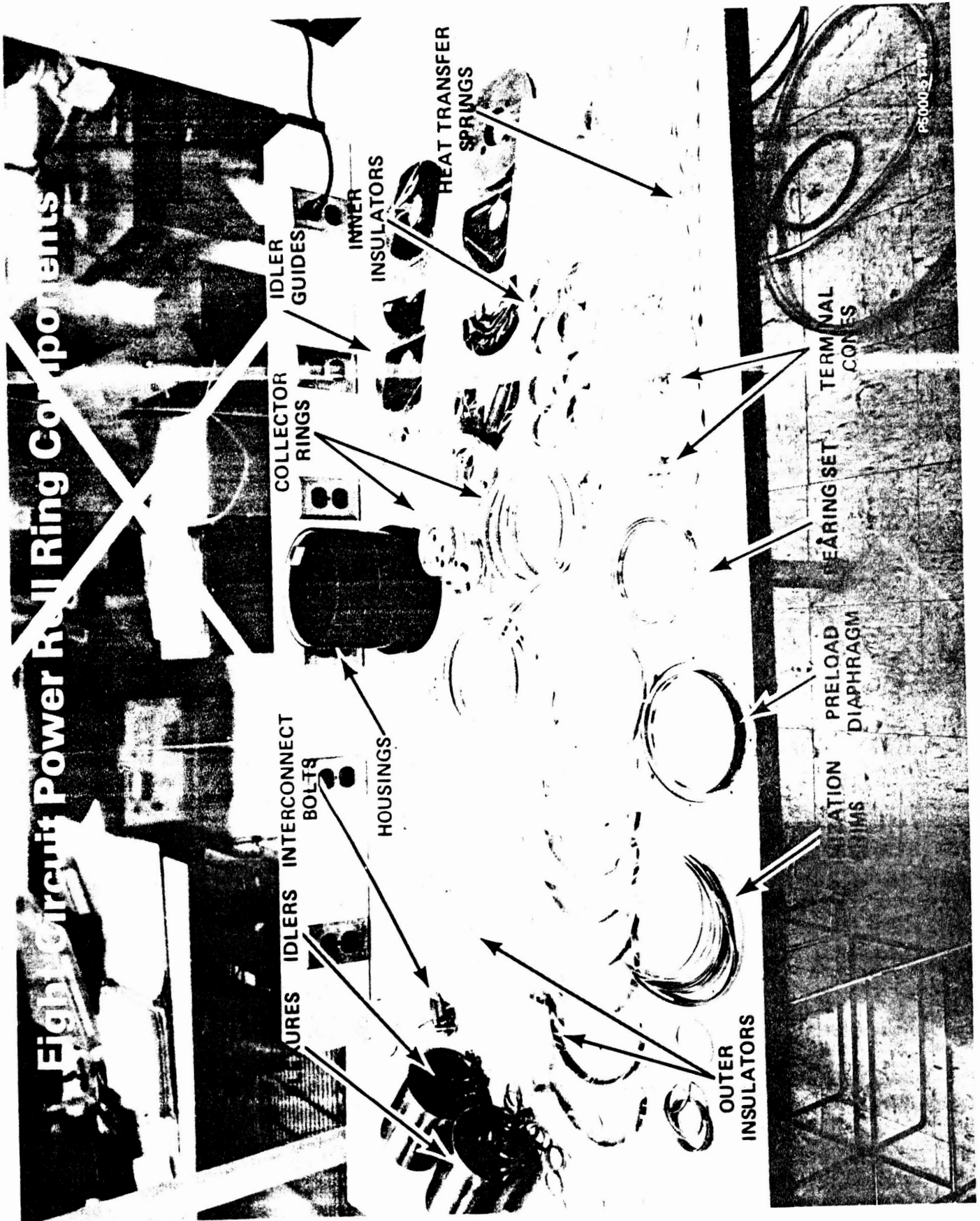


FIGURE 12

After the Inner and Outer Housings were assembled with the Bearing/Diaphragm assembly the rotational torque was measured and the circuit assembly was initiated. The most critical phase of the assembly consisted of the assembly of each Ring set and the verification of the axial alignment of the Inner and Outer Rings. This sub-assembly process is documented in this report as Appendix G. A photograph was taken of the EU looking down into the Housing cavity after step "n" of the procedure described in Appendix G. This photograph is included in this report as Figure 13. This figure also shows the other circuit and heat transfer components discussed.

After all of the circuit components had been assembled the Inner and Outer Housing termination members were assembled. These members provide axial clamping of all of the components as well as an effective mechanical overlapping non-contact, labyrinth seal.

- e. TF Assembly - The assembly of the Test Fixture (TF) was rather straight forward and followed the assembly details delineated in Appendix H.

Figure 14 is a photograph which shows the heat exchange manifold in the bottom of the vacuum Base Plate of the TF. The manifold, which is machined directly into the plate provides $1,806 \text{ cm}^2$ (280 in^2) of heat exchange area which is located directly adjacent to the exchange area from the EU base. Figure 15 is a photograph of the Base Plate after being sealed by the Cover Plate and 3M-EC-1675 sealant.

Figure 16 is a view of the completed TF prior to assembly of the EU. This figure provides a good view of the control panel.

Figure 17 is a close-up of the surface of the TF vacuum Base Plate which shows the EU-to-TF adapter Ring. This Adapter provides an efficient heat transfer interface and provides rotational clearance for the Inner Housing interconnecting cables for circuits 1 through 4.

Figure 18 is a photograph of the under side of the TF and shows additional details of the various sub-components. Comparison can be made between the details of Figure 18 and those shown on the even numbered pages of the document of Appendix H.

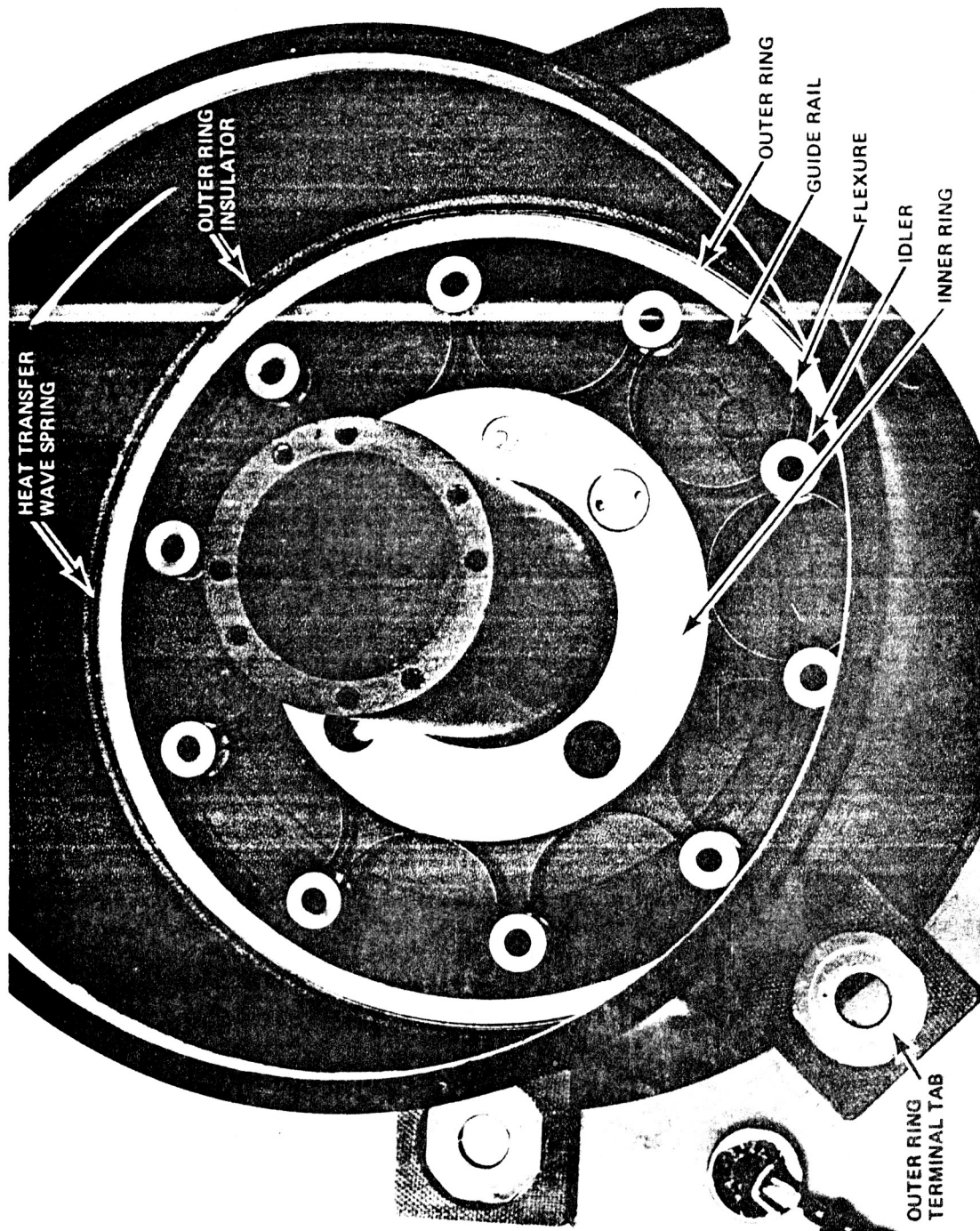
2.3 TESTING

2.3.1 Single Circuit Tests

During the fabrication of the components for the complete EU a special static test fixture was fabricated to provide a means of optimizing the heat transfer between the collector Rings and the EU Housing. (This optimization was described in section 2-1.4 of this report.) A single circuit was assembled in the test fixture and eleven copper/constantan thermocouples were attached per Test Procedure 5240-080741. This procedure is included as Appendix D of this report.

Fifteen different design configurations were assembled into the fixture and tested. These configurations provided various means of transferring the heat from the collector Rings to the Housings. Parameters which were

TYPICAL POWER TRANSFER COMPONENT LAYOUT



ORIGINAL PAGE IS
OF POOR QUALITY

FIGURE 13

455-05-26

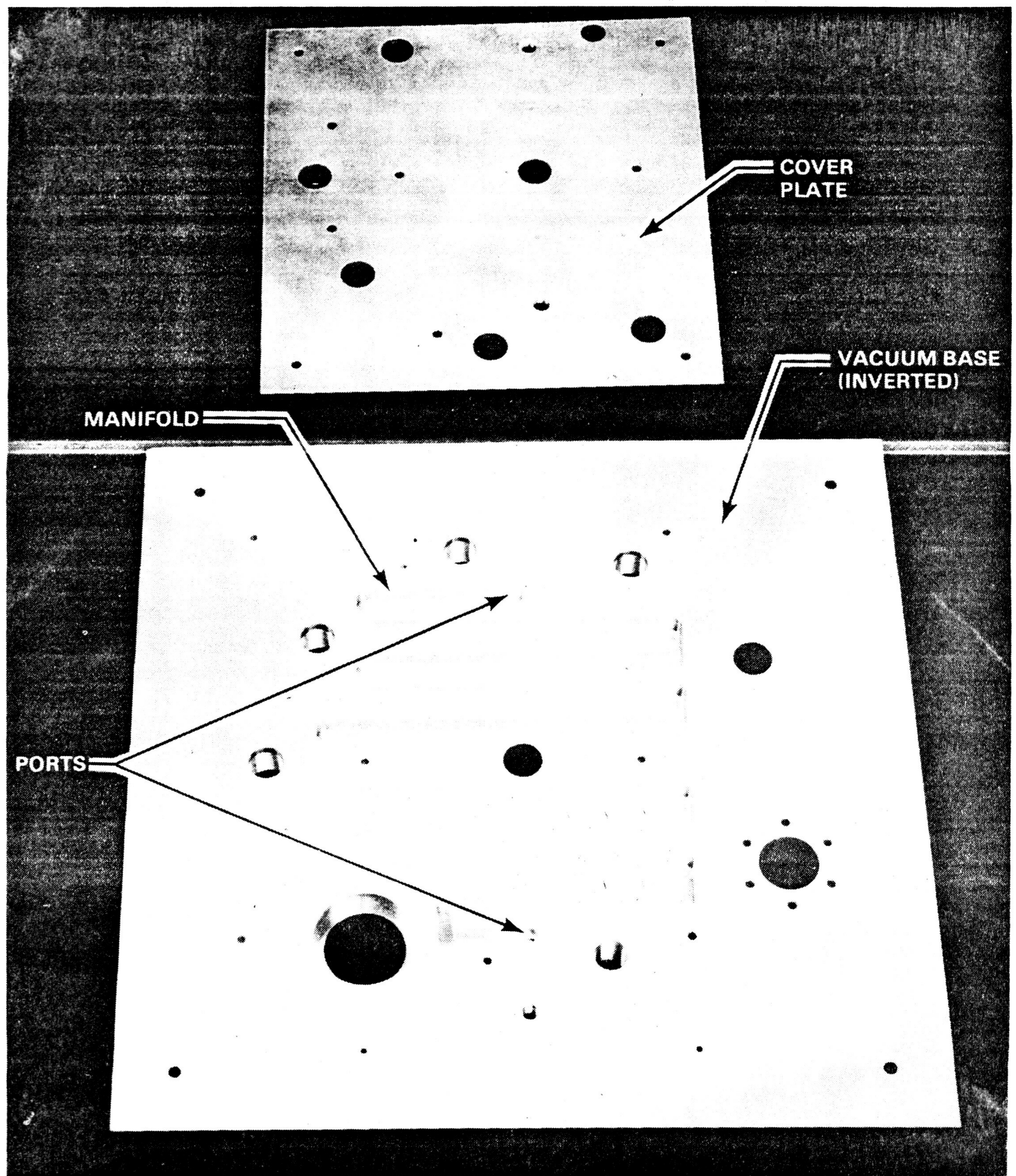


Figure 14

Vacuum Base Heat Exchange Manifold

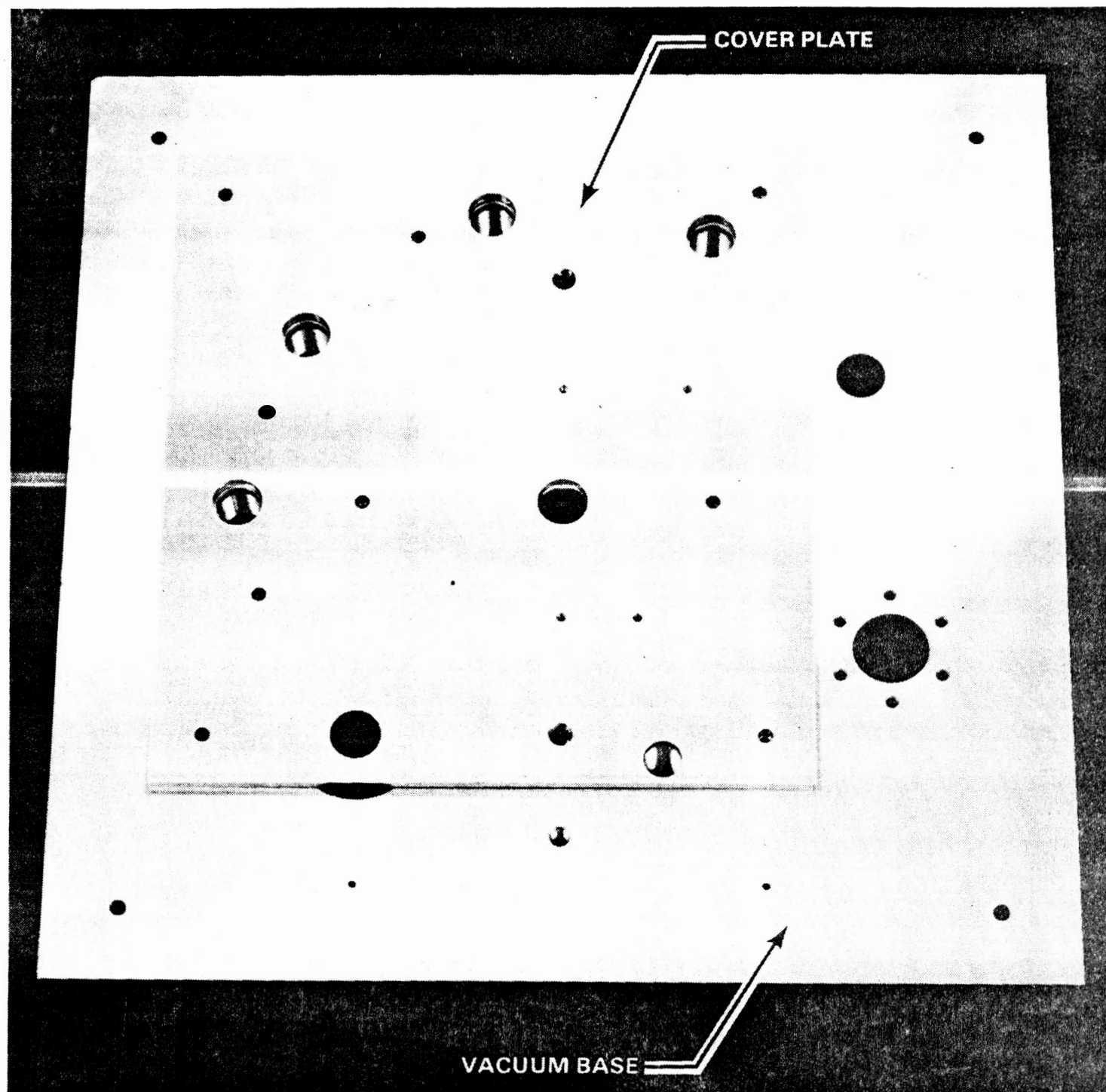


Figure 15

Vacuum Base With Sealed Manifold

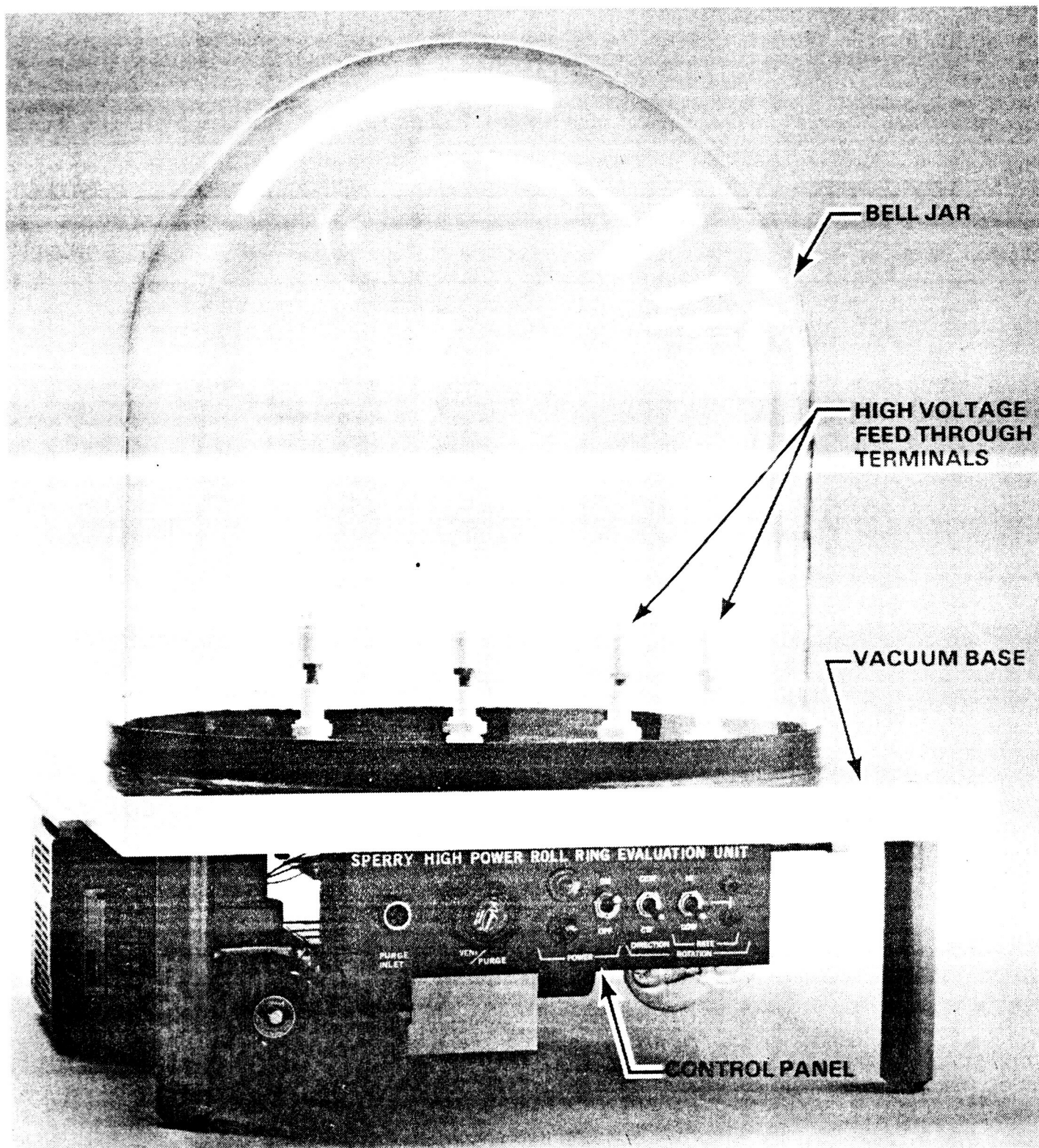


Figure 16

High Power Roll Ring Test Fixture

ORIGINAL PAGE IS
OF POOR QUALITY

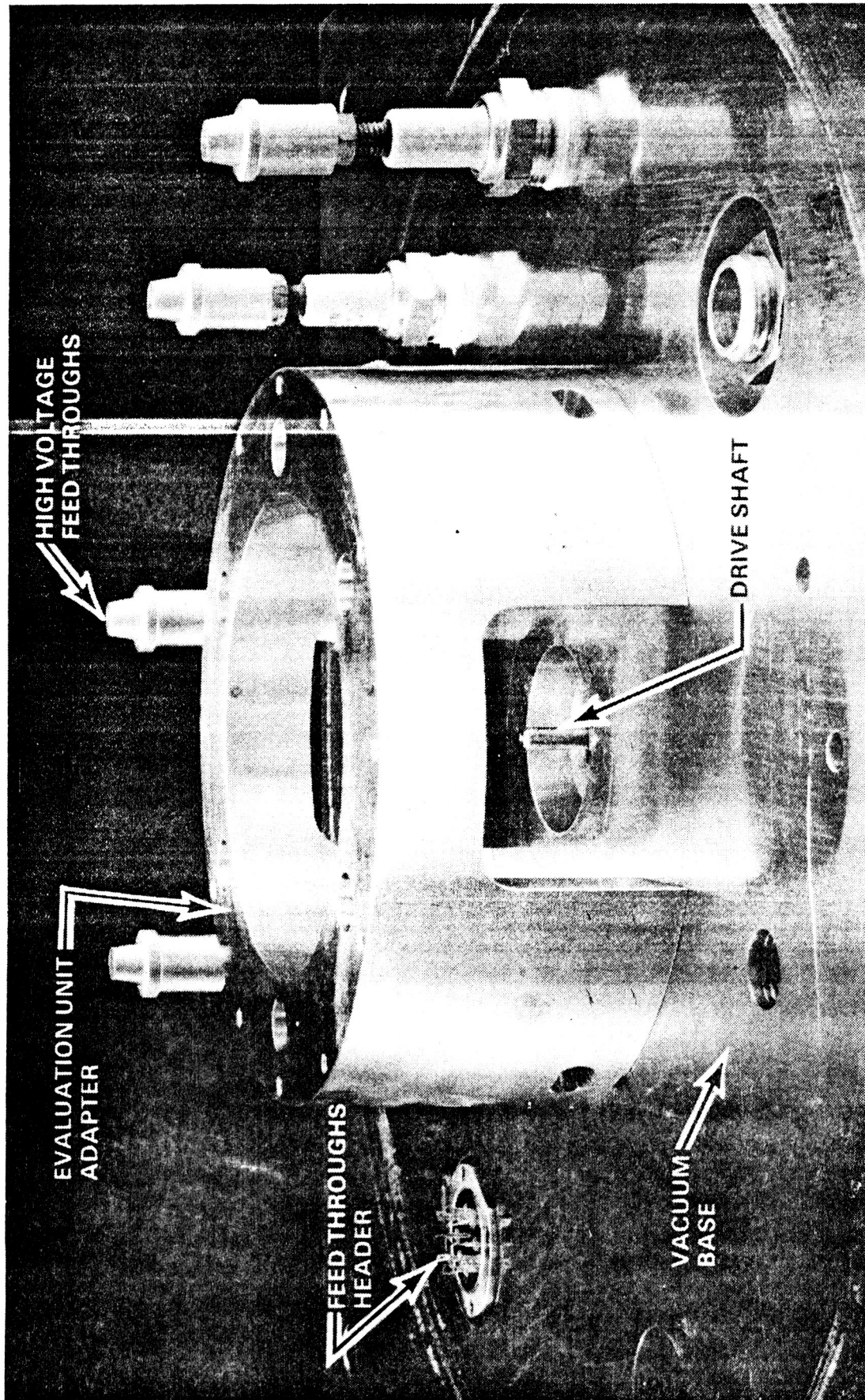


Figure 17

Test Fixture Base and Adapter

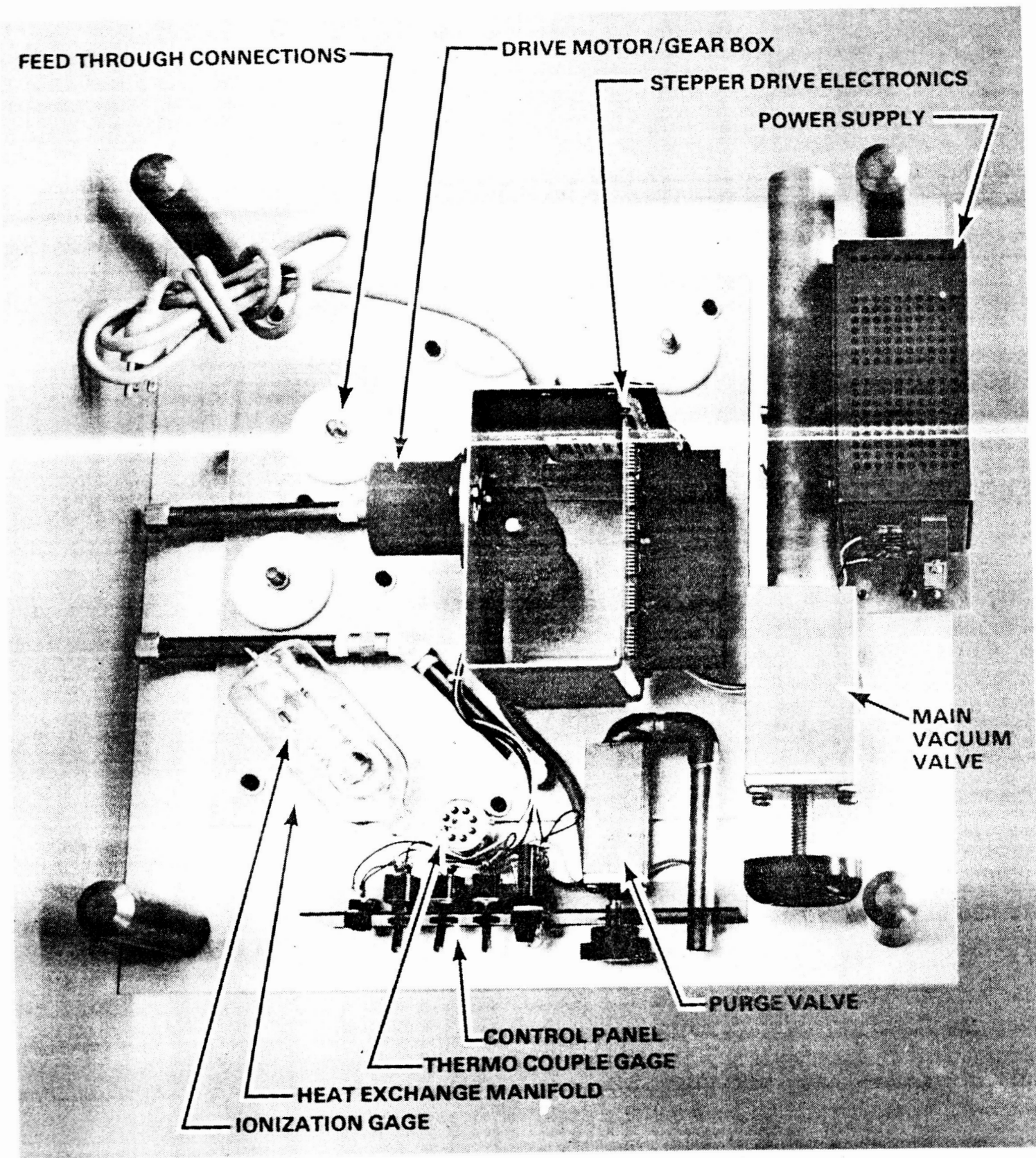


Figure 18

ORIGINAL PAGE IS
OF POOR QUALITY

Bottom View of Test Fixture

varied were contact pressure, effective surface roughness (area), interface material (machined phenolic, copper, epoxy and grease) and interface orientation (Wave Spring location). This test sequence revealed that little was to be gained by improving the surface finish unless it could be vastly improved. Of major importance was the determination that for the particular Wave Spring design fabricated the heat transfer was optimum for a given annulus radial dimension. The reason this is believed to be true is discussed in the "Design" section (2-1) of this report. This radial dimension, which represents a spring deflection of 35 percent of free height and 350 percent of Spring material thickness, was used in the EU.

2.3.2 MULTI CIRCUIT TESTS

After completing the initial assembly of the EU a set of measurements were made to verify design and assembly adequacy prior to initiating the performance tests. The result of these measurements and a brief discussion of each follows:

- a) DC Low Current Resistance - Since the original and the revised groove configurations of the EU have slightly different Flexure/Ring groove interfaces the low current circuit resistance is also different. Table VI below summarizes the two sets of resistances. These resistances were measured with a low current milliohm meter. The modulation resistance is the variation of the average resistance when the EU rotates.

<u>CIRCUIT NUMBER</u>	<u>RESISTANCE (MILLIOHMS)</u>		<u>RESISTANCE MODULATION (MILLIOHMS)</u>	
	<u>Original</u>	<u>Final</u>	<u>Original</u>	<u>Final</u>
1	(0.45)	(0.47)	(+0.02)	
2	(0.46)	(0.48)	(+0.01)	
3	(0.45)	(0.47)	(+0.02)	
4	(0.46)	(0.48)	(+0.01)	
5	0.50	(0.50)	+0.02	
6	0.51	(0.48)	+0.04	
7	0.52	(0.50)	+0.02	
8	0.48	(0.48)	+0.01	
Spec. Req.	<1.00	<1.00	<+0.25	

LOW CURRENT CIRCUIT RESISTANCE
TABLE VI

b. Insulation Resistance - The high voltage insulation resistance of each circuit of the EU was checked with respect to the EU Housings and with respect to adjacent circuits. Table VII below summarizes the readings taken.

<u>CIRCUIT NUMBER</u>	<u>INSULATION RESISTANCE</u>	
	<u>AT 1K VOLTS (M OHMS)</u>	
	<u>CRKT/GRND</u>	<u>CRKT/CRKT</u>
1	50K	100K
2	30K	100K
3	50K	100K
4	30K	100K
5	60K	200K
6	60K	200K
7	60K	200K
8	50K	
Spec. Req.	>10.0	>10.0

INSULATION RESISTANCE
TABLE VII

The EU has acceptable insulation between adjacent circuits as well as to the respective grounds.

c) Capacitance - An estimate was made in the original proposal as to the potential circuit-to-circuit and the circuit-to-ground capacitive coupling. As the summary data in Table VIII below shows, the capacitance in the completed EU is considerably greater than the predictions. If this turns out to be a problem when the EU is conducting an AC voltage the design would require modification to reduce the values. These design mods would likely result in a larger unit. The measured capacitance values are as shown in the table. No explanation can be given for the variation of the readings from circuit-to-circuit.

<u>CIRCUIT NUMBER</u>	<u>CAPACITANCE (PFD)</u>	
	<u>CIRCUIT/CIRCUIT</u>	<u>CIRCUIT/GROUND</u>
1	2000	1590
2	2000	1440
3	2000	1570
4	980	1440
5	1080	1010
6	860	1130
7	710	1020
8		850
Spec. Req.	<150	<300

CAPACITIVE COUPLING

TABLE VIII

d) Torque - The torque measured on the various EU builds varied over a wide range. This characteristic was not observed in previous builds of the initial 2 circuit prototype unit. It is believed to be associated with not-quite-optimum design clearances in the multi-circuit axial tolerance stackup of the EU. The torque per circuit was typically 0.7 Newton cm (1.0 oz-in) and the bearing torque was on the order of 4.2 Newton cm (6.0 oz-in). This resulted in a complete EU torque of 10 Newton cm (14.0 oz-in).

After the first build of the EU the torque level increased approximately 300 percent shortly after initiating the vacuum test phase. The unit was disassembled to determine the cause. The only discrepancy which could be located was that three of the 10 Idlers on the bottom (No. 1) circuit were found to be in an inner, instead of an outer location relative to the Flexure/Flexure small gap. After conducting a number of experiments to attempt to cause the Idlers to traverse the gap by applying modest levels of radial forces but without success it was concluded that the Idlers must have been assembled in the incorrect position.

The Idler Guides were modified by adding shoulders to the Guides which restricted the Idler radial freedom, the EU was re-assembled and vacuum test data was taken. During the final phases of this testing (approximately 30 hours total) the unit again momentarily stalled the TF. The EU was then removed from the TF and carefully disassembled to determine the cause of the torque change. (The torque change had subsequently disappeared). No obvious cause was evident during disassembly. A set of tests were conducted and piece part measurements made to determine the cause but none could be found nor could the torque increase be duplicated.

These tests consisted of assembling only two circuits with a special upper Idler Guide which was modified to provide a means of observing the operation of the upper circuit components. Subsequent testing at 5 rev/min in vacuum both with and without current did not reveal any anomalous behavior other than occasional flutter of some Flexures. The latter was characterized by a small deviation of the Flexure from a rolling plane normal to the rotation axis.

Since this behavior is influenced by the Flexure capture stiffness which is, in turn, controlled by the Ring groove radii, Flexure radii and groove-to-groove space it is not easily modified. This capture quality is characterized by the "stability ratio" and the "straddle angle" and is improved by a reduced ratio and increased angle respectively. This ratio and angle are traded off with "conformity" which relates to the contact current density. It had previously been assumed that stability ratios <1 and straddle angles >10 were acceptable. The EU design had a ratio of 0.51 and an effective angle of 13 degrees in contrast to the original prototype module of 0.27 and 17 degrees respectively. This trade-off provided a reduction of current density from 650K amps/inch² to 50K amps/inch².

Since the Flexure rolling deviation was small and infrequent and because dynamic modifications would be time consuming a decision was made to retrofit a partial EU with Teflon flexure guides to limit the rolling excursion and related torque change. The unit was then placed into an operational mode for sufficient time to assure that future operation would be acceptable. Subsequent tests for 110 hours (33K revs) in vacuum were acceptable from a performance standpoint. After disassembly and inspection, however, it was observed that one circuit had several small Teflon particles from the occasional Flexure contact.

It was observed during tear down that some Flexures were very stable (small lateral deviations) while others were very unstable. Subsequent examination on a comparator at 100X revealed a variance of the straddle angle from 8 degrees on the unstable Flexures to 18 degrees on the stable Flexures. This variation was related to the close conformity of the Flexure radius and Ring groove radii. Small variations of plating thickness were adequate to introduce the variation. This sensitivity could be avoided by a small reduction of the conformity and would only force a small increase in related current density.

It was decided at this point that a change of the Flexure/Ring groove interface was necessary to eliminate the plating sensitivity, to improve the Flexure dynamics and to reduce the Flexure lateral excursions. The design modifications forced by the unacceptable Flexure dynamics involved the Ring groove transverse radius and basic groove diameters as well as the Flexure contact groove radius and radius center location. Layouts were made to provide a means of selecting the groove radii which would not necessitate a change of the Flexure preload, Idler diameters and Idler Guide contact radii. An acceptable design configuration was selected which could be implemented without scrapping any components. Contacts with the plating vendor provided a means of building up the Ring grooves with copper 0.005 inches thick which provided a base from which the new groove could be machined. After the new grooves were formed and the Flexure corner radii were modified the parts were all replated. The numerically controlled machining process made it possible to relocate the Flexures and Rings in the machine and re-machine the grooves and tracks with a revised computer control tape.

The EU was then reassembled a third time. It was observed during this reassembly that the Flexure rolling trajectory was much more stable and that the Flexures would even snap back into the track after being

nudged out of position. The unit was then placed back into test. The torque increased approximately 200 percent in test but then appeared to level off at this value. It is probable that the Flexure kinematics are still not optimum but vastly improved from that of the initial design. The increase in torque is anticipated to result from occasional light rubbing contact of a few Flexures from time to time with the face of the Idler Guide rails.

e) Low Voltage/High Current Tests - Throughout the test sequence just described the EU was subjected to current testing from 50 to 200 amps but always at a voltage level of <10 volts. The general procedure described in Appendix I was used as a baseline for conducting these tests. This procedure describes both the integration of the EU into the TF and the actual EU tests. Figure 19 is a photograph of the EU set-up on the TF ready for cabling into the TF terminals. Figure 20 is a photograph of the EU set up for Inner Housing temperature testing.

A considerable quantity of data was taken during these various tests in a number of configurations for both the original and the revised Flexure/Ring groove interface. The steady state temperature as well as the effective circuit resistance under current were essentially the same for both configurations. Table IX summarizes the resistance and steady state temperature measured during these tests. The raw data is available for review but is not included as a part of this report.

Tests "a" and "b" in Table IX were conducted to determine the Inner Housing temperature as well as the relationship of this temperature to rotation. Since the ball bearings provide the only thermal path from the Inner to the Outer Housing it was suspected that the effective thermal conductivity of the bearing might change with rotation. A thermocouple was attached to the Housing adjacent to Circuit Number 1. The two lead wires were brought out on upper circuits 7 and 8. The remaining six circuits were set-up in a series string to conduct current. The results of these tests show that the rotation of the Inner Housing introduces a temperature increase of the Housing of 6 to 8 percent. The temperature change at the Inner Ring is not known but assumed to be on the same order.

Tests "c" and "d" are typical of those taken to determine the influence of the number of active circuits upon the steady state temperature and the repeatability of the voltage drop, resistivity and temperature readings. As can be seen from the test summaries, these parameters are not only consistent from run to run but also indicate that the heat transfer of the Housing members does not saturate when all eight circuits are activated. The influence on the Inner Housing assembly is not known.

An attempt was made to measure the steady state temperature of all of the circuits with mixed success. The temperature readings tended to be inconsistent when more than one thermocouple was connected to the multiple pin header in the vacuum plate. These readings showed a reduced temperature on some of the circuits above circuit no. 1 and slightly greater temperature levels on others which did not seem consistent.

ORIGINAL PAGE IS
OF POOR QUALITY

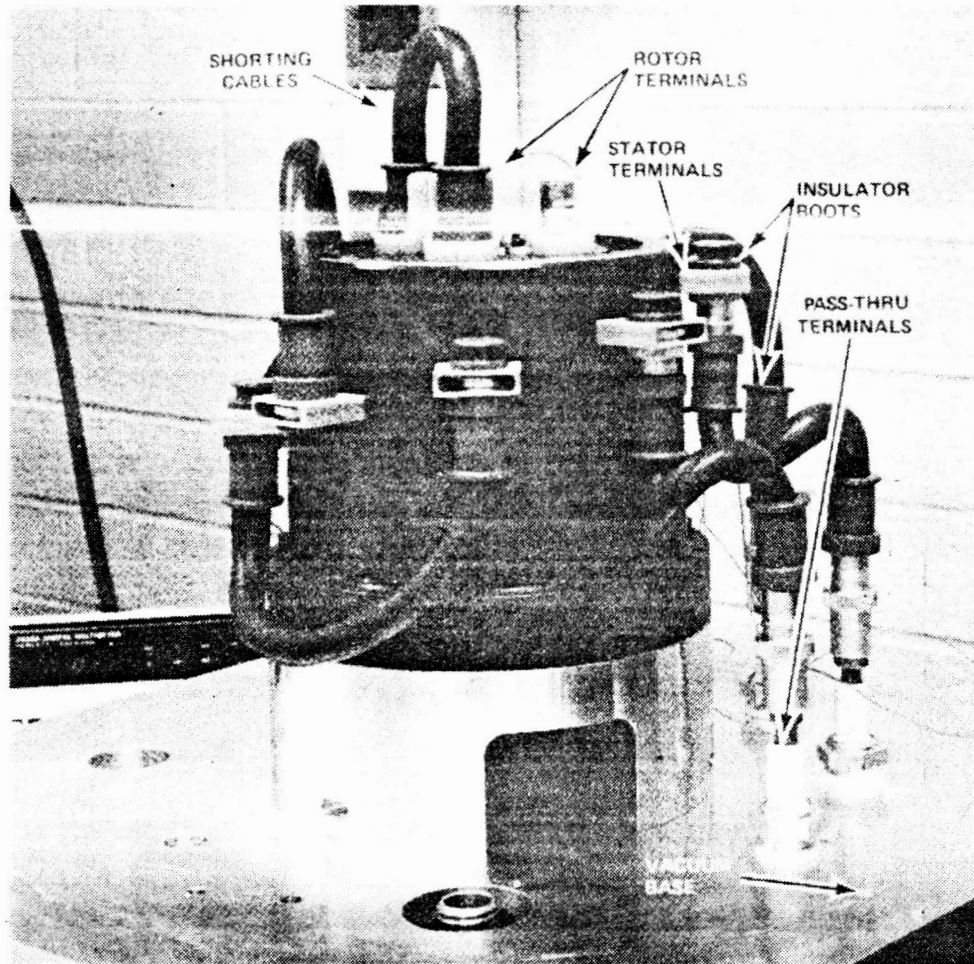


Figure 19

**Ro'l Ring Evaluation Unit
Mounted on Test Fixture**

ORIGINAL PAGE IS
OF POOR QUALITY

ROLL RING EVALUATION UNIT
SET-UP FOR TEMPERATURE TESTING

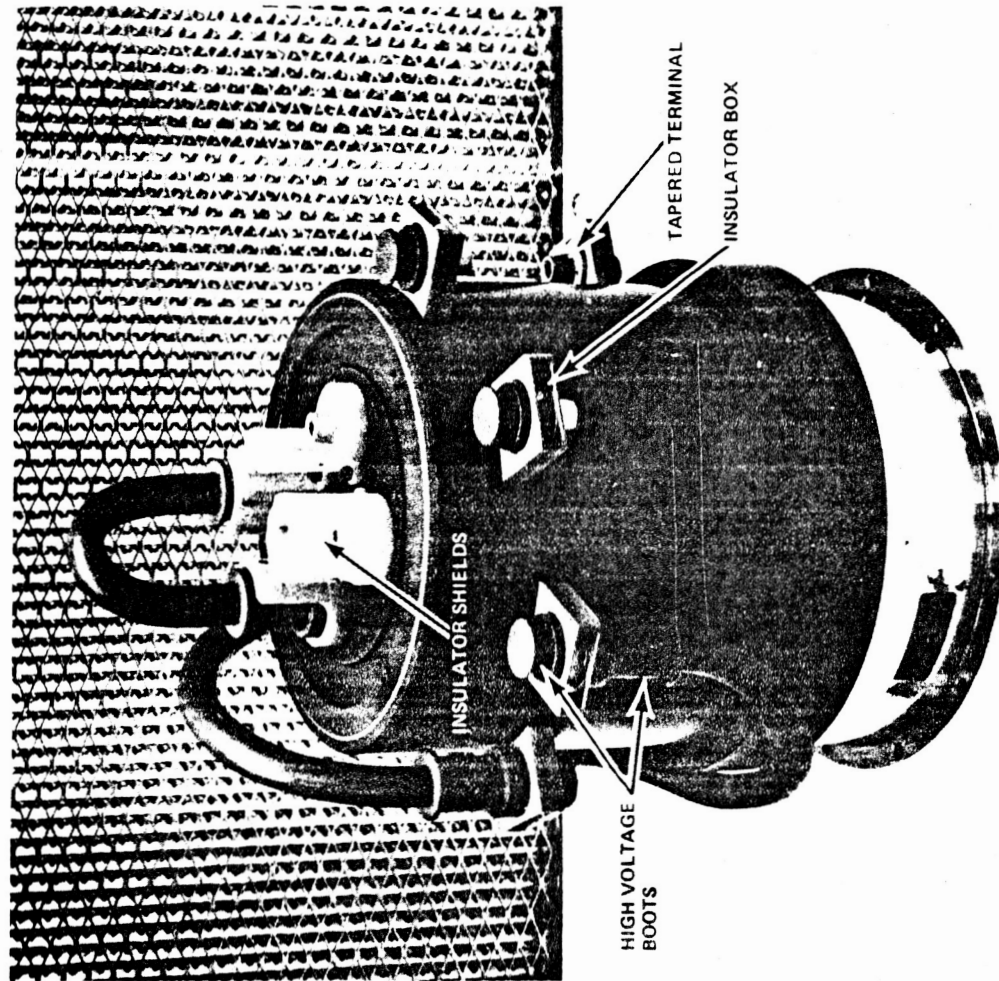


FIGURE 20

The power transfer efficiency, e_T , may be determined by reducing the power transferred across the EU by the " $I_C^2 R_T$ " losses such that

$$e_T = \frac{EI_T - I_C^2 R_T}{EI_T}$$

Figure 21 identifies the relationship of this transfer efficiency with the source voltage, E, for the EU for various power levels. The efficiency of transfer shown in the figure is unequalled by any other known transfer device. The efficiency for instance at a 250 volt source at a power level of 50KW is 99.96 percent which exceeds the specification requirement of 95.0 percent.

CIRCUIT	CURRENT (AMPS)	VOLTAGE DROP(mv)	DERIVED RESISTANCE (milli ohms)		STEADY STATE TEMPERATURE ($^{\circ}$ C)	
			AVERAGE	MODULATION	RING	HOUSING

a. Initial Configuration/Power on Circuits 1-6/Static

1	100	85.1	0.37	---	47	34
1	150	132.7	0.39	---	68	42
1	150	136.3	0.40	---	68	43
1	200	184.2	0.41	---	95	50
1	200	185.6	0.42	---	100	54

b. Initial Configuration/Power on Circuits 1-6/5 rev/min

1	50	42.0/43.9	0.38	± 0.02	31	28
1	100	86.9/90.4	0.39	± 0.02	47	36
1	150	134.5/138.1	0.40	± 0.01	70	46

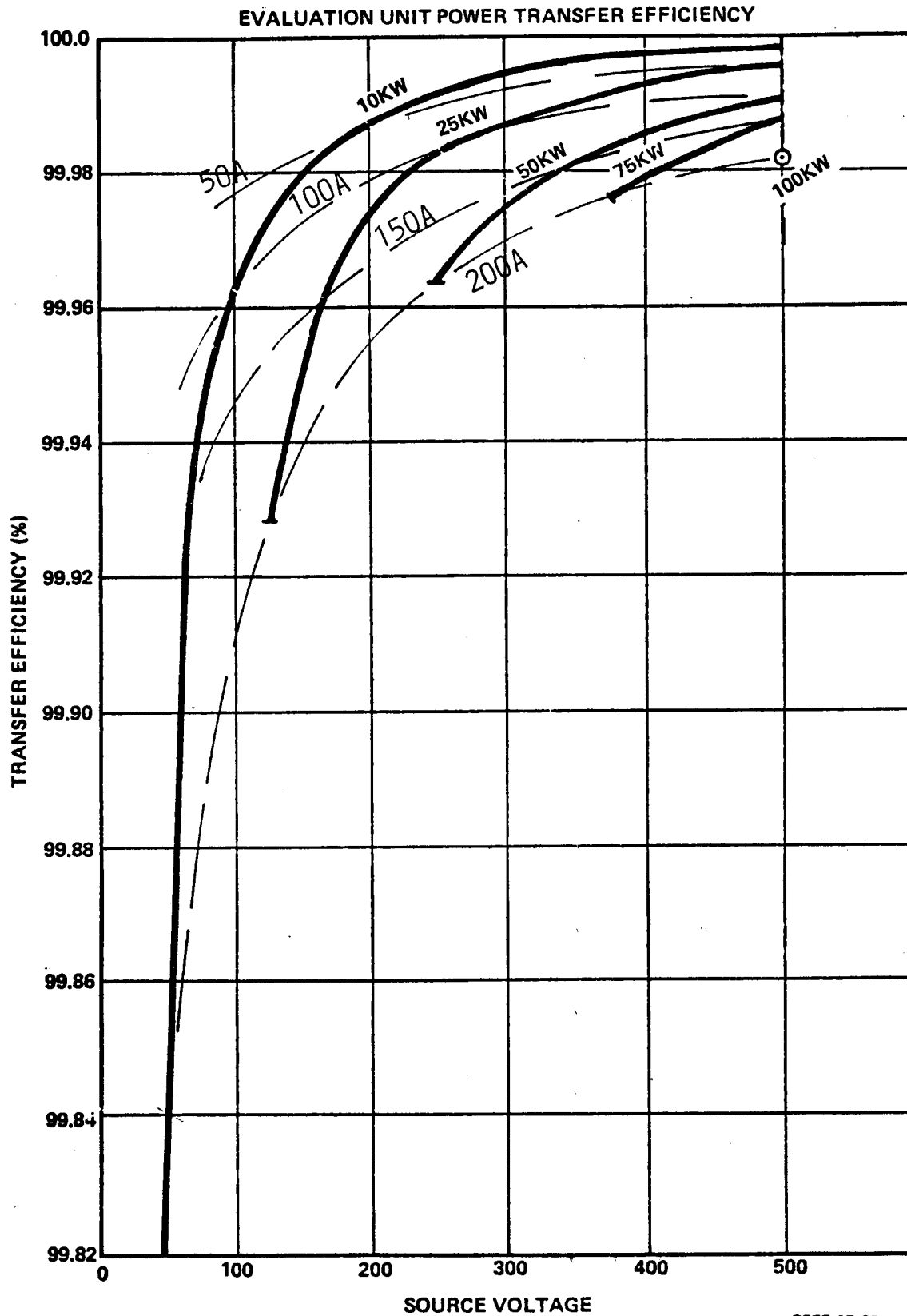
c. Initial Configuration/Power on Circuits 1 and 2/5 rev/min

2	154	150/158	0.45	± 0.03	74	---
2	154	150/160	0.45	± 0.03	73	---

d. Final Configuration/Power on all circuits/5 rev/min

1	152	138/143	0.41	± 0.02	65	---
1	151	139/142	0.41	± 0.01	69	---

RESISTANCE AND TEMPERATURE SUMMARY OF POWER TESTS
TABLE IX

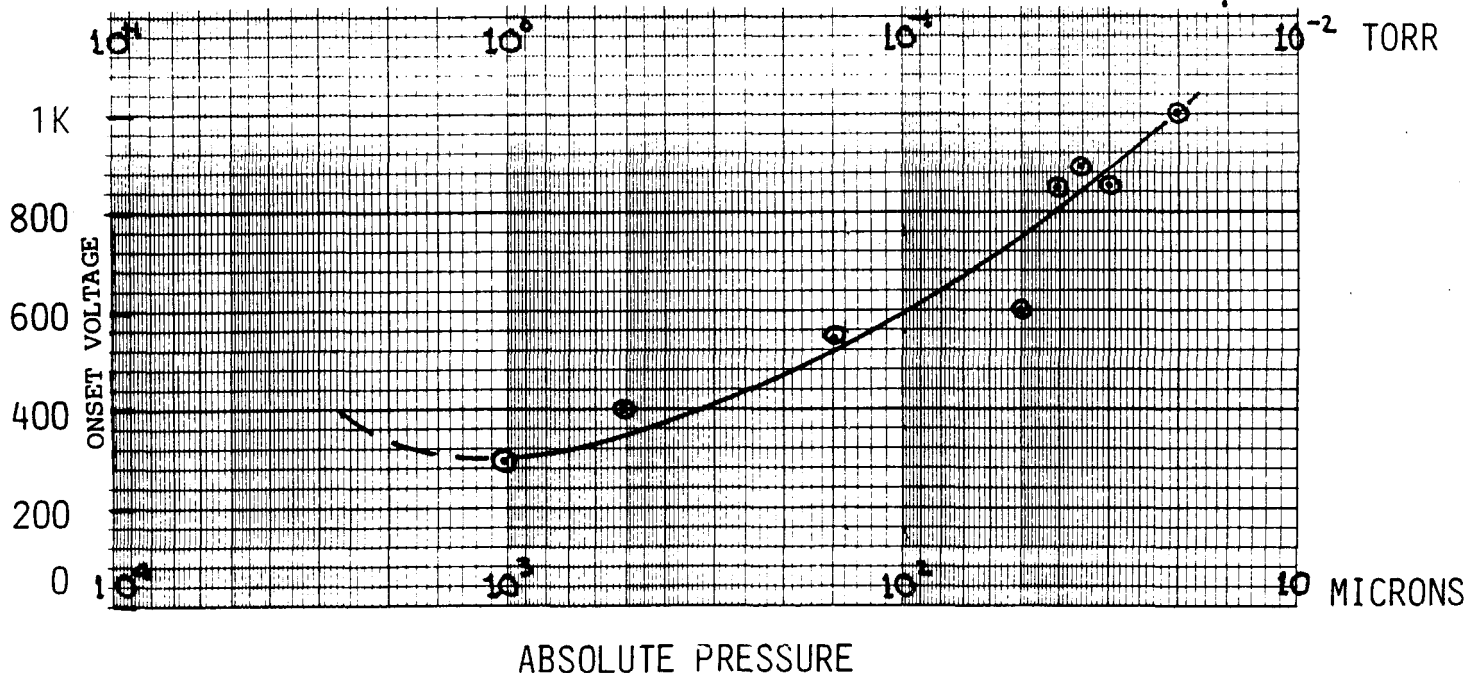


S855-05-29

f) High Voltage/Low Current Tests - After completing the high current tests the EU was subjected to 500 volt testing with a 250 ohm load resistor. The unit was wired with alternating polarity to impose a worst case scenario for potential voltage break-down and/or plasma generation. The unit was wired as follows: Power supply (+) to $1_S - 1_R - 3_S - 3_R - 5_S - 5_R - 7_S - 7_R$ to load resistor to $8_S - 8_R - 6_S - 6_R$ to power supply (-). The "S" and "R" subscripts denote stator and rotor respectively.

The unit was pumped down all night such that the chamber pressure was 2×10^{-3} Torr. The power supply was switched on and 500 volts was applied to the EU. The current was 1.8 amps. The unit was turned off to open the bell jar so that a loose monitor wire could be insulated. While pumping the chamber back down the power supply was again switched on and set at 500 volts. The pressure in the chamber was greater than 10^{-3} Torr so that the ionization gage was not operable. It is estimated from the time the valve had been open that the pressure was approximately 1000 microns (1mm Hg). A plasma abruptly formed in the chamber, the power supply surged to >10 amps and the breaker turned the unit off.

Since it was not anticipated that a plasma would form at a pressure as high as 1000 microns a set of tests were conducted to determine the relationship of the plasma on-set voltage with absolute pressure. A thermocouple gage (part of the TF) was used to monitor the pressure and the feedthrough header was used to determine plasma formation. A low current high voltage megohmmeter was used as the supply. One leg of the supply was attached to two pins on the header and the other leg of the supply was attached to the TF Base. The results of this test are plotted in Figure 2.2 below:



PLASMA ONSET VOLTAGE RELATED TO CHAMBER PRESSURE
FIGURE 22

The EU was disconnected from the load and supply and checked to determine the damage caused by the plasma. This check, revealed that although the insulation resistance to ground was $>2 \times 10^3$ M ohms at 10^3 volts circuits 1 and 2 were shorted together with a 10^3 ohm short even in air.

The unit was removed from the TF and disassembled to determine the source. It was determined that plasmas had formed internally at each of the Connecting Bolts at the points that the Bolts immersed from the clearance holes in Inner Rings 1 and 8. The plasma between the clearance hole in Inner Ring 1 had been severe enough as to burn through the insulation on the connecting bolt on circuit 2. The resulting metal ion transfer from the hole wall in the Ring to the connecting Rod resulted in a metallic build up which produced the short.

The sleeve insulators on the Connecting Rods were replaced with a more substantial Nylon tube Insulator and the EU was rewired so as to not impose the worst case polarity between adjacent circuits. Circuits 1 through 4 were assigned one polarity while circuits 5 through 6 were assigned the other. Figure I-2 of Appendix I identifies this wiring technique.

The EU was reassembled for the fourth time with these modifications and final performance checks were made. These checks, which included high current (150 amps at 8 volts) testing, high voltage insulation resistance measurements and high voltage testing in air, were all satisfactory. The high current test results were summarized as tests "d" in Table IX and the high voltage test results are summarized in Table X below. This is the configuration of the unit as it was shipped for full power testing at the Lewis Research Center.

<u>VOLTAGE</u>	<u>CURRENT</u> (Amps)	<u>VOLTAGE DROP</u> (MV) 1-3	<u>DERIVED RESISTANCE</u> (Milliohms)
100	0.4	0.3	0.32
200	0.8	0.6	0.32
300	1.1	0.95	0.38
400	1.5	1.3	0.38
500	1.85	1.6	0.38

SUMMARY OF HIGH VOLTAGE TESTING IN AIR # 5RPM
TABLE X

3. CONCLUSIONS AND RECOMMENDATIONS

It is concluded that although a number of problems had to be solved during the development of this first multi-hundred kilowatt rotary power transfer device, these problems were all of a design "learning curve" type. None of the problems are believed to be of a state-of-the-art level. The high voltage plasma breakdown was more a result of lack of familiarity with testing at high voltage in vacuum than of design inadequacy. Some of the latter was true, however, which dictates that a design change at the terminations would increase the operating margin. Power transfer at levels and efficiencies never before achieved have been demonstrated. It now remains to demonstrate how long this efficiency of transfer can be maintained.

It could also be concluded that the EU as it is presently configured could be used to test at current and voltage levels of up to 200 amps and 500 volts simultaneously provided that the proper testing procedures for vacuum are followed.

Although the torque levels and life are anticipated to be acceptable for future testing additional development in the area of Flexure/Idler/Ring groove relationships is required to properly understand the mechanisms involved. Another design related area of uncertainty is the effect of multi-circuits on axial dimensional stack-up and associated clearance effects with and without temperature.

A set of recommendations can be made based upon the results of the EU/TF development.

- a) Power testing of the EU should be gradually increased from approximately 50 amps to 200 amps at a potential of 200 volts or less prior to initiating higher voltage testing.
- b) Since the present configuration of the EU and the TF does not represent an application from the standpoint of heat transfer from both Housings, the maximum allowable operating power based on temperature should be adjusted accordingly.
- c) Testing at levels of 250 volts or more should only be conducted at standard pressure or at an absolute pressure of $<10^{-4}$ Torr.
- d) When testing the EU at a potential >250 volts the EU should be allowed to outgas in stages as the unit heats up to prevent setting up localized zones within the EU which could support a plasma.
- e) The EU should be evaluated for the transfer of both DC and AC power since there are no known bars to the transfer of AC current at almost any frequency.
- f) A set of design/tests should be conducted in which the stability of the Flexures is optimized by way of the Flexure/Ring groove interface design.

g) Future units utilizing many circuits should provide greater internal clearances to accomodate thermally induced strain especially in the axial direction.

h) A set of design/tests should be conducted in which further improvements of heat transfer between the current collector Rings and the Housings result. This would result in greater operating margins at maximum power levels.

REFERENCES

1. U.S. Patent Number 4,098,546, "Electrical Conductor Assembly".
2. U.S. Patent Number 4,372,633 "High Current Roll Ring Assembly".
3. Jacobson, Peter, High Voltage Rotary Power Transfer Device, paper presented at the 19th Intersociety Energy Conversion Engineering Conference, 19-24 August 1984, San Francisco, California.
4. Love, A.E.H., A Treatise on the Mathematical Theory of Elasticity, Dover Publications.
5. Smith, D.W., "Beryllium Copper Fatigue in Roll Ring Flexure Configurations", Sperry Roll Ring Tech Report No. 7, 25 February 1982.
6. Porter, R.S., "Determination of Flexure Deflection for a Standard Roll Ring Redundant Interface", Sperry Roll Ring Tech Report No. 9, 1 July, 1981.
7. Barkin, P. and Tuohy, E. J., "A Contact Resistance Theory for Rough Hemispherical Silver Contacts in Air and in Vacuum", IEEE Trans. PAS84, No. 12, December 1965, pp 1132-1149.
8. Sperry computer program, "BBLOAD".
9. Roark, R.J., "Formulas for Stress and Strain", Mc Graw Hill Book Co., 4th Edition, 1965, Table X, Case 20, p 222.

APPENDIX A

FLEXURE BENDING STRESS & STIFFNESS

APPENDIX A

FLEXURE BENDING STRESS AND STIFFNESS

Bending Stress

The bending stress distribution of a preloaded flexure is as shown in Figure A-1 below. The magnitude of this stress may be determined (4) by assuming the flexure is a thin elastic ring deformed in a single plane by equal and opposite forces F_R . The radial deflection, Y_R , is related to the location angle, θ , taken from the normal load, F_R , by:

$$Y_R = \frac{F_R r^3}{E_1 I} \left[-\frac{1}{\pi} + \frac{\sin \theta}{4} + \frac{\pi \cos \theta}{8} - \frac{\theta' \cos \theta}{4} \right] \quad (A - 1)$$

NOTE: Y_R = half of the total deflection and is + toward the centerline.

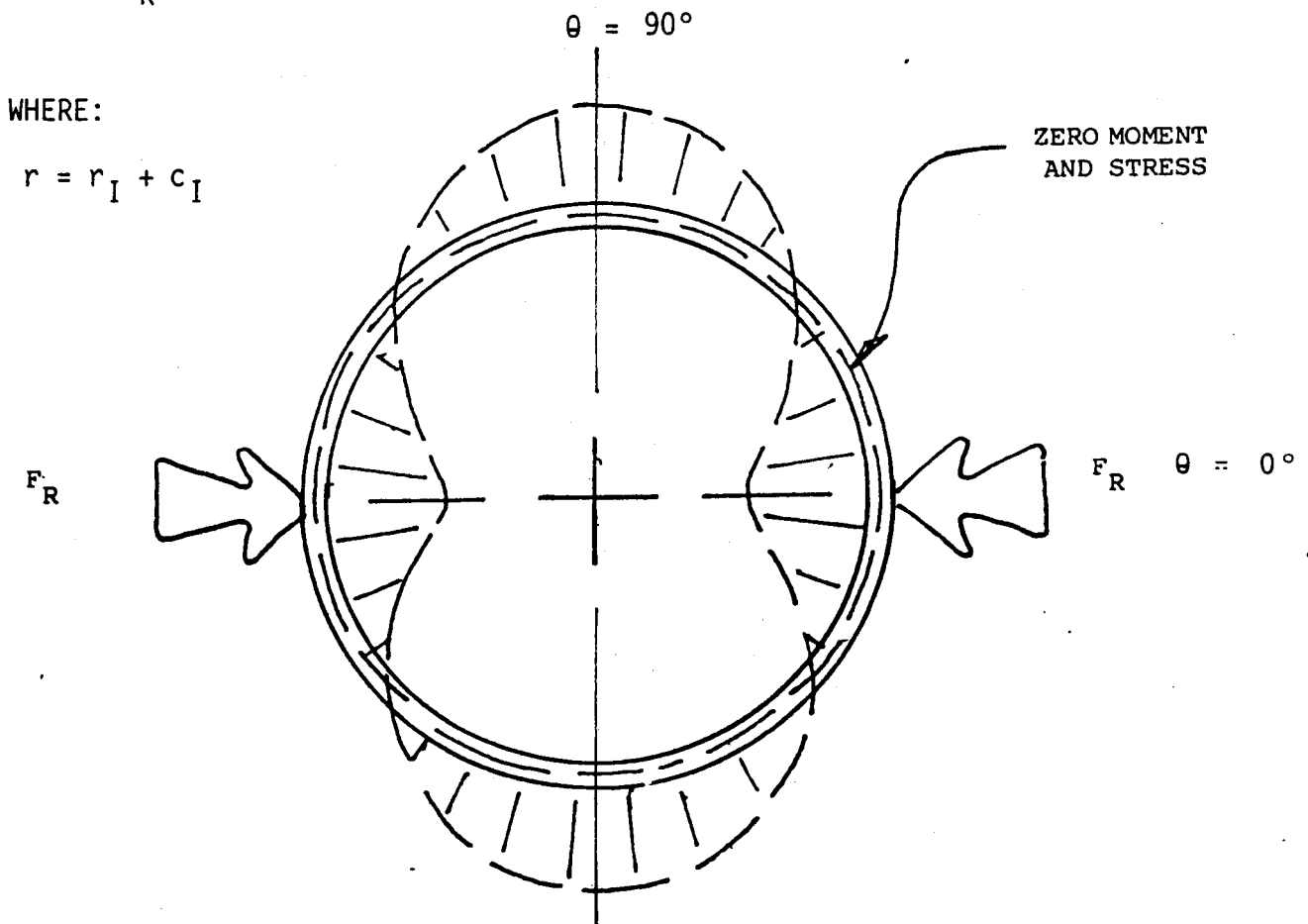


FIGURE A-1 - FLEXURE PRELOAD AND BENDING STRESS DISTRIBUTION

The bending moment, M, is related as follows:

$$M = F_R r \left[\frac{\sin \theta}{2} - \frac{1}{\pi} \right] \quad (A-3)$$

The bending stress at the load point, $\rho_{B/0}$, is related to the moment, M, by:

$$\begin{aligned} \rho_{B/0} &= \frac{MC}{I} \quad \theta = 0 \\ &= \frac{-0.318 F_R r c_I}{I} \quad \text{at the inside fiber} \quad (A-4) \\ &\quad \quad \quad (- \text{ denotes tension}) \end{aligned}$$

$$= \frac{0.318 F_R r c_O}{I} \quad \text{at the outside fiber} \quad (A-5)$$

and the stress at the free loop, $\sigma_{B/90}$

$$\begin{aligned} \rho_{B/90} &= \frac{MC}{I} \quad \theta = 90 \\ &= \frac{0.182 F_R r c_I}{I} \quad \text{at the inside fiber} \quad (A-6) \\ &\quad \quad \quad (- \text{ denotes tension}) \end{aligned}$$

$$= \frac{-0.182 F_R r c_O}{I} \quad \text{at the outside fiber} \quad (A-7)$$

Bending Stiffness

The effective flexure stiffness, K, may be derived from the deflection equation (A-1) by letting $\theta = 0 = 180^\circ$:

$$\begin{aligned} K &= \frac{F_R}{2Y_R} \quad \theta = 0 \\ &= \frac{6.7214 E_1 I}{r^3} \quad (A-8) \end{aligned}$$

SECTION SECOND MOMENT

The second moment of the Flexure section may be derived by deriving the second area moment about the flexure minor radius center (axis X-X) and transposing to the neutral axis 0-0. Reference is made to Figure A-2 for this analysis.

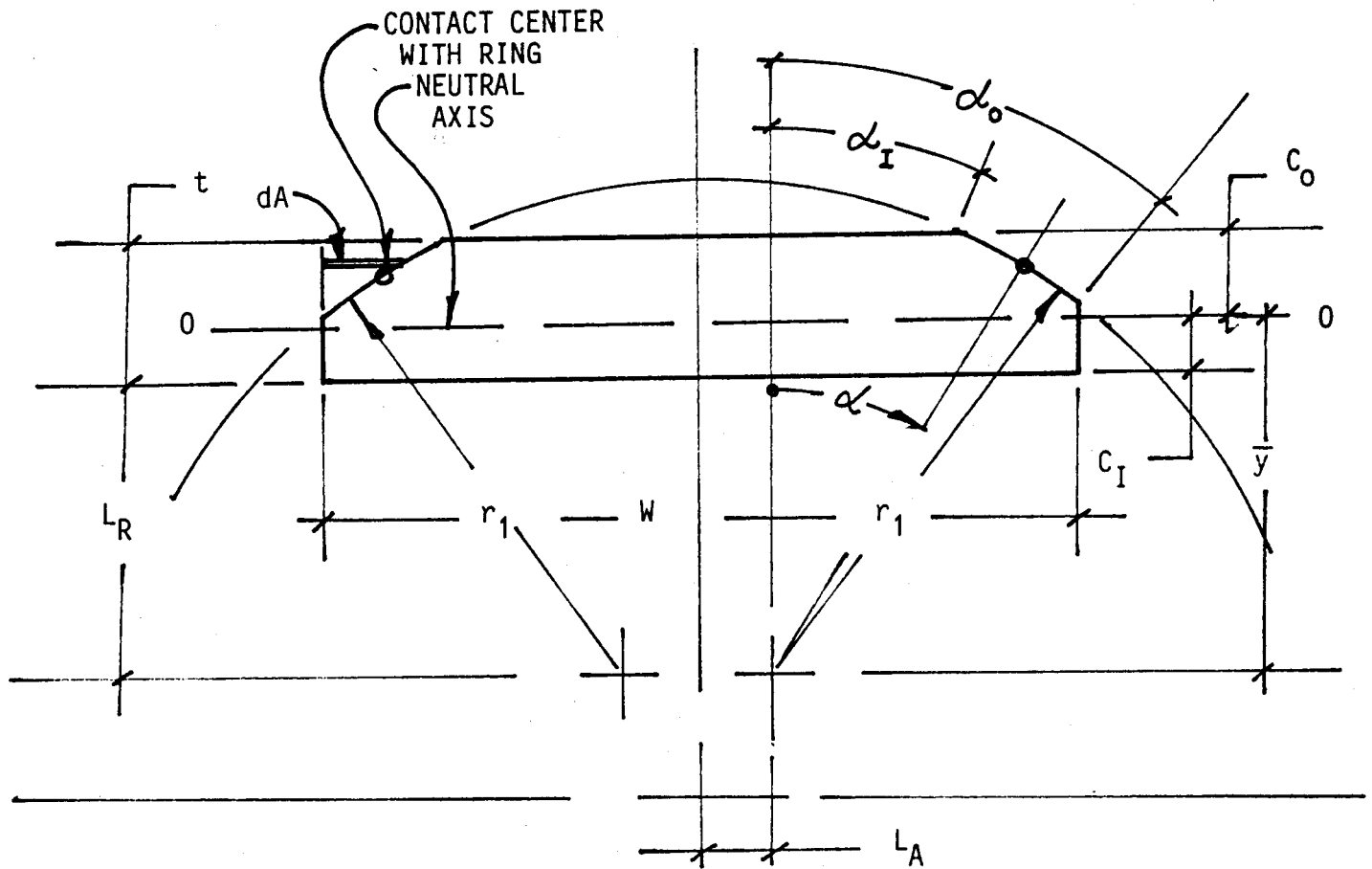


FIGURE A-2 CROSS SECTION OF FLEXURE

The cross section area of the Flexure, A , may be derived by subtracting the two corner areas from the total rectangular area as follows:

$$X = L_R r_1 \sin \alpha \quad (A-9)$$

$$Y = r_1 \cos \alpha \quad (A-10)$$

$$dy = -r_1 \sin \alpha \quad (A-11)$$

$$\begin{aligned} da &= r_1 (\sin \alpha_0 - \sin \alpha) dy \\ &= r_1^2 (\sin^2 \alpha - \sin \alpha \sin \alpha_0) d\alpha \end{aligned} \quad (A-12)$$

and

$$A_F = w t - 2 \int_{\alpha_0}^{\alpha_I} r_1^2 (\sin^2 \alpha - \sin \alpha \sin \alpha_0) d\alpha$$

$$= w t - r_1^2 (\alpha_I - \alpha_0 - 0.5 \sin 2\alpha_I + 0.5 \sin 2\alpha_0 + 2 \cos \alpha_I \sin \alpha_0) \quad (A-13)$$

The first area moment about axis X-X may be derived from equations A-10 and A-12:

$$\begin{aligned}
 yA &= wt(L_R + t/2) - 2r_1^3 \int_{\alpha_0}^{\alpha_I} (\cos \alpha \sin^2 \alpha - \cos \alpha \sin \alpha \sin \alpha_0) d\alpha \\
 &= wt(L_R + t/2) - r_1^3 [2\sin^3 \alpha_I + \sin^3 \alpha_0 - 3\sin^2 \alpha_I \sin \alpha_0] \quad (A-14)
 \end{aligned}$$

The second area moment about axis X-X may also be derived from equations A-10 and A-12:

$$\begin{aligned}
 y^2 A &= I_{xx} \\
 &= wt \left[(L_R + t/2)^2 + t^2/12 \right] - 2r_1^4 \int_{\alpha_0}^{\alpha_I} (\cos^2 \alpha \sin^2 \alpha - \cos^2 \alpha \sin \alpha \sin \alpha_0) d\alpha \\
 &= wt \left[(L_R + t/2)^2 + t^2/12 \right] - r_1^4/12 \left[3(\alpha_I - \alpha_0) + 3\sin^3 \alpha_I \cos \alpha_I - \right. \\
 &\quad \left. 3\sin \alpha_I \cos^3 \alpha_I + 8\sin \alpha_0 \cos^3 \alpha_I - 5\sin \alpha_0 \cos^3 \alpha_0 - 3\sin^3 \alpha_0 \cos \alpha_0 \right] \quad (A-15)
 \end{aligned}$$

The neutral axis of the section is located at a distance, \bar{y} from the axis X and may be determined from equation A-13 and A-14:

$$\bar{y} = \frac{yA}{A_F} \quad (A-16)$$

The inertia about the neutral axis, I, may be derived from the relationships governing area translations which are equations A-13, A-15 and A-16:

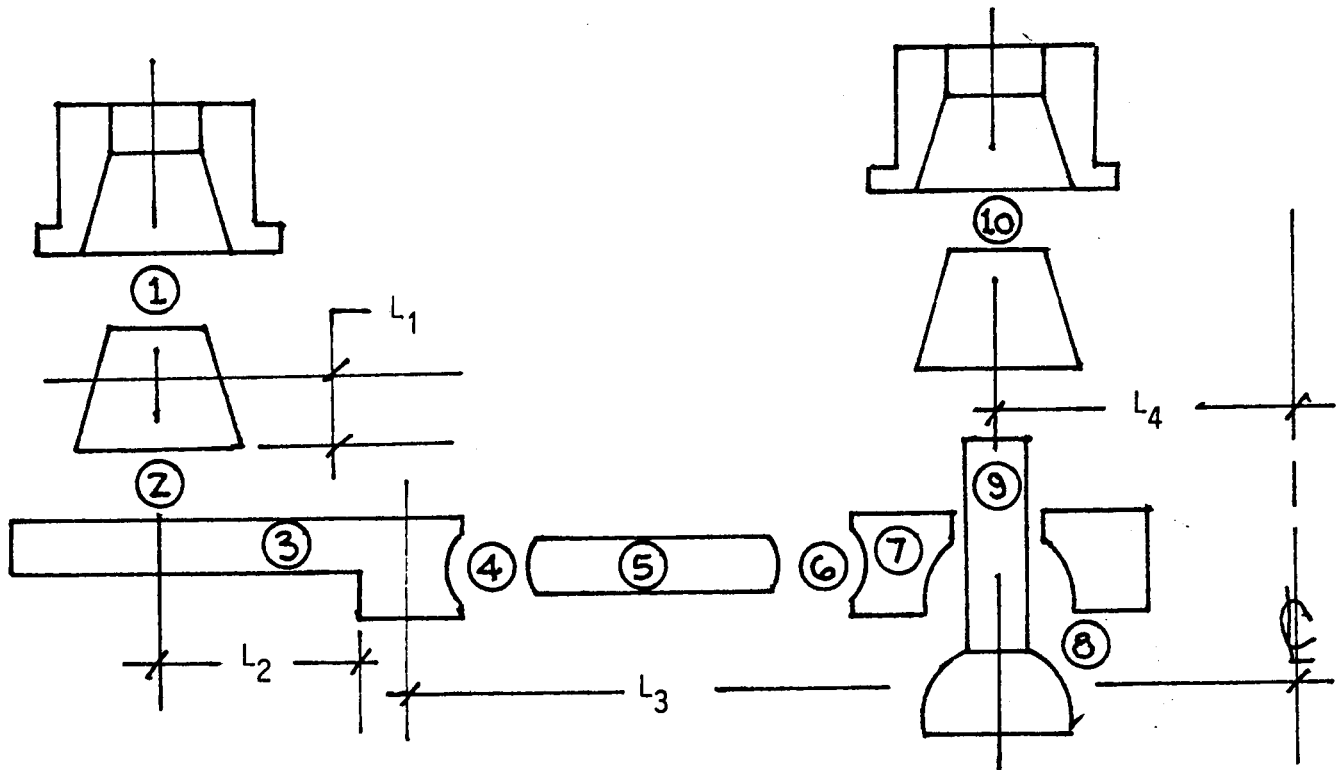
$$\begin{aligned}
 I &= I_x - A_F \bar{y}^2 \\
 &= y^2 A - A_F \bar{y}^2 \quad (A-17)
 \end{aligned}$$

APPENDIX B
CIRCUIT RESISTIVITY ANALYSIS

APPENDIX B

CIRCUIT RESISTIVITY ANALYSIS

The terminal-to-terminal resistance of each circuit may be derived by considering the total parallel path. Referring to the equivalent circuit below the resistance elements may be assigned:



$$R_1 = \frac{\rho_{TC} L_1}{A_1}$$

Where:

ρ_{TC} = Resistivity of tellurium copper = $\left(\frac{101}{93}\right) 1.724 = 1.87 \mu \text{ ohm cm}$

L_1 = Mean length of terminal to centroid of cone.
= 0.370 in

A_1 = Effective cross sectional area

$$= \frac{\pi}{4} \left[(0.5)^2 - (0.25)^2 \right]$$

$$= 0.147 \text{ in}^2$$

$$R_1 = \frac{(1.87 \times 10^{-6})(0.37)}{(0.147)(2.54)} = 1.8 \times 10^{-6} \text{ ohm}$$

$$R_2 = 0$$

R_3 consists of the parallel paths $R_{(n)}$ (where "n" represents the 10 flexure contacts) in series with the tab resistance R_T .

$$R_T = \frac{L_2 \rho_B}{A_2}$$

Where:

$$\rho_B = \text{Resistivity of leaded brass} = 6.63 \times 10^{-6} \text{ ohm cm}$$

$$L_2 = \text{The effective length from the tab/cone mounting center to the outer ring OD.}$$

$$= 0.80 \text{ in.}$$

$$A_2 = \text{Cross section area of tab}$$

$$= (0.94)(0.15)$$

$$= 0.14 \text{ in}^2$$

$$\& R_T = \frac{(6.63 \times 10^{-6})(0.80)}{(0.14)(2.54)} = 14.9 \times 10^{-6} \text{ Ohm}$$

$$R_{(2)} = \frac{2L_3 \pi \rho_B}{10A_3}$$

Where:

$$L_3 = \text{Mean radius of outer ring}$$

$$= 3.1 \text{ in.}$$

$$A_3 = \text{Outer ring cross section}$$

$$= (0.2)(0.28)$$

$$= 0.056 \text{ in}^2$$

$$R_{(2)} = \frac{(2)(3.1) \pi (6.63 \times 10^{-6})}{(10)(0.056)(2.54)} = 90.8 \times 10^{-6} \text{ Ohm}$$

Since there are 2 $R_{(2)}$ paths the equivalent $R_{(2)}$ path resistance $R'_{(2)}$ is:

$$R'_{(2)} = 45.4 \times 10^{-6} \text{ ohm}$$

In a similar manner

$$R'_{(3)} = \left(\frac{2L_3 \pi \rho}{10A_3} \right) \left(\frac{2}{2} \right) = 90.8 \times 10^{-6} \text{ ohm}$$

$$R'_{(4)} = \left(\frac{2L_3 \pi \rho}{10A_3} \right) \left(\frac{3}{2} \right) = 136.2 \times 10^{-6} \text{ ohm}$$

$$R'_{(5)} = \left(\frac{2L_3 \pi \rho}{10A_3} \right) \left(\frac{4}{2} \right) = 181.6 \times 10^{-6} \text{ ohm}$$

$$R'_{(6)} = \left(\frac{2L_3 \pi \rho}{10A_3} \right) \left(\frac{5}{2} \right) = 227 \times 10^{-6} \text{ ohm}$$

$$(R'_{(3)} + R'_{(4)}) = \frac{(90.8)(136.2)(10^{-6})}{90.8 + 136.2} = 54.5 \times 10^{-6} \text{ ohm}$$

$$(R'_{(5)} + R'_{(6)}) = \frac{(181.6)(227)(10^{-6})}{181.6 + 227} = 100.9 \times 10^{-6} \text{ ohm}$$

$$(R'_{(3)} + R'_{(4)} + R'_{(2)}) = \frac{(54.4)(45.4)(10^{-6})}{54.5 + 45.4} = 24.8 \times 10^{-6} \text{ ohm}$$

$$(R'_{(2)} + R'_{(3)} + R'_{(4)} + R'_{(5)} + R'_{(6)}) = \frac{(24.8)(100.9)(10^{-6})}{24.8 + 100.9} = 20 \times 10^{-6} \text{ ohm}$$

and

R_3 = Total outer ring resistance

$$= (15 + 20) \times 10^{-6}$$

$$= 35 \times 10^{-6} \text{ ohm}$$

R_4 = Total equivalent contact resistance at flexure/ring groove interface.

R_c = Resistance of each interface

$$= \frac{\rho_F + \rho_R}{4} \left(\frac{\pi}{A_c} \right)^{0.5} \quad (\text{Ref 7})$$

Where

ρ_F = Resistivity of flexure surface material

ρ_R = Resistivity of ring groove surface material

A_C = Contact area = $1.8 \times 10^{-4} \text{ in}^2$ (Ref 8)

Since $\rho_F = \rho_R = \rho_{\text{Gold}} = 2.2 \times 10^{-6} \text{ ohm cm}$

$$\begin{aligned} R_C &= \frac{\rho_{\text{Gold}}}{2} \left(\frac{\pi}{A_C} \right)^{0.5} \\ &= \frac{(2.2 \times 10^{-6})}{(2)(2.54)} \left[\frac{\pi}{1.8 \times 10^{-4}} \right]^{0.5} \\ &= 57.2 \times 10^{-6} \text{ ohm} \end{aligned}$$

and

$$R_4 = \frac{R_C}{2n} \quad \text{for 2 contacts/flexure}$$

Where

n = Number of flexures = 10

$$\begin{aligned} R_4 &= \frac{57.2 \times 10^{-6}}{(2)(10)} \\ &= 3 \times 10^{-6} \text{ ohm} \end{aligned}$$

R_5 = Resistance of flexures

R_F = Resistance of each flexure

$$= \left(\frac{\pi D_F \rho_F}{2A_F} \right) \frac{1}{2}$$

Where

$$D_F = \text{Flexure Diameter} = 1.28 \text{ in.}$$

$$\begin{aligned} A_F &= \text{Cross sectional area of flexure} \\ &= 2.26 \times 10^{-3} \text{ in}^2 \quad (\text{Appendix A}) \end{aligned}$$

$$\begin{aligned} \rho_F &= \text{Resistivity of Beryllium Copper flexure material} = 7.19 \times 10^{-6} \text{ ohm cm} \\ &= 1.26 \times 10^{-3} \text{ ohms} \end{aligned}$$

$$R_F = \frac{\pi (1.28)(7.19 \times 10^{-6})}{(2.54)(4)(2.26 \times 10^{-3})}$$

$$\begin{aligned} R_5 &= \frac{R_F}{n} \\ &= \frac{1.26 \times 10^{-3}}{10} \end{aligned}$$

$$= 126 \times 10^{-6} \text{ ohm}$$

$$R_6 \approx R_4 = 3 \times 10^{-6} \text{ ohm}$$

$$R_7 = \text{Resistance of the Inner Ring}$$

The worst case resistance is that of the number 4 and number 5 rings since these rings have the largest number of connecting bolt clearance holes. Each of these rings have 3 holes in addition to the tie bolt hole.

$$\begin{aligned} R_7 &= \left[\left(\frac{2 \pi L_4 \rho_7}{4A_7} \right) + \left(\frac{2 \pi L_4 \rho_7}{4A_7} \right) + \left(\frac{L_5 \rho_7}{A_7 - A_H} \right) \right] \frac{1}{2} \\ &= \frac{\pi L_4 \rho_7}{2A_7} + \frac{\pi L_5 \rho_7}{2(A_7 - A_H)} \end{aligned}$$

Where

$$\rho_7 = \text{Resistivity of leaded brass inner ring} = 6.63 \times 10^{-6} \text{ ohm cm}$$

$$L_4 = \text{Mean radius of Inner Ring} = 1.40 \text{ in}$$

$$A_7 = \text{Cross sectional area of inner ring}$$

$$= (0.38)(0.69)$$

B-5

$$= 0.26 \text{ in}^2$$

A_H = Cross sectional area of hole in inner ring

$$= (0.38)(0.44)$$

$$= 0.17 \text{ in}^2$$

L_5 = Effective length of hole restriction in inner ring

$$\approx 0.25 \text{ in}$$

$$R_7 = \frac{(1.4)(6.63 \times 10^{-6})}{(2)(0.26)(2.54)} + \frac{(0.25)(6.63 \times 10^{-6})}{2(0.26 - 0.17)}$$

$$= 22.1 \times 10^{-6} + 9.2 \times 10^{-6}$$

$$= 31 \times 10^{-6} \text{ ohm}$$

R_8 = Resistivity of spherical socket in inner ring

$$= \frac{\rho_{\text{GOLD}}}{2} \left(\frac{\pi}{A_S} \right)^{0.5}$$

Where

A_S = Socket contact area

$$= 2\pi R (R - \sqrt{R^2 - r_1^2} - R + \sqrt{R^2 - r_2^2})$$

$$= 2\pi R (\sqrt{R^2 - r_1^2} + \sqrt{R^2 - r_2^2})$$

$$r_1 = \sqrt{R^2 - a^2}$$

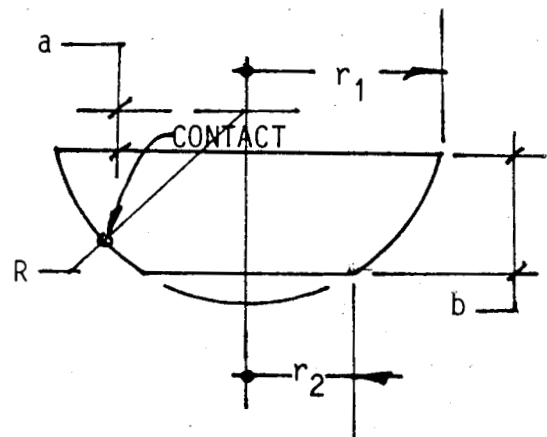
and

$$r_2 = \sqrt{R^2 - (a+b)^2}$$

$$\therefore A_S = 2\pi R(2a + b)$$

$$= 2\pi(0.23) [(2)(0.02) + 0.153]$$

$$= 0.28 \text{ in}^2$$



$$a = 0.235 \sin 5^\circ = 0.02$$

$$b = 0.153$$

$$R_8 = \frac{2.2 \times 10^{-6}}{(2)(2.54)} \left[\frac{1}{0.28} \right]^{0.5} = 1.5 \times 10^{-6} \text{ ohm}$$

R_9 = Total connector bolt resistance

$$= R_S + R_T$$

Where

R_S = Resistance of shank of bolt

R_T = Resistance of thread of bolt

Also

$$R_S = \frac{\rho_{TC} L_S}{A_S}$$

Where

L_S = Length of unthreaded shank length

A_S = Area of shank

$$= \frac{\pi D_S^2}{4}$$

D_S = Diameter of shank = 0.312 in.

$$A_S = \frac{\pi (0.312)^2}{4} = 0.077 \text{ in}^2$$

$$R_{S/in} = \frac{(1.87 \times 10^{-6})(1.0)}{(0.077)(2.54)} = 9.6 \times 10^{-6} \text{ ohm/in (Tellurium Copper)}$$

$$R_T = \frac{\rho_{TC} L_T}{A_T}$$

Where

L_T = Effective length of thread (to centroid)

$$= 0.25 \text{ in}$$

A_T = Area of thread at minor diameter, D_T

$$\begin{aligned}
&= \frac{\pi D_T^2}{4} \\
&= \frac{\pi (0.261)^2}{4} \\
&= 0.053 \text{ in}^2
\end{aligned}$$

And

$$R_T = \frac{(1.87 \times 10^{-6})(0.25)}{(0.053)(2.54)} = 3.5 \times 10^{-6} \text{ ohm}$$

And

$$R_9]_{\text{DN1}} = (0.81 - 0.77)(9.6 \times 10^{-6}) + 3.5 \times 10^{-6} = 3.9 \times 10^{-6} \text{ ohm}$$

$$R_9]_{\text{DN4}} = (2.58 - 0.77)(9.6 \times 10^{-6}) + 3.5 \times 10^{-6} = 21 \times 10^{-6} \text{ ohm}$$

$$R_{10} = R_1 = 1.8 \times 10^{-6} \text{ ohm}$$

$$R_S = \text{Total system resistance } (\mu\text{ohm})$$

$$= R_1 + R_2 + R_3 + R_4 + R_5 + R_6 + R_7 + R_8 + R_9 + R_{10}$$

$$= 1.8 + 0 + 35 + 3 + 126 + 3 + 31 + 1.5 + (4 \text{ to } 21) + 1.8$$

$$= 207 \mu \text{ ohm to } 224 \mu \text{ ohm}$$

APPENDIX C
DIAPHRAGM DESIGN ANALYSIS

APPENDIX C

DIAPHRAGM DESIGN

Assume a fixed/fixed diaphragm with outer radius "a" and inner radius "b".
The axial deflection, y, is:

$$y = \frac{3W(m^2 - 1)}{4\pi m^2 E t^3} \left[a^2 - b^2 - \frac{4a^2 b^2}{a^2 - b^2} \left(\ln \frac{a}{b} \right)^2 \right] \quad (\text{Ref 9})$$

where:

W = Axial (central) force

E = Material elastic modulus

t = Diaphragm thickness

m = $\frac{1}{\nu}$

ν = Poissons ratio

a = 3.15 in

b = 2.625 in

m = $\frac{1}{0.3} = 3.3$

E = 30×10^6 LB/IN² (17-4PH)

t = 0.012 in

K' = Axial compliance

= $\frac{y}{W}$

$$= \frac{(3) [(3.3)^2 - 1]}{4\pi (3.3)^2 (30 \times 10^6) (0.012)^3} \left[(3.15)^2 - (2.625)^2 - \frac{(4)(3.15)^2 (2.625)^2}{(3.15)^2 - (2.625)^2} \left(\ln \frac{3.15}{2.625} \right)^2 \right]$$

$$= 4.18 \times 10^{-3} [9.9225 - 6.8906 - (90.2035)(0.03324)]$$

$$= 1.40 \times 10^{-4} \text{ IN/LB}$$

$$\equiv 7.16 \times 10^3 \text{ LB/IN}$$

$$P_0 = \frac{3W}{2\pi t^2} \left[1 - \frac{2b^2}{a^2 - b^2} \left(\ln \frac{a}{b} \right) \right] \quad (\text{Ref 9})$$

$$\rho_o \left[\begin{array}{l} = \frac{(3)(10)}{2\pi(0.012)^2} \left[1 - \frac{2(2.625)^2}{(3.15)^2 - (2.625)^2} \left(\ln \frac{3.15}{2.625} \right) \right] \\ W = 10 \text{ Lb} \\ = 5,679 \text{ LB/IN}^2 \end{array} \right]$$

$$\rho_I = \frac{3W}{2\pi t^2} \left[1 - \frac{2a^2}{a^2 - b^2} \left(\ln \frac{a}{b} \right) \right] \quad (\text{Ref 9})$$

$$\rho_I \left[\begin{array}{l} = \frac{(3)(10)}{2\pi(0.012)^2} \left[1 - \frac{2(3.15)^2}{(3.15)^2 - (2.625)^2} \left(\ln \frac{3.15}{2.625} \right) \right] \\ W = 10 \text{ LB} \\ = -6411 \text{ LB/IN}^2 \end{array} \right]$$

Let $t = 0.008$ in

$$K^1 = \left(\frac{0.012}{0.008} \right)^3 1.40 \times 10^{-4} = 4.7 \times 10^{-4} \text{ IN/LB}$$

$$\& K = 2,116 \text{ LB/IN}$$

Max stress is at hole:

$$\rho_I \left[\begin{array}{l} = \left(\frac{0.012}{0.008} \right)^2 (6411) = 14,425 \text{ LB/IN}^2 \\ W = 10 \text{ LB} \end{array} \right]$$

If $y = 0.010 \text{ IN} \pm 0.002$

$$\text{Min } W = (2116)(0.008) = 17 \text{ LB}$$

&

$$\text{Min } \rho_I = \frac{17}{10} (14,425) = 24.5 \text{ K LB/IN}^2$$

&

$$\text{Max } W = (2116)(0.012) = 25.4 \text{ LB}$$

&

$$\text{Max } \rho_I = \frac{25.4}{10} (14,425) = 36.6 \text{ K LB/IN}^2$$

APPENDIX D

HIGH POWER ROLL RING
SINGLE CIRCUIT HEAT
TRANSFER OPTIMIZATION
TEST PROCEDURE 5240-080741

SINGLE CIRCUIT TEST

Objective - The objective of this set of tests is to provide actual thermal mapping of key areas of the high power roll ring module resulting from self heating effects while conducting 150 amp and to select an optimum heat transfer shim thickness and interface configuration.

- a) Disassemble test set-up on Turbo Pump baseplate.
- b) Seal-off vacuum throat with plate and "Duc Seal".
- c) Locate area on base plate which provides 100% area contact with Base PN 072041 and drill and tap three 3/8-24UNF-2B 0.50 deep holes on 6.250 dia circle. (These holes would be 5.413 inches apart). Chamfer leading edge of threaded holes to assure that no protrusions exist. Remove seal.
- d) Secure Base to base plate with three 3/8 - 24 cap screws 3 inches long. Apply thin film of Andok "C" grease to interface prior to attachment.
- e) Assemble single circuit High Power Roll Ring (HPRR) module with bearings lightly preloaded. Use special Inner Housing PN 5240-050341 and Clamping Plate PN 5240-050342 for this unit. Roller Guide PN 5240-050447 and Housings PN 5240-052445 and 5240-050341 are to be un-coated.
- f) Attach thermocouples to module components as shown in Figure 1 locations A-K using Bacon Labs LCA-4 adhesive. Clarification of these locations is as follows:

<u>Location</u>	<u>Description</u>	<u>Lead Dressing</u>	<u>Header Pins</u>
A	Inner Housing wall centered on ring adjacent to other thermocouples	Out bottom thru slot in base	A1,2
B	Outer surface of Spring PN 5240-051041-2 on inboard convolution	Out top thru hole in Plate PN 5240-050342	A3,4
C	Inner surface of Spring on outboard convolution	On top through hole in plate	A5,6
D	On wall of 0.437 dia hole in Ring PN 5240-011842A	Out top thru hole in Barrier PN 5240-050446 and Guide PN 5240-050447	A7,8
E	On ID of Flexure PN 5240-011843 at center of Idler and Inner Ring contact span	Out top thru hole in Guide and under Barrier	B1,2

F	On tab of Outer Ring PN 5240-011841 on offset side just outside spring OD	Out windows in Housing and Insulation PN 5240- 050843	B3,4
G	Outer surface of spring PN 5240-051041-1 on inboard convolution	Out windows in Housing and Insulator	B5,6
H	Inboard surface of spring on outboard Convolution	Out windows in Housing and insulator	B7,8
I	Outer Housing wall centered on ring adjacent to other thermocouples	(none required)	C1,2
J	Inner Housing lower cavity adjacent to upper bearing	Out bottom thru slot in Base	C3,4
K	Bearing hub OD of Bearing Housing PN 5240-050744	Out bottom thru slot in base	C5,6

NOTE: Attach copper to "odd" numbered pins.

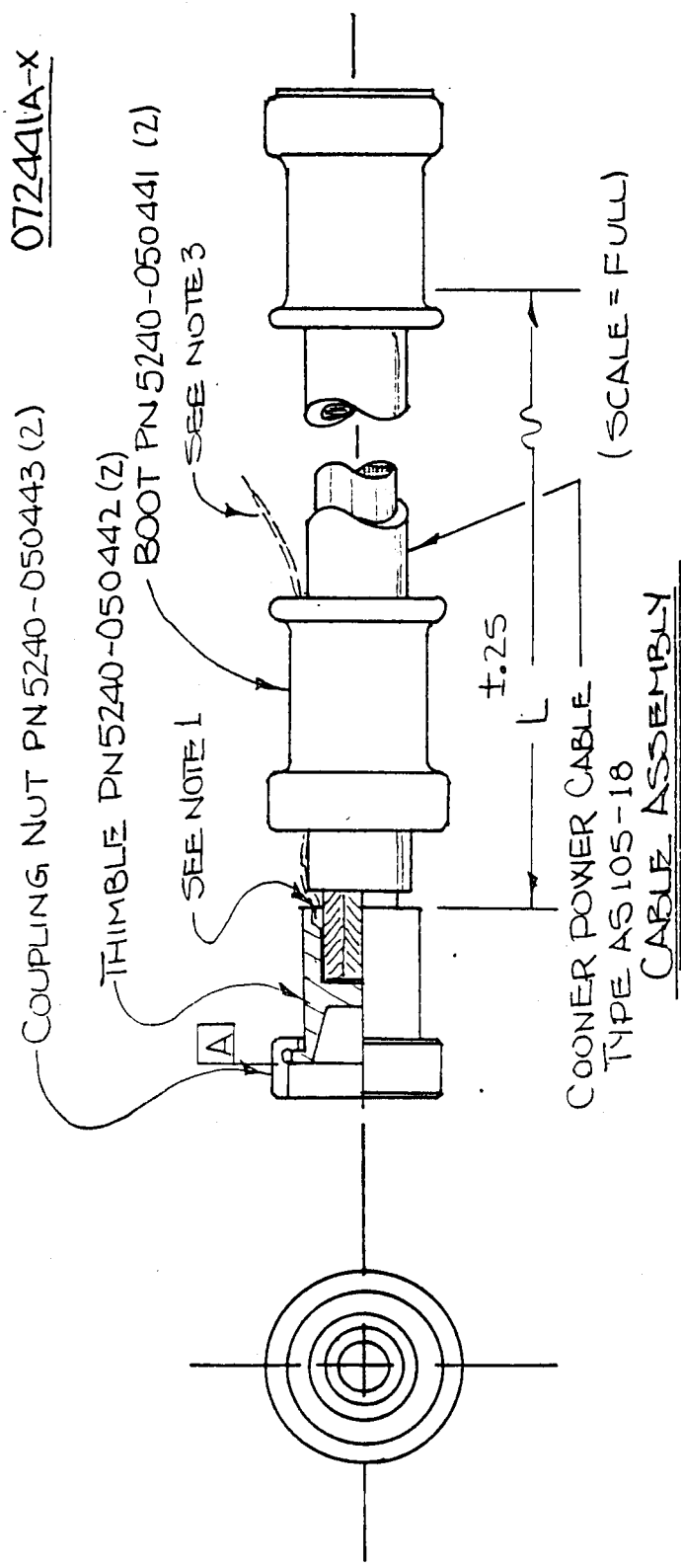
- g) Mount assembly to Base with twelve 10-32 cap screws 1 1/4 inches long.
- h) Construct two cables of appropriate length per Cable Assembly PN 072441-X except one end to terminate into soldered flat connector compatible with feed-throughs in vacuum plate.
- i) Attach cables to Contact Cones PN 5240-050741 and feed thru and connect thermocouple leads to header in baseplate. (Refer to paragraph 6)
- j) Attach two #22 AWG lead wires on each power cable to header pins D1 - D4 in base plate.
- k) Make external connections to resistive load and high current power supply. connect thermocouple lead-wires to A-K pairs maintaining copper-copper and constantine-constantine matching. (Refer to paragraph f)
- l) Mount bell-jar and pump down system to 10^{-3} Torr. (Mechanical pump only)
- m) Power-up system and measure steady state temperature at points A-K at 150 Ampere reference current. Maintain the current throughout the test by adjusting the power supply voltage as the unit heats up and the resistance increases. Temperature readings are to be taken at 15 minute intervals over the first 60 minutes of test and at 30 minute intervals thereafter. The refrigeration cycle of the Turbo Pump is to be operated during these tests to maintain the Vacuum Base at room temperature. This test step will require an 8 hour time period.

- n) Measure the voltage drop across the terminal cones using cable lead wire connections. Calculate the resistance of the circuit by dividing the instantaneous voltage drop by the associated current.
- o) Repeat steps "m" and "n" for various Shim thicknesses, two and three parallel Wave Springs PN 5240-051041-1 and -2, Insulator PN 5240-050843 with external pores sealed with materials such as Vacuum Grease, Torr Seal epoxy and copper plating and segmented shims (one per Spring convolution).
- p) Select the configuration which results in a minimum temperature of the highest temperature component. (Usually the Flexure PN 5240-011843)

APPENDIX E

CABLE ASSEMBLY DETAILS

PN 5240-072441-X

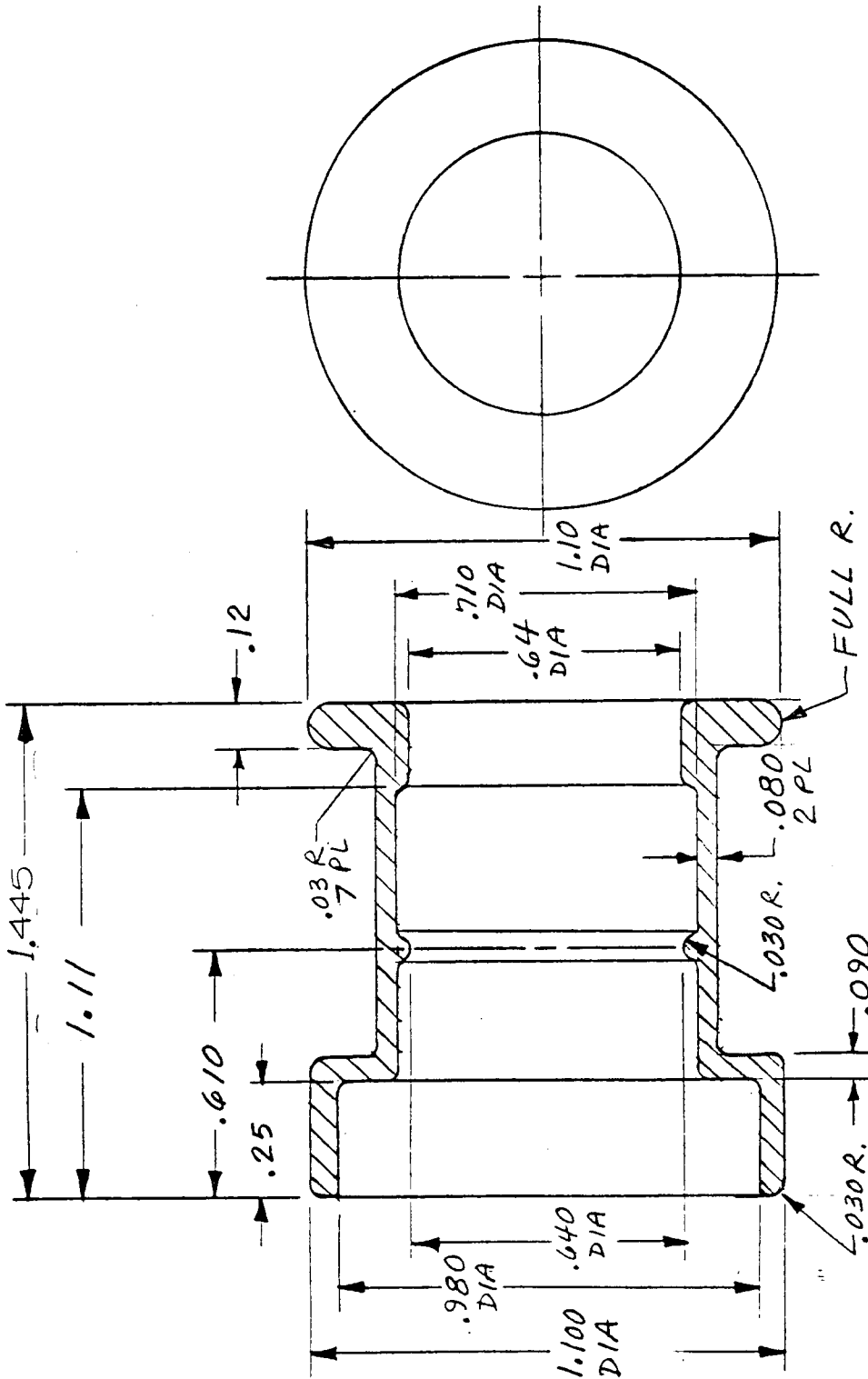


NOTES:

1. ASSEMBLE COMPONENTS AS SHOWN IN SECTIONAL VIEW. SLIDE "COUPLING NUT" BACK ON "THIMBLE" SUCH THAT SURFACE **A** MAY BE APPLIED TO HOT PLATE AT 400/450°F. APPLY SOLDER AT CAVITY PROVIDED UNTIL CUP IS FULL. FORM COMPLETE MENISCUS AT ENTRY. USE 60/40 TIN/LEAD SOLDER (89-003) WITH 2.2% ROSEN CORE PER M. 690,452-1.
2. STRIP 0.562 INSULATION FROM CABLE PRIOR TO SOLDERING.
3. ATTACH #22 AWG LEAD 20" LONG TO THIMBLE AT CUP FILLER CAVITY (RED INSULATION) ON DOUBLE DASH NUMBER UNITS. FEED LEAD UNDER BOOT AS SHOWN.

DASH NO.	"L" (IN)
1	6
2	8
3	10

ORIGINAL PAGE IS
OF POOR QUALITY



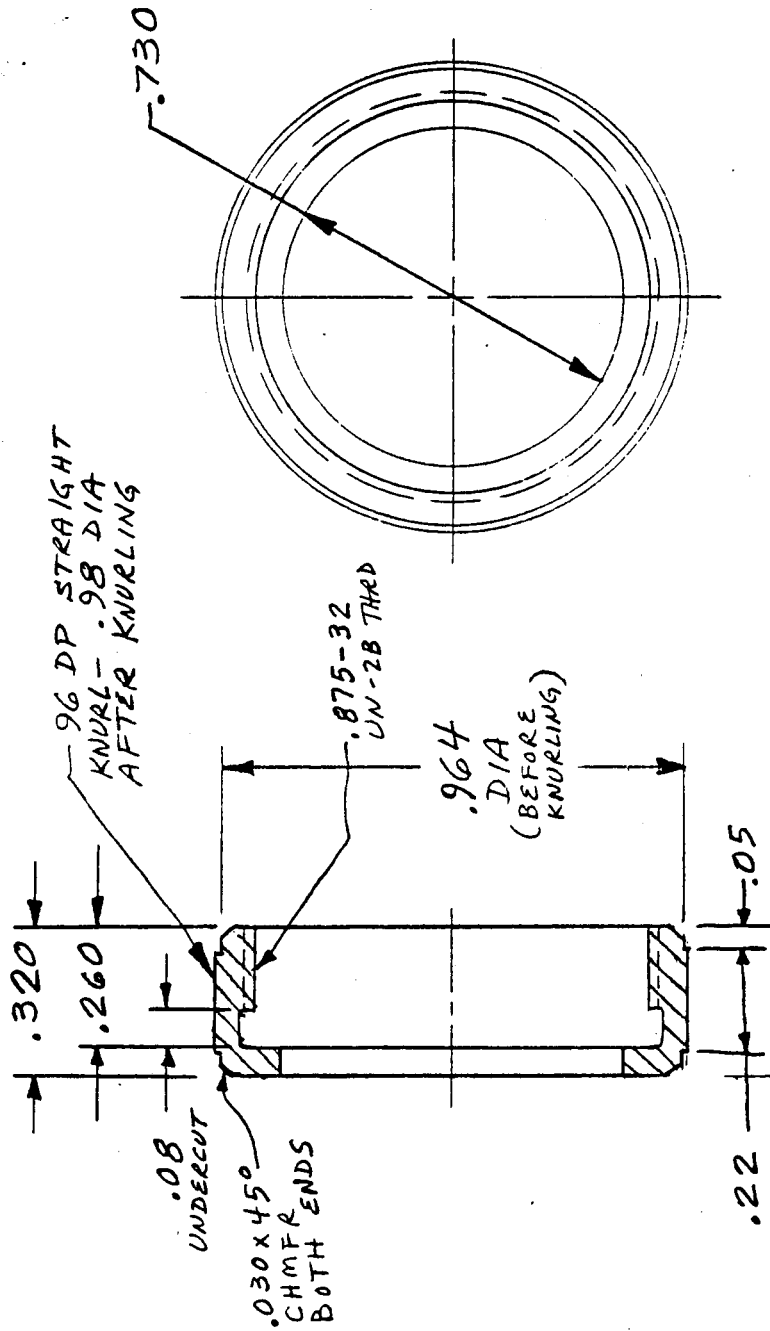
NATL
SILICONE RUBBER (F# 539)
CURE 170HRS AT 75°F + 2HRS AT 250°F + 2HRS AT 275°F +
2HRS AT 300°F + 2HRS AT 325°F + 2HRS AT 350°F.

.XXX ±.010 .XX ±.02

BOOT, RUBBER

W.F. MADAY
24 MAY '84

5240-050441



MATL

LEADED BRASS (06-024)

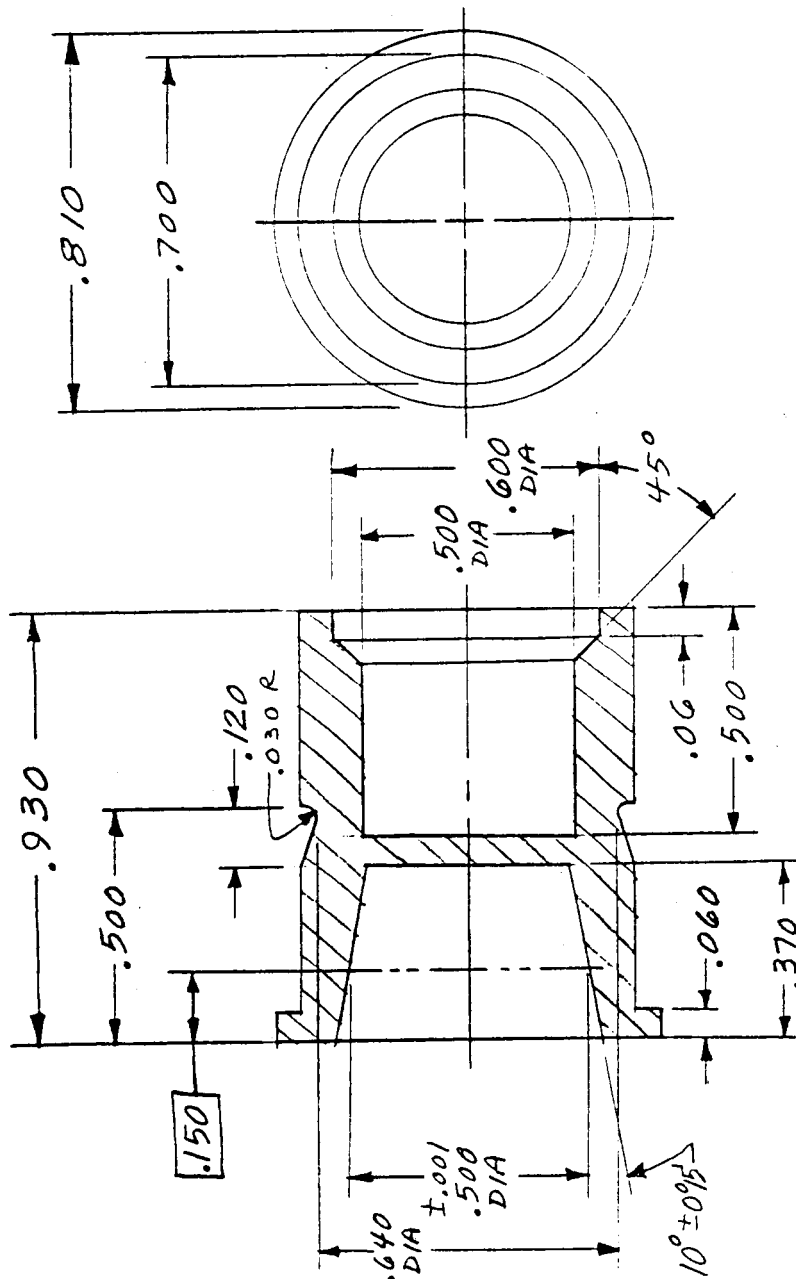
FINISH

COPPER FLASH (50 μ INCH)
 SULFAMATE NICKEL (125 \pm 50 μ INCH)
 OROSENE 999 COBALT GOLD (125 \pm 50 μ INCH)
 .XXX \pm .005 .XX \pm .01

NUT - COUPLING

W.F. MADAY
 13 APR. '84

5240-050443A



MATL

TELLURIUM COPPER ALLOY C14500 (13-040)

FINISH

COPPER FLASH (50μ INCH)

SULFAMATE NICKEL (125 ± 50μ INCH)

OROSENE 999 COBALT GOLD (125 ± 50μ INCH)

.XX.X ±.005

.XX.X ±.01

ANG. ± 2°

THIMBLE-TERMINAL

W.F.MADAY

11 MAY '84

5240-050442A

APPENDIX F

BEARING PRELOAD PROCEDURE

5240-080841

BEARING PRELOADING

This procedure provides a means of establishing a proper bearing axial preload. The final assembly will provide a rigid "DB" preload arrangement with a 0.010 ± 0.002 inch axial deflection. This correlates with a theoretical axial preload of 21 ± 5 pounds.

- a) Mount a Kaydon KB45 "Real-Slim" bearing into the Stator Housing PN 5240-050343 bore with the preload shoulder on the outer race located away from the Housing conductor cavity.
- b) Secure the Kaydon KB45 bearing in the Housing by threading a Bearing Outer Nut PN 5240-050749 (relieved face away from bearing) into engagement with the bearing face. Torque to 50 inch pounds using a 5.094 inch spanner with 0.125 inch diameter pins.
- c) Mount another Kaydon KB45 bearing into the Bearing Housing PN 5240-050744 with the preload shoulder on the outer race located adjacent to the diaphragm.
- d) Secure the Kaydon KB45 bearing in the Housing by threading a Bearing Outer Nut PN 5240-050749 (relieved face away from bearing) into engagement with the bearing face. Torque to 50 inch pounds using a 5.094 inch spanner with 0.125 inch diameter pins.
- e) Position a Bearing Spacer PN 5240-050747 into the cavity adjacent to the previously installed bearing.
- f) Fit the latter Bearing/Housing subassembly into the Stator Housing PN 5240-050343 and secure with 8 number 6-32 Allen head cap screws (safety wire type) 0.375 inches long. Do not tighten screws at this time.
- g) Mount the body of an indicator on the Stator Housing PN 5240-050343 and position the stylus against the outboard surface of the Bearing Housing PN 5240-050744 adjacent to the nut.
- h) Insert the bearing trunnion of the Rotor Housing PN 5240-052445 into the bearing bores from the conductor cavity side of the Housing Subassembly. It will be necessary to position the Bearing Spacer PN 5240-050747 to facilitate this operation.
- i) Mount a Bearing Inner Retainer PN 5240-050748 into the outboard end of the trunnion of the Rotor Housing PN 5240-052445 using 8 number 6-32 Allen head cap screws (safety wire type) 0.375 inches long. Tighten screws sequentially alternating across the diameter such that the diaphragm of the Bearing Housing PN 5240-050744 is gradually preloaded as indicated by the position indicator installed in step "g". The proper deflection is a 0.010 ± 0.002 inch axial distortion of the diaphragm when the 6-32 screws have been torqued to 20 inch pounds. If the deflection of the diaphragm is less than 0.008 inches, lap the

axial dimension of the Bearing Spacer PN 5240-050747 an amount equal to 80 percent of the difference between the indicator reading and 0.010 inches. The total variation of the Spacer width should not exceed 0.0002 inches. Record the final diaphragm deflection.

NOTE: Thoroughly wash the Spacer after each lapping operation prior to re-assembling.

j) Secure the 8 number 6-32 screws retaining the Bearing Housing PN 5240-050744 to the Stator Housing PN 5240-050343 by torquing to 20 inch pounds.

APPENDIX G

RING SET ASSEMBLY PROCEDURE

5240-021851

NOTE: The Ring must be properly centered radially in order that the Insulator can be fully seated.

k) Insert the proper Connecting Bolt PN 5240-050448 through the hole provided in the Inner Ring into firm engagement with the spherical seat in the Ring.

l) Invert assembly, insert the proper Insulator Tube PN 5240-021351-X over the Bolt, assemble the Housing Insulator PN 5240-050743 over the Bolt and into the Housing cavity and thread a Terminal Cone PN 5240-050741 onto the Bolt PN 5240-050448. Secure the Cone to a torque of 50 inch pounds. Lock the Cone onto the Bolt with a 0.312 - 24UNF X.375 set screw.

m) Lock the Bolt into the Ring by threading a Nut PN 5240-050449 into the threaded cavity of the Ring to a 50 inch pound torque.

n) Carefully insert 10 Flexures PN 5240-010951 and 10 Idlers PN 5240-011841 into the annulus space between the two Ring grooves. The Flexures should be spread with a pair of Teflon or Nylon rods at insertion to allow their clearing the Ring shoulders. The circumferential clearance between the Flexures should be taken up as each Flexure/Idler pair is inserted such that there is adequate space to insert the tenth pair.

o) Slide a Roller Guide PN 5240-050447 (cavity down) over the Insulator Spacer PN 5240-050445 and firmly against the Inner Ring PN 5240-011842 by rotating the Inner Housing assembly while maintaining light pressure on the Guide. The 10 Idlers will be heard to snap into place.

p) Repeat steps "a" through "o" for each of the consecutive S/N 2 through S/N 8 circuit sets. It will be necessary to use greater axial hold-down forces as the number of circuits increases in order to obtain consistent readings. Note that the Bolts PN 5240-050448 reverse their orientation at circuit number 5, and that a solid Barrier PN 5240-021352 is used between circuits 4 and 5.

RING SET ASSEMBLY

This procedure is required to establish the proper Ring to Ring axial alignment and to assure that the radial run-out is acceptable.

- a) Insert a Barrier PN 5240-050446 into the Housing cavity and into proper angular orientation with the terminal holes.
- b) Insert an Outer Ring PN 5240-011841, S/N 1, into the cavity of the Outer Ring Insulator PN 5240-050843. Both the Insulator and the Ring tabs should be up.
- c) Fold the split ends of the Outer Ring Insulator PN 5240-050843 as required, insert into the lowest window of the Stator Housing PN 5240-050343 and assure firm seating against the shoulder.
- d) Slide a split Insulator Spacer PN 5240-050445, a shim PN 5240-102941-1 and a wave spring PN 5240-051041-2 into the cavity of the Inner Ring PN 5240-011842, and position firmly against the seat in the Ring.
- e) Slide a Roller Guide PN 5240-050447 (cavity up) over the Insulator Spacer PN 5240-050445 and firmly against the Insulator Barrier PN 5240-050446.
- f) Slide Inner Ring PN 5240-011842, S/N 1, (counter-bore down) over the Insulator Spacer PN 5240-050445 and firmly against the Roller Guide PN 5240-050447. Rotate the Ring into proper angular alignment with the threaded socket hole and the designated terminal hole.
- g) Determine the axial alignment of the Inner Ring PN 5240-011842 by measuring the vertical position relative to the Outer Ring PN 5240-011841 in four locations on each ring adjacent to the ring grooves. The rings are properly aligned when the surface of the Inner is 0.046 inches \pm .005 above the surface of the Outer. The axial TIR of the Inner shall be <0.008 inches. If the relative axial position is greater than 0.050 inches correct by adding appropriate shims below the Outer Ring. If the relative axial position is less than 0.041 inches correct by adding appropriate shims below the Inner Ring. Record all final measurements. The readings are to be taken as increasing from the top of the Outer Housing which establishes the "zero" position.

NOTE: Assure that the components are held down securely during these and following measurements.

- h) Insert the Shim PN 5240-102941-2 into the cavity between the Outer Ring PN 5240-011841 and the Outer Insulator PN 5240-050843.
- i) Thread in the Wave Spring PN 5240-051041-1 into the cavity between the Outer Ring and the Shim.
- j) Insert the Outer Cap Insulator PN 5240-050844 (notch down) into the Stator Housing PN 5240-050343 and into firm engagement with the Outer Ring PN 5240-011841.


APPENDIX H

HIGH POWER ROLL RING

EVALUATION UNIT

TEST FIXTURE


5240-010152

ENGINEERING SPECIFICATION		SECURITY NOTATION		SPEC NO. 5240-010152		REV LTR																										
		TYPE OF SPECIFICATION		FSCM NO.		INITIAL RELEASE DATE 85-01-29																										
DIVISION SPACE		DEPARTMENT NO 5240		PRODUCT LINE NO.		CLASS C																										
				CONTRACT NO. NAS3-24264																												
TITLE HIGH POWER ROLL RING EVALUATION UNIT TEST FIXTURE																																
PREPARED BY				APPROVED BY SECTION HEAD		APPROVED BY DEPARTMENT HEAD																										
DATE				DATE		DATE																										
REF AWAEB/PSAEB NO.		CHECKER		PRODUCT DESIGN CHECKER (AW/PS CRITICAL DOCUMENTS ONLY)		COGNIZANCE OF QE SUPVR (PRODUCTION CRITICAL TEST AND CALIB DOCUMENTS ONLY)																										
NOTES: FOR REVISION RECORD, SEE PAGE CR-2.																																
PAGE INDEX																																
CR 5	REV SYM	PG	121	122	123	124	125	126	127	128	129	130	131	132	133	134	135	136	137	138	139	140	141	142	143	144	145	146	147	148	149	150
CR 4	REV SYM	PG	91	92	93	94	95	96	97	98	99	100	101	102	103	104	105	106	107	108	109	110	111	112	113	114	115	116	117	118	119	120
CR 3	REV SYM	PG	61	62	63	64	65	66	67	68	69	70	71	72	73	74	75	76	77	78	79	80	81	82	83	84	85	86	87	88	89	90
CR 2	REV SYM	PG	31	32	33	34	35	36	37	38	39	40	41	42	43	44	45	46	47	48	49	50	51	52	53	54	55	56	57	58	59	60
CR 1	REV SYM	PG	1	2	3	4	5	6	7	8	9	10	11	12	13	14	15	16	17	18	19	20	21	22	23	24	25	26	27	28	29	30
		SECURITY NOTATION		AW/PS CRITICAL NOTATION		CR-1 PAGE CONTROL RECORD																										

H-1

TITLE			
HIGH POWER ROLL RING EVALUATION UNIT TEST FIXTURE			
PREPARED BY		APPROVED BY SECTION HEAD	APPROVED BY DEPARTMENT HEAD
DATE		DATE	DATE
REF AWAEB/PSAEB NO.	CHECKER	PRODUCT DESIGN CHECKER (AW/PS CRITICAL DOCUMENTS ONLY)	COGNIZANCE OF QE SUPVR (PRODUCTION CRITICAL TEST AND CALIB DOCUMENTS ONLY)

FOR REVISION RECORD, SEE PAGE CR-2.

	H-2		CR-1 PAGE
---	-----	--	--------------

ENGINEERING SPECIFICATION

SECURITY NOTATION

SPEC NO. 5240-010152

FSCM NO.

A
REV LTR

REV LTR

SEE FIRST PAGE FOR PROPRIETARY OR DATA RIGHTS NOTATIONS.

5

10

15

20

25

30

35

40

45

$\frac{3}{8}$ -16 ALLEN HD CAP SCREW $1\frac{1}{2}$ LONG (4 REQD)

10-32 ALLEN
HD CAPSCREW
 $1\frac{1}{2}$ LONG
(12 REQD)
(20 IN LB)

(TOP VIEW)

BASE PLATE
PN 072444

$\frac{3}{8}$ -16 ALLEN HD
CAP SCREW $2\frac{3}{4}$ LONG
(6 REQD)
(75 IN LB)

BASE
PN 072041

2.50

ASSEMBLY DETAILS



SECURITY NOTATION

SUPPLEMENTS

1
PAGE

ENGINEERING SPECIFICATION

SECURITY NOTATION

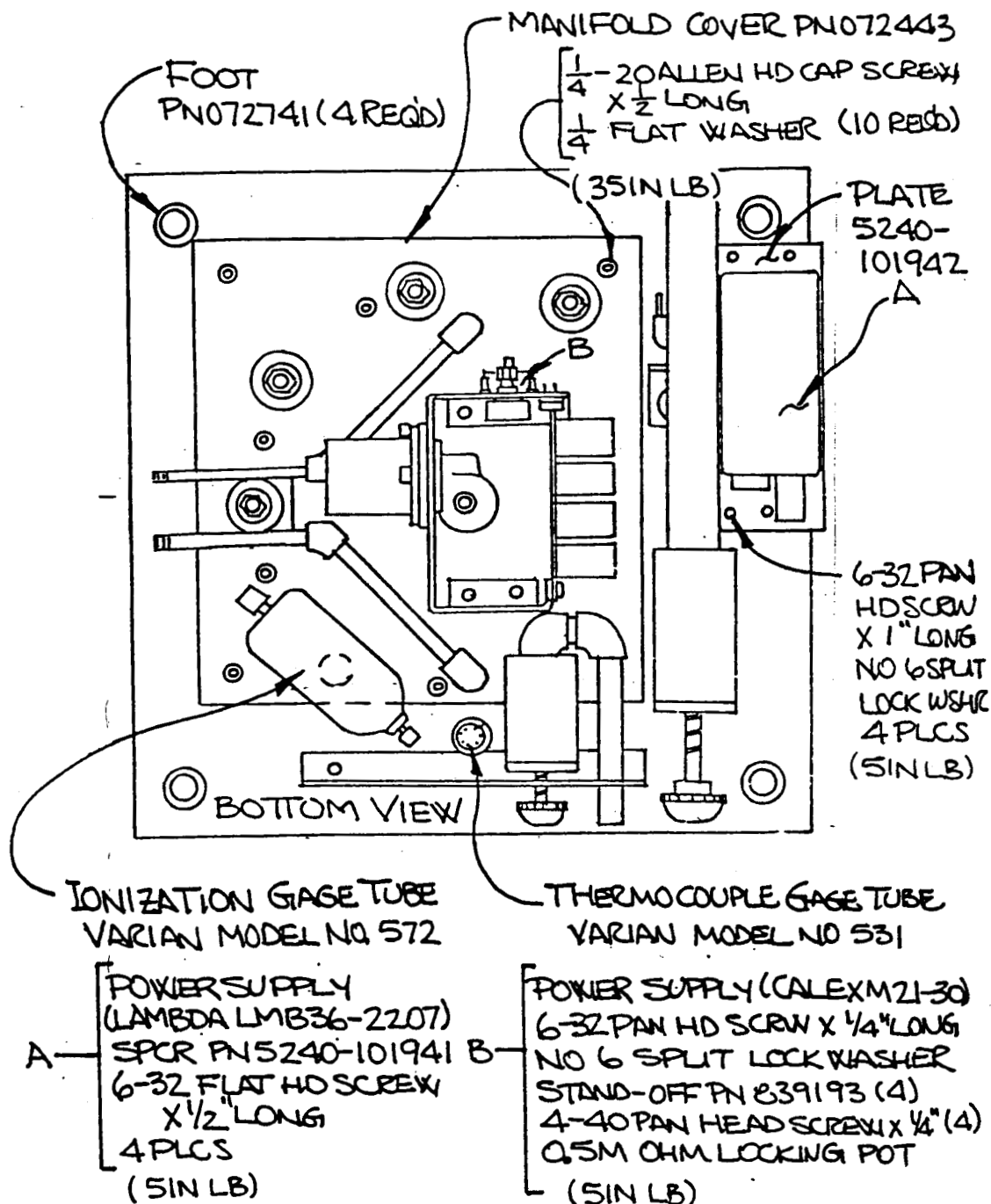
SPEC NO. 5240-010152

FSCM NO.

REV LTR

REV LTR

SEE FIRST PAGE FOR PROPRIETARY OR DATA RIGHTS NOTATIONS.



ASSEMBLY DETAILS



SECURITY NOTATION

SUPPLEMENTS

2
PAGE

H-4

ENGINEERING SPECIFICATION

SECURITY NOTATION

SPEC

NO. 5240-010152

FSCM

NO.

A

REV LTR

REV LTR

SEE FIRST PAGE FOR PROPRIETARY OR DATA RIGHTS NOTATIONS.

5

10

15

20

25

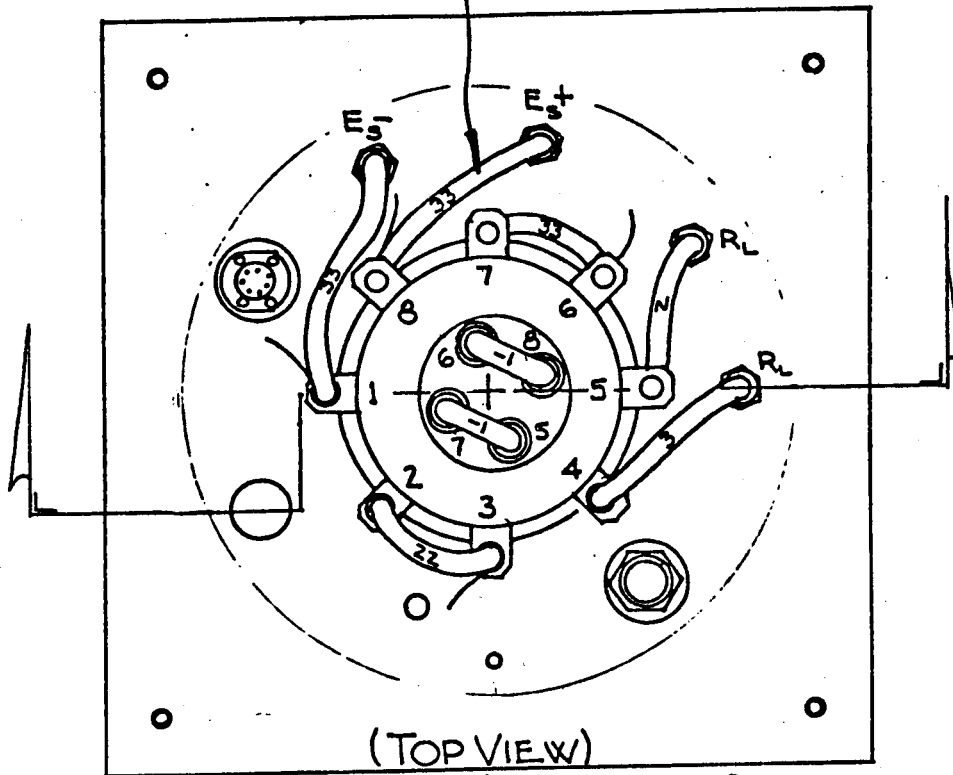
30

35

40

45

CABLE ASSEMBLY
PN 072441-X (10 REQD)

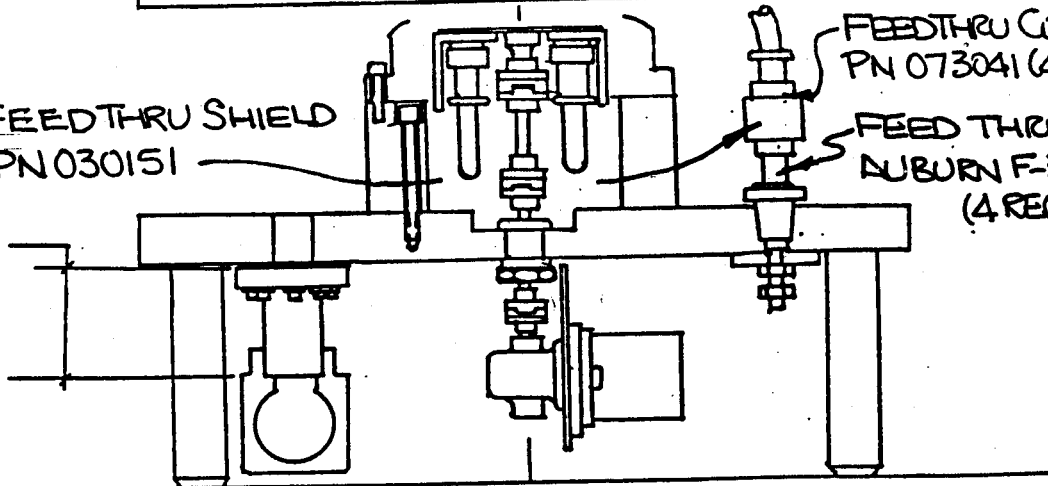


FEEDTHRU SHIELD
PN 030151

2.50

FEEDTHRU CONTACT
PN 073041 (4 REQD)

FEED THRU
AUBURN F-310-H
(4 REQD)



INTERCONNECT DETAILS

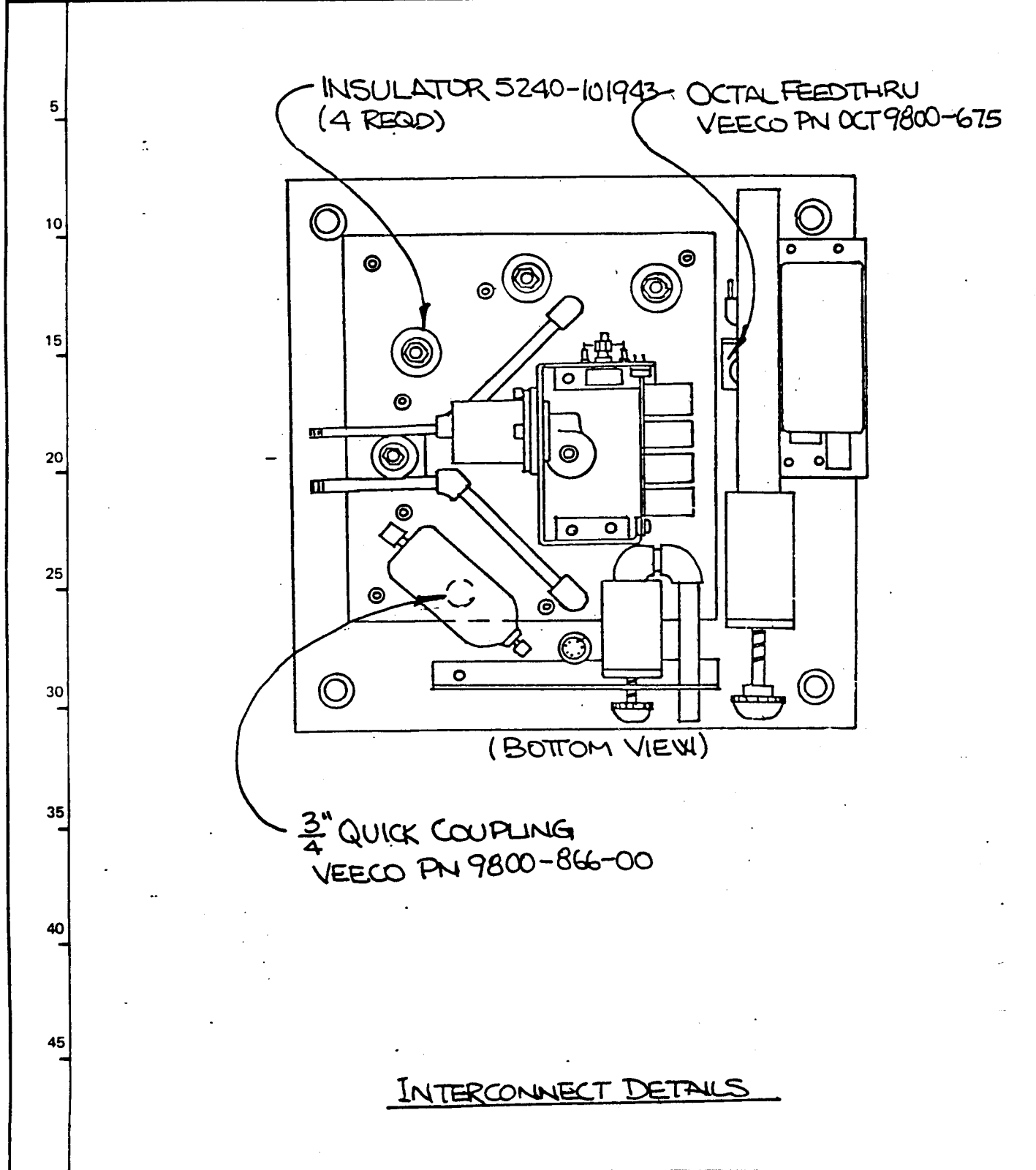


SECURITY NOTATION

SUPPLEMENTS

3
PAGE

REV LTR	SEE FIRST PAGE FOR PROPRIETARY OR DATA RIGHTS NOTATIONS.
------------	--



ENGINEERING SPECIFICATION

SECURITY NOTATION

SPEC NO. 5240-010152

FSCM NO.

A

REV LTR

REV LTR

SEE FIRST PAGE FOR PROPRIETARY OR DATA RIGHTS NOTATIONS.

5

10

15

20

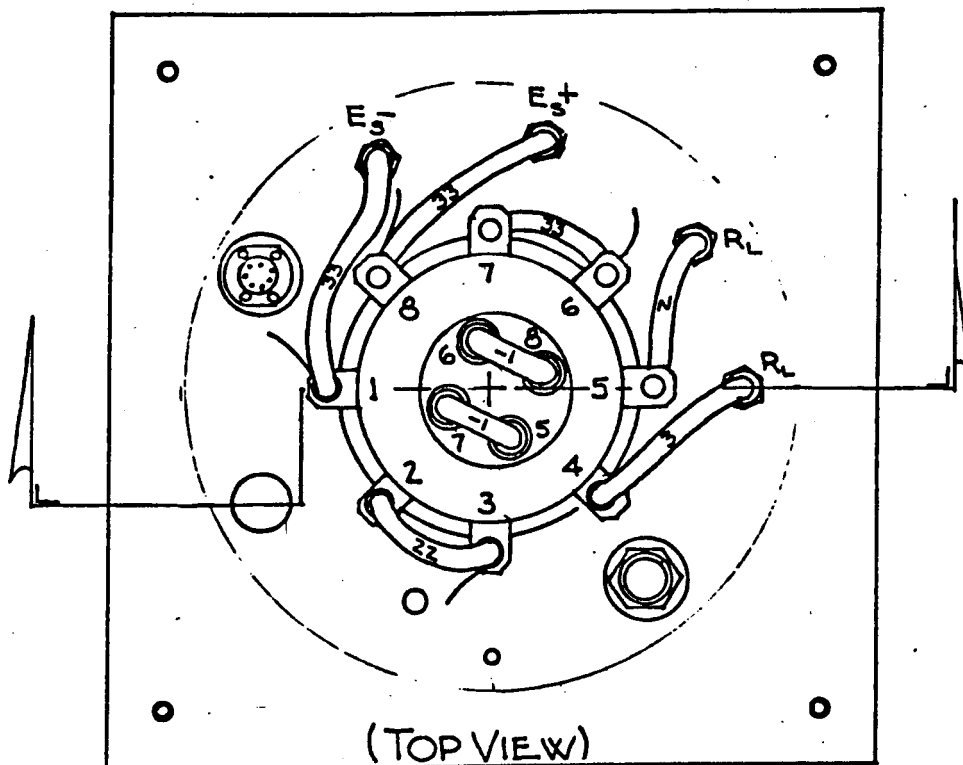
25

30

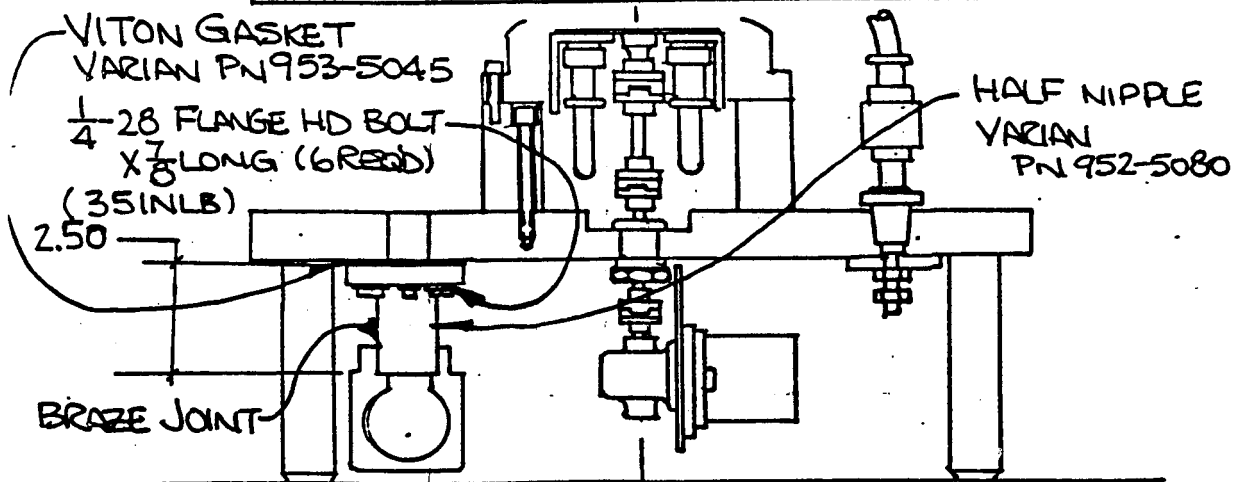
35

40

45



(TOP VIEW)



BRAZE JOINT

PLUMBING DETAILS



SECURITY NOTATION

SUPPLEMENTS

5
PAGE

ENGINEERING SPECIFICATION

SECURITY NOTATION

SPEC

NO. 5240-010152

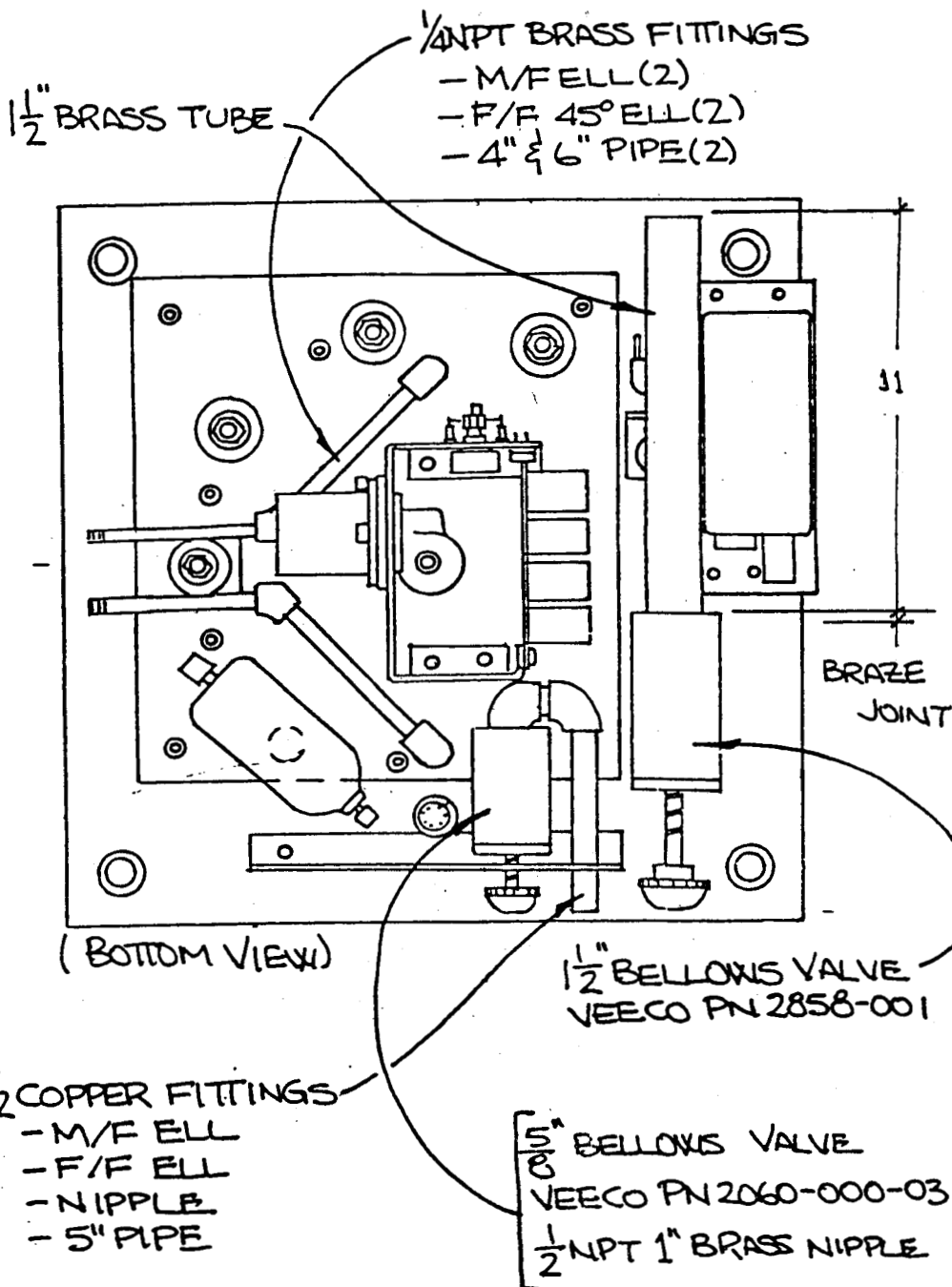
FSCM

NO.

REV LTR

REV LTR

SEE FIRST PAGE FOR PROPRIETARY OR DATA RIGHTS NOTATIONS.



PLUMBING DETAILS



SECURITY NOTATION

SUPPLEMENTS

6
PAGE

ENGINEERING SPECIFICATION

SECURITY NOTATION

SPEC NO. 5240-010152

FSCM NO.

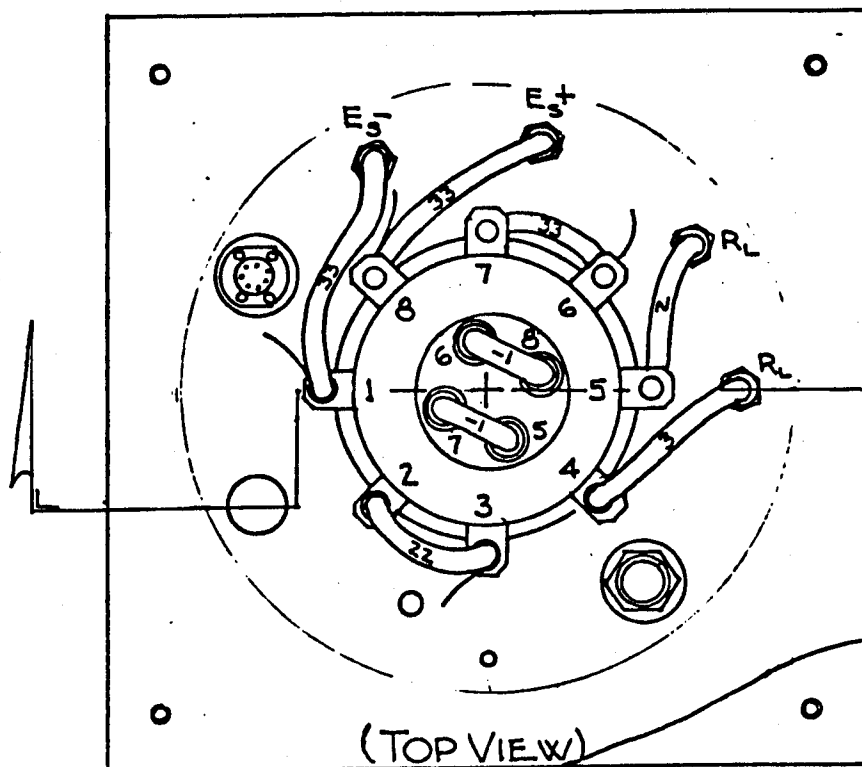
A

REV LTR

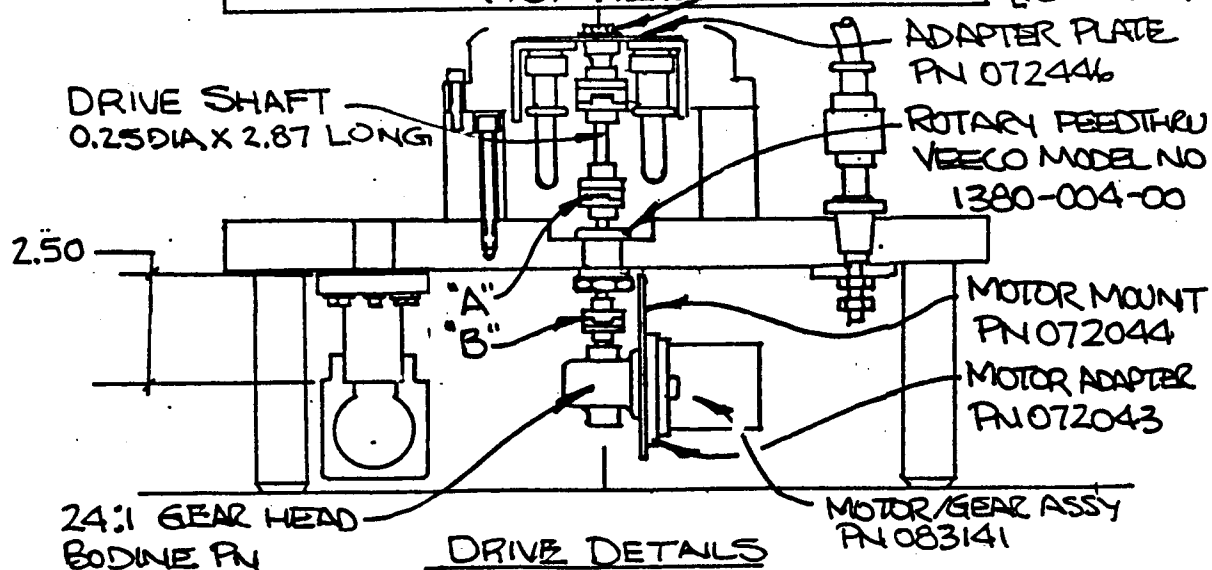
REV LTR

SEE FIRST PAGE FOR PROPRIETARY OR DATA RIGHTS NOTATIONS.

"A" = COUPLER STERLING PN G401-4 (2)
 "B" = COUPLER STERLING PN G401-4 & -5



1/4-24 HEX NUT
 SPLIT LOCK WASHER
 (50 IN LB)



SECURITY NOTATION

SUPPLEMENTS

7
 PAGE

ENGINEERING SPECIFICATION

SECURITY NOTATION

SPEC

NO. 5240-010152

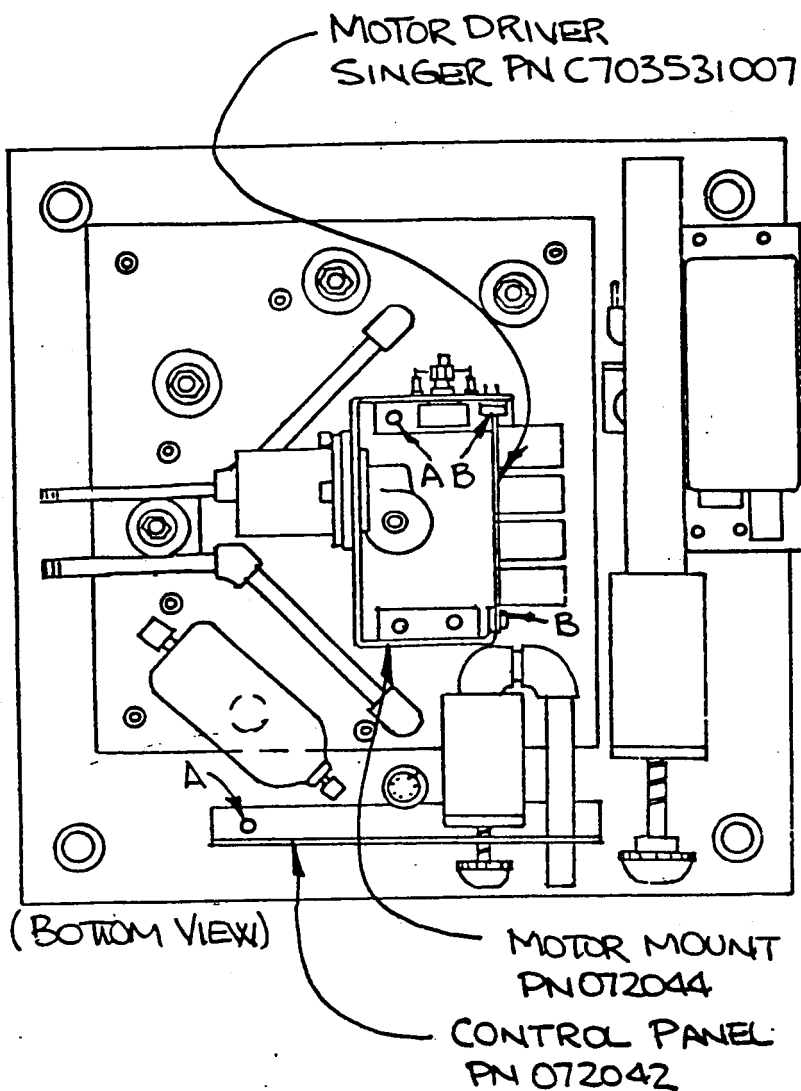
FSCM

NO.

REV LTR

REV LTR

SEE FIRST PAGE FOR PROPRIETARY OR DATA RIGHTS NOTATIONS.



"A" = 10-32 PAN HEAD SCREWS $\times \frac{1}{4}$ LONG;
#10 SPLIT LOCK WASHERS (6 REQD)
(20 IN LB)
"B" = 6-32 PAN HEAD SCREWS $\times \frac{1}{4}$ LONG;
#6 SPLIT LOCK WASHERS; 6-32 HEX NUT (4 REQD)
(5 IN LB)

DRIVE DETAILS



SECURITY NOTATION

SUPPLEMENTS

8
PAGE

ENGINEERING SPECIFICATION

SECURITY NOTATION

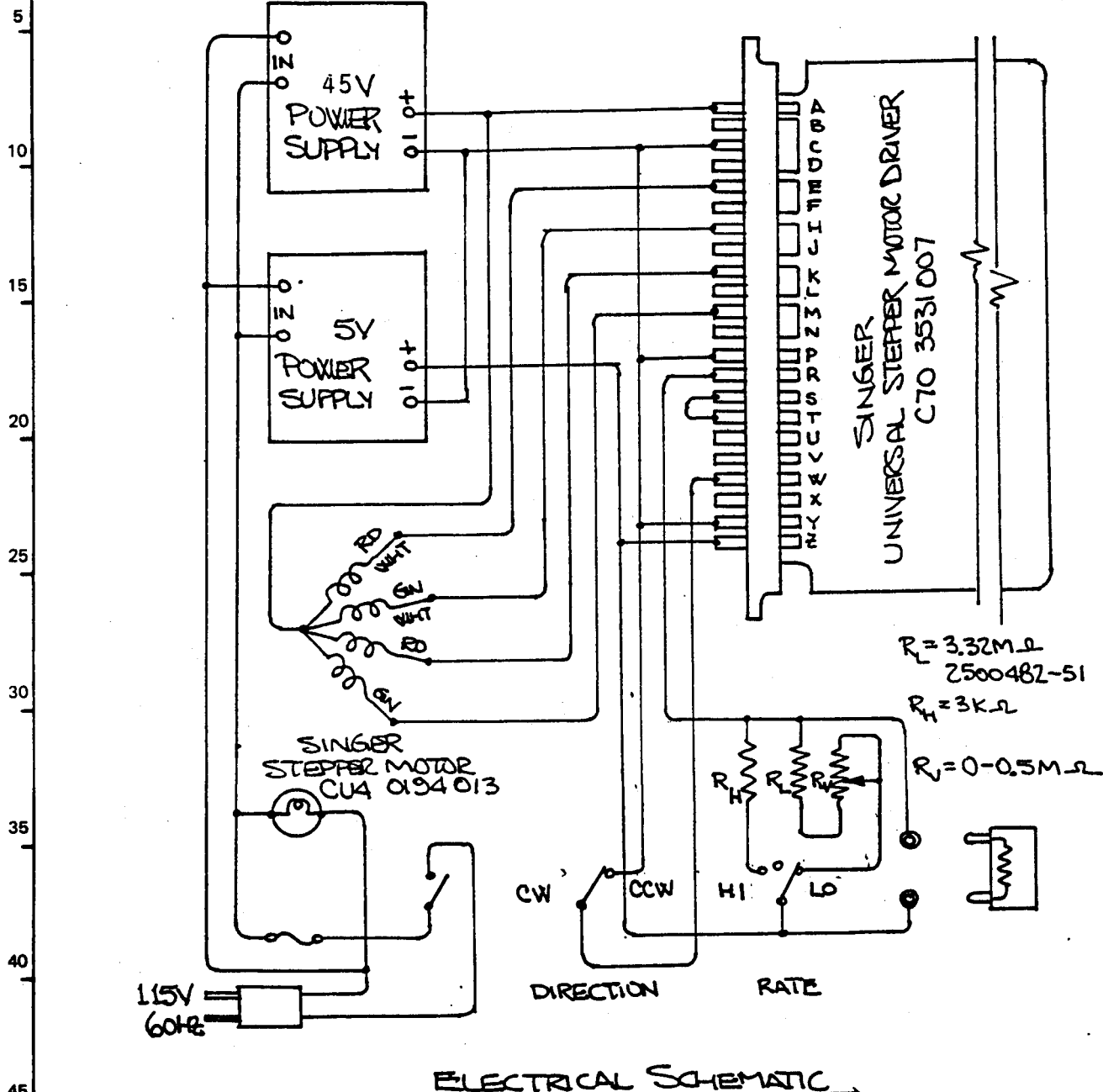
SPEC NO. 5240-010152

FSCM NO.

REV LTR

REV LTR

SEE FIRST PAGE FOR PROPRIETARY OR DATA RIGHTS NOTATIONS.



SECURITY NOTATION

SUPPLEMENTS

9
PAGE

**ENGINEERING SPECIFICATION
REVISION RECORD**

SECURITY NOTATION

SPEC
NO. 5240-010152

FSCM
NO.

REV LTR

SEE FIRST PAGE FOR PROPRIETARY OR DATA RIGHTS NOTATIONS

REV LTR	PAGE	DESCRIPTION	DATE AND APPROVAL



SECURITY NOTATION

REVISION RECORD

10

PAGE

APPENDIX I

EB FOR SET UP & TEST
OF
HIGH POWER ROLL RING
EVALUATION UNIT
EB 011451

TABLE OF CONTENTS

PARAGRAPH	PAGE
1. SCOPE -----	1
2. APPLICABLE DOCUMENTS -----	1
3. APPLICABLE EQUIPMENT -----	1
4. PREPARATION OF TEST FIXTURE -----	2
4.1 VACUUM SYSTEM -----	2
4.2 PURGING SYSTEM -----	2
4.3 BASE PLATE CONTROL SYSTEM -----	2
4.4 CONTROL PANEL -----	2
5. INTEGRATION OF ENGINEERING UNIT WITH TEST FIXTURE -	4
6. TEST PROCEDURE -----	4
6.1 HIGH CURRENT TESTING -----	4
6.2 HIGH VOLTAGE TESTING -----	8
6.3 HIGH POWER TESTING -----	9
7. POST TEST CONSIDERATIONS -----	10
8. DOCUMENT CONTROL -----	11

ENGINEERING BULLETIN

Engineering bulletin for the Set Up and Test of High Power Roll Ring Evaluation Unit Part No. 5240-010151.

1. SCOPE

This engineering bulletin identifies the instrumentation, procedures and precautions necessary for setting up the High Power Roll Ring Evaluation Unit (EU), Part Number 5240-010151 for test on the related Test Fixture (TF), Part Number 5240-010152 and for execution of these tests.

2. APPLICABLE DOCUMENTS

	<u>ITEM NUMBER</u>
High Power Roll Ring Evaluation Unit	5240-010151
Evaluation Unit Test Fixture	5240-010152
Cable Assembly	5240-072441-xx

3. APPLICABLE EQUIPMENT

	<u>PART NUMBER</u>
Vacuum Roughing Pump	Welch Model No. 1397 or equivalent
Ionization Gage Control	Veeco, Model RG-830 or equivalent
Vacuum Gauge Control	Veeco Model TG-70 or equivalent
Mechanical Trap	Perkin Elmer Model No. 231-1622 or equivalent
Temperature Sensor	Minimate Thermo electric or equivalent
Current Meter	F.W. Bell Model CG100D or equivalent
Milliohmmeter	Hewlett Packard Model 4328A or equivalent
High Voltage Ohmmeter	Freed Transformer Co. Megohmmeter Model 1620C or equivalent

4. PREPARATION OF TEST FIXTURE PN 5240-010152

The following auxiliary equipment is required to support this procedure.

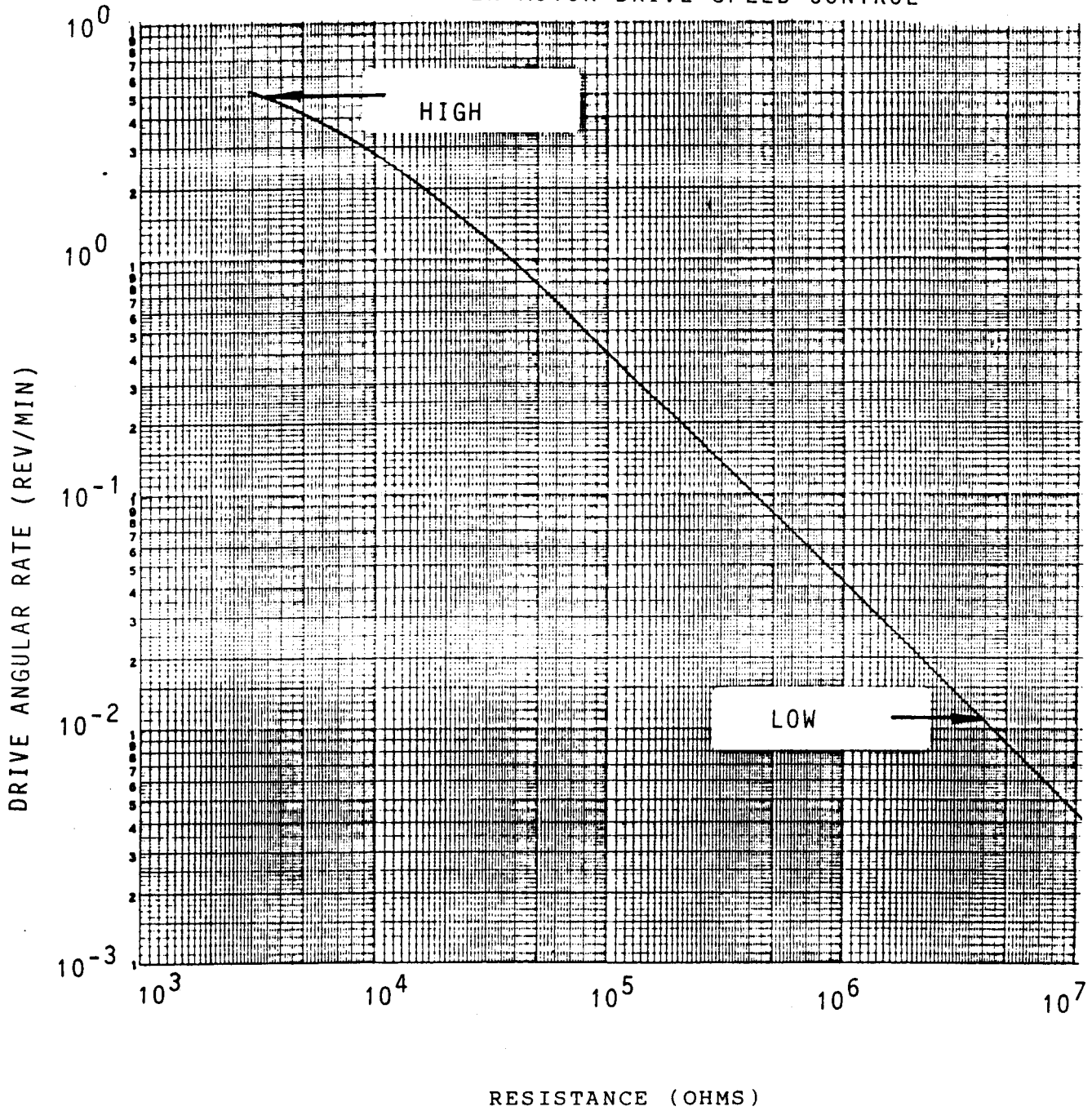
4.1 Vacuum System - A mechanical roughing pump such as Welch Model No. 1397 is required along with a suitable flexible vacuum line. The attachment at the Test Fixture (TF) is a 1 1/2 inch copper line. If a vacuum of <0.5 milli Torr is desired for a test duration of greater than 50 hours a suitable additional pumping system is required between the TF and the roughing pump. The use of a mechanical trap such as Perkin Elmer Model 231-1622 between the TF and the pumping system is also recommended. The TF is equipped with a standard ionization gage and a thermocouple gage to facilitate the pressure monitoring. Monitoring equipment such as Veeco Models RG-830 and TG-70 may be used.

4.2 Purging System - Although not essential it is preferred to back fill the vacuum system with an inert gas such as dry N₂ prior to opening the chamber for any reason. To accomplish this back-filling process a dry N₂ tank, regulator and suitable set of adapters and purging line is required. The attachment at the TF is a 1/2 inch copper line.

4.3 Base Plate Control System - Since most testing of the EU will be accomplished with the TF set up on a poor heat sink, (such as a Formica bench top), it is necessary to provide a source of heat extraction from the TF Base Plate. To accomplish this temperature control, a suitable heat extraction medium is required such as LN₂ or chilled water. This medium is to be connected to the two male 1/4 inch NPT fittings provided on the TF. Two fittings are provided such that a closed chilled water system may be incorporated with the TF or, in the case of LN₂ use, one fitting will accomodate the supply while the other can be connected to a short vent line. A copper/constantan thermocouple is attached to the heat exchange manifold on the TF to provide for a monitor of the Base Plate temperature. A temperature sensor such as a Minimate Thermo Electric is required to translate the thermocouple signal.

4.4 Control Panel - The TF is provided with an integral stepper drive motor and supply and a control panel for this and other functions. This panel has a power on switch which controls the 115 volt/60 Hz line power to the motor electronics. The EU drive direction control switch is labeled CW/CCW for clockwise and counterclockwise EU drive respectively, as viewed from above the EU. The drive speed is selectable with another switch labeled "High" for a 5 rev/min drive rate and "LO" for a 360 degree/90 min rotational rate. This switch also has a center position which provides for alternate speeds by inserting a selected resistor mounted onto a standard General Radio double male plug into the sockets provided to the right of the speed select switch on the control panel. The relationship of this resistance to drive speed is as shown in Figure 1.

STEPPER MOTOR DRIVE SPEED CONTROL



5. INTEGRATION OF EU WITH TF

This procedure covers the integration of the EU with the TF and connection of the system to the external power supply and resistive loads for test. Cables PN 5240-072441-XX are used to provide the various interconnects and EU to TF connections. Cables between the TF and the supply and the resistive load may be made up of 1/0 or larger welding cable and conventional spade lug fittings. The actual cable connections are discussed in Section 6.1 to follow.

The TF Base Plate feedthrough terminals marked "P_S+" and "P_S-" are to be connected to the power supply and the two marked "R" are to be connected to the resistive load except when only 2 circuits are being tested. In this event only the "P_S+" and "P_S-" feedthrough terminals are used.

It should be noted here that only even numbers of circuits can be evaluated since connections between the EU and the TF are not possible when odd numbered groups of circuits are used.

Reference should be made to TF Assembly Drawing Part Number 5240-010152 during preparation for, and execution of, testing of the EU. This document contains TF assembly information.

If the EU has been disassembled from the TF for any reason, it should be reassembled per the details given in document 5240-010152. The base PN 072041 is mounted to the Base Plate PN 072444 and the EU is mounted to the Base per sheet 1 of the document 5240-010152. Care should be exercised during this assembly to assure that the two interfaces between these two components are clean and free of burrs and protrusions since all of the heat generated in the EU is conducted through these interfaces and related components. The cables PN 072441-X are attached to the EU and between the EU and the TF per sheet 3 of 5240-010152. Note that the interconnections shown on sheet 3 are for a full 8 circuit test only. Other test arrangements are connected as discussed in section 6.1. The mechanical drive configuration is as shown on sheet 7 of 5240-010152. Care should be taken to assure that the couplings are properly meshed without binding during drive reassembly.

6. TEST PROCEDURE

This procedure establishes general test configurations and procedures for each of three test profiles. It does not provide a detailed overview of the many variations of test profiles which are possible with the EU and the TF.

6.1 High Current Tests

a. Set-up

After assembling the EU onto the TF as described in the previous section, the interconnect cables may be connected in a variety of ways to accommodate the number of circuits in test. The inventory of cables supplied with the TF provide for maximum flexibility in this regard. When only two circuits are to be tested one terminal of the resistive

load must be connected to the power supply directly and the remaining two terminals on the supply and the load may be connected to the EU through two of the feedthroughs. When four or more circuits are to be tested the resistive load may be located anywhere along the series string of circuits. The location of the load resistance is not important when conducting high current, low voltage tests. Figure 2 is an electrical schematic of one of many possible cabling configurations for an eight circuit test.

The Locking Quills on the cables should be torqued by hand to a "finger tight" condition only or a torque value of approximately 10 inch pounds. After Securing the cable the assembly should be checked with a reversing radial force to assure that the interface is tight.

CAUTION: The cables, EU and vacuum chamber TF components should be handled with nylon gloves or finger cots and not with unprotected fingers. This will minimize the introduction of body oils and other organic contaminants to the vacuum chamber. All tools used on the EU and TF must be clean and free of organic contaminants.

Pliers or other tools should not be used on the Cable terminations as the connections are designed to not require large clamping torques. The Boots on the cables should be pushed back away from the Locking Quills from the outer end of the cable so as to not over stress the Boot resulting in a tear crack. After the connection has been made and the Locking Quill is tight the Boot may be pushed back into position from the flanged end of the Boot.

The cables provided with the TF include some with monitoring lead wires attached to one end. These cables are designated with double digit dash numbers. Since all connections are reversible and interchangeable, they may be connected with the monitor leads located at almost any desired terminal.

When the resistance under load is desired for any circuit pair the monitor leads must be located at EU terminals of that pair. The other end of these leads may be soldered to any pair of pins on the monitor connector FT2. The voltage measured on these monitor leads while the circuit pair is under current represents the voltage drop across the pair and the interconnecting cable on the rotating side of the EU. An average circuit resistance may be derived by dividing the measured voltage drop by the current, subtracting the interconnect cable resistance and dividing the remainder by two. Table I provides the required information on the cables to make this determination.

ENGINEERING SPECIFICATION

SECURITY NOTATION

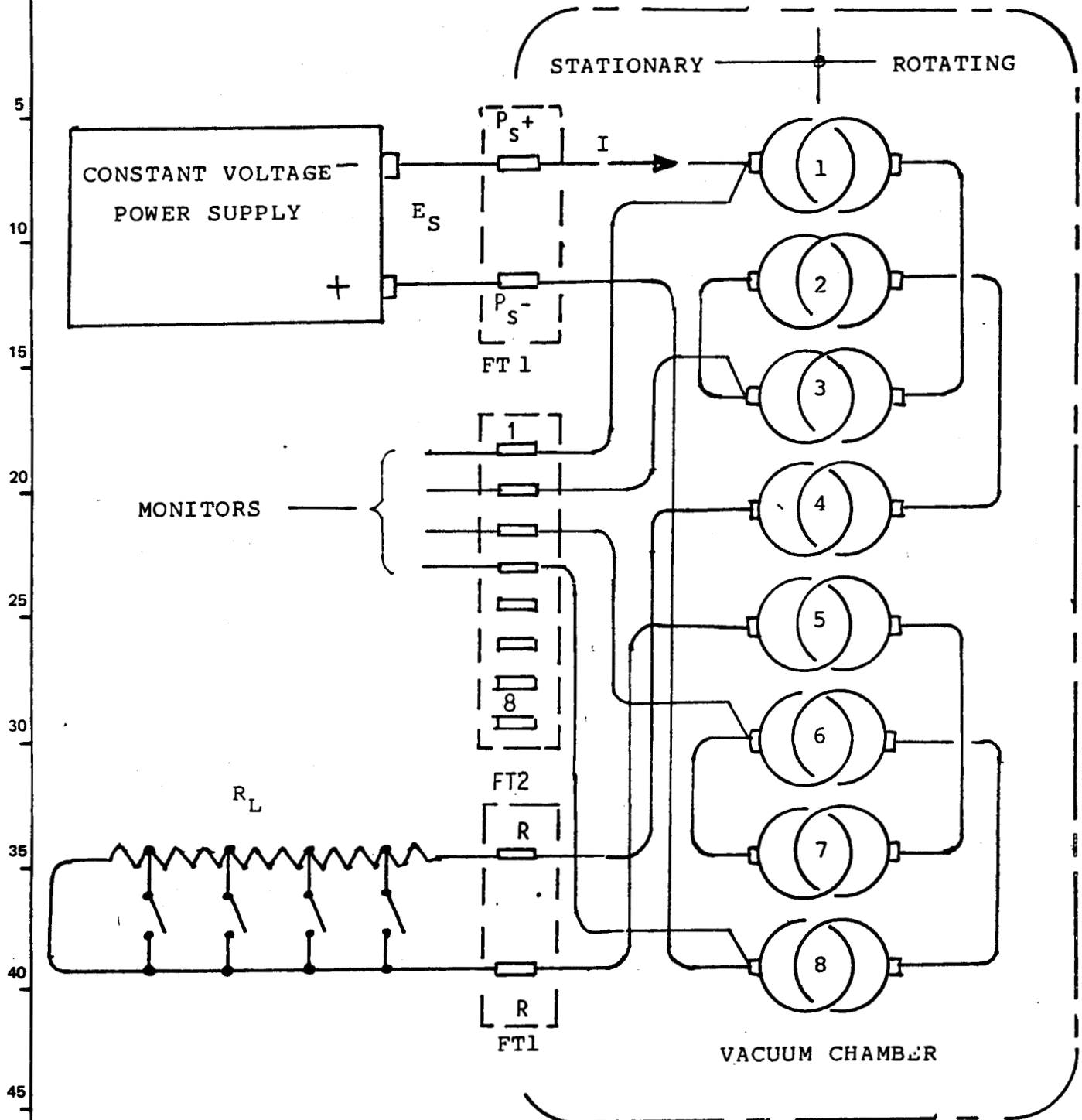
SPEC
NO. EB 011451

FSCM
NO.

REV LTR

REV
LTR

SEE FIRST PAGE FOR PROPRIETARY OR DATA RIGHTS NOTATIONS.



ELECTRICAL SCHEMATIC FOR OPERATIONAL TESTS

FIGURE 2



SECURITY NOTATION

SUPPLEMENTS

PAGE

<u>CABLE DASH NUMBER</u>	<u>LENGTH (Inches)</u>	<u>RESISTANCE (Milliohms)</u>
1	6	0.07
2	8	0.09
3	10	0.11
11	6	0.07
22	8	0.09
33	10	0.11

CABLE PN 5240-072441-XX RESISTANCE
TABLE I

A similar voltage drop under load may be measured by locating monitor leads at alternate locations. The average circuit resistance may then be derived by calculating the total circuit resistance, subtracting the total resistance of all intermediate cables and dividing the remainder by the number of circuits between monitor points.

The actual test current is most conveniently measured by using a portable current sensor on any of the external TF cables. A sensor such as F.W. Bell Model CG 100D hand held current meter provides a precise means of measuring this current and also provides an output voltage jack such that a voltage proportional to current may be recorded if desired.

If temperature measurements are to be made during test the sensor leads may be connected to the monitor connector FT2. The mating octal connector on the FT2 interconnector must be wired in a manner compatible with the sensor connections on the vacuum side of the TF. If copper/constantan thermocouples are used to monitor the temperature, similar lead materials must be located on both sides of the junctions so as to minimize temperature measurement errors. These errors are related to the Baseplate and Feedthrough Terminal (FT2) temperature and are also minimized by maintaining the Baseplate at a given reference temperature.

The steady-state reference temperature of a given circuit may be monitored by attaching a temperature sensor to the Cable Coupling Nut of the appropriate Cable Assembly Part Number 5240-072441-XX. The sensor may be inserted under the lip of the Boot on this Cable Assembly and thus held into contact with the nut.

If the temperature of a point on the rotating assembly is to be measured on approximation of the temperature may be made by attaching a suitable temperature sensor on the location and bringing the signal out to the stationary region through two of the vacant power transfer circuits. The lead wire material should be matched across both sides of each of the two roll Ring circuits to minimize measurement errors associated with temperature differences in the transfer circuits.

b. Test

After setting the EU and TF up for test the test chamber should be pumped down, for a vacuum test, in a conventional manner. A screen shield should be placed around the bell jar during vacuum testing to avoid the possibility of injury should an implosion of the jar occur. This could occur only if the jar is struck by an object while under a pressure differential. The thermocouple gage is provided on the test chamber to monitor the absolute pressure in the vacuum chamber until the pressure is $<10^{-3}$ Torr (1 micron). At lower pressures the ionization gage on the TF should be used. It should be noted here that a small amount of outgassing of the EU cables and other organic material in the test chamber when the unit is under test is normal and will decrease with time. This outgassing material will result in an initial small absolute pressure increase which is normal.

Electrical power may be applied to the EU as a ramp or as a step. The EU need not be rotating when conducting current. It will be noted, however, that the voltage drop across the unit will fluctuate slightly (about ± 2 percent) because of minute resistance changes while rotating. The AC component of this voltage drop represents the resistance modulation and the mean component the absolute circuit resistance.

After application of power the base temperature must always be monitored to assure the unacceptable thermal excursions do not occur. If the TF is mounted on a poor heat transfer medium, such as a formica bench top, the only significant mode of heat transfer will be by means of the heat exchanger built into the vacuum base of the TF. The thermal lag of the TF makes temperature control of the base difficult unless a temperature controlled valve is used to gate the LN_2 or chilled water heat exchange medium.

The EU has a thermal time constant of approximately 30 minutes. The total system should be at a thermal equilibrium condition within one working day.

6.2 HIGH VOLTAGE TESTS

a. Set-up

The procedures defined in section 6 are applicable for the high voltage tests. The electrical schematic shown in Figure 1 imposes the least probable case condition for electrical breakdown since the polarity reverses between circuits 1-4 and 5-8. Alternate configurations are possible as long as the load resistance is located between all circuits selected from the 1 through 4 group and those in the 5 through 8 group. The EU has been designed to accommodate the high voltage separation between these two groups only. Note that the electrical location of the resistive load effects the voltage distribution throughout the EU.

Care should be exercised dressing, connecting and insulating the various monitor lead wires so as to not impose a possibility for

voltage breakdown. The thermocouples should be electrically insulated from the terminals or other current conducting members of the EU so as to avoid shorting out the high voltage with a test instrument external to the EU or TF.

It is probable that a plasma will occur between any two exposed circuit components, terminations or TF Base at voltage differences exceeding 250 volts in a pressure range of 10 to 10^3 microns (10^{-2} to 1 mm Hg) which have even near line of sight orientation. For this reason the Insulating Boots must be firmly pressed into position prior to conducting any test. Under no circumstances should voltages exceeding 200 volts be applied in a pressure range of 1 to 10^4 microns (10^{-3} to 10 mm Hg). All monitor and thermocouple leads must be properly insulated prior to applying the high voltage.

b. Test

For test currents of <50 amps it is possible that no heat extraction from the TF base plate will be required to maintain the base at a relatively constant temperature.

In the interest of personnel safety it should be obvious that test voltages as high as 500 volts can be lethal and should be respected at all times. If in doubt, "don't." It is recommended that all test instruments be connected to the TF prior to application of power. If test currents exceed 5 amps at voltages as high as 500 volts the bell jar must be protected by a suitable metal safety shield.

As is true in any vacuum testing, a screen shield should be placed around the bell jar during vacuum testing to avoid the possibility of injury should an implosion of the jar occur. This is especially important when testing at high voltage since a breakdown plasma developed in the vicinity of a feedthrough terminal can develop a rapid leak and possible implosion.

An external dielectric failure or breakdown or a plasma during high voltage testing should be visible as a red to blue glow in the vicinity of the problem. An internal (or external) breakdown should be detectable as a change (increase) of the current and voltage drop across the EU. The power supply must be provided with a suitable adjustable current sensor and voltage breaker.

Prior to initiating the high voltage testing a high voltage ohmmeter such as Freed Megohmmeter Model 1620C should be connected between the TF Base and the EU to assure that the dielectric resistance is greater than 200 M ohms. The power supply must be disconnected prior to making this test. This test should be repeated periodically to verify that dielectric degradation has not occurred.

When any high voltage test is initiated after the EU has been exposed to a laboratory ambient, or after any wiring/cabling modifications have been made, the current and voltage should be increased slowly to allow organic contaminants to be sublimed. This procedure will minimize only tendency to form plasma discharge paths which would act as short cir-

cuit to the supply. The temperature of the unit should be allowed to increase slowly which will enhance the "cleaning" process. It may be necessary to increase/decrease the voltage in cycles while maintaining current/temperature to reach a desired operating voltage.

6.3 High Power Tests

a. Set-up

The set-up of the EU and TF for testing at both high voltage and at high current simultaneously require the procedures of the high current testing (section 6.1) combined with the procedures/precautions of the high voltage tests (section 6.2).

b. Test

Test results at a given current level should be comparable for all supply voltages provided that a dielectric breakdown does not occur. Since the destructive potential of a breakdown is related to source voltage level the EU should be initially evaluated at low voltage levels at high current and at high voltage levels at low current to establish the loss/heat management and dielectric integrity respectively.

It should be noted that the voltage drop within circuits 1 through 4 and circuits 5 through 8, within the EU is extremely small regardless of source voltage unless a dielectric breakdown between the two groups occurs. Should this materialize the majority of the source voltage would then appear across the breakdown propagating a failure which would likely be destructive.

The same precautions relative to bell jar shielding discussed in section 6.1 and 6.2 are also applicable to the high power testing.

The transfer efficiency e_t of a given circuit of the EU maybe determined by first calculating the heating loss P_L of the circuit.

$$P_L = I^2 R_C$$

Where

$$R_C = \text{Effective circuit resistance}$$

$$I = \text{Transfer current}$$

now

$$e_T = \frac{E_s I - P_L}{E_s I}$$

where

$$E_s = \text{Supply voltage}$$

7. POST TEST CONSIDERATIONS

It is a good practice to measure and record the resistance at various locations on the EU both before and after testing as a reference. These measurements may be made by applying a known current (>1 amp), measuring the voltage drop at the desired location and deriving the resistance. The alternate technique would be to use a conventional low current milliohm meter such as Hewlett Packard Model 4328A. If resistance is measured directly at a low current this value will be approximately 30 percent higher than that calculated from a measured voltage drop. The reason for the difference is the sensitivity of the contact surfaces to airborne organic contaminants. These surface film contaminants do not degrade the performance of the EU as the normal currents will break through these films through a fritting action.

During extended periods of storage the EU should be protected from the external contaminating environment by leaving it under the TF bell jar, preferably under at least a partial vacuum or atmosphere of inert gas such as nitrogen. Short exposures to standard laboratory atmospheres should not be harmful to the EU.

8. DOCUMENT CONTROL

No changes may be made to this document without engineering approval.

DISTRIBUTION LIST

Pub. No. (TBD)

March 1985

Final Report No. CR-174832

Customer: Lewis Research
Center

Copy No.	Recipient	Mail Station	Life No.	Signature and Date
1-12	Lewis Research Center (Via B. Wallace)	I26D2		
13	F. Blatter	P30E2		
14	G. Driskill	13K		
15	. Failla	2H29A2		
16	B. Goetz	I26D2		
17	P. Jacobson	N30D3		
18	B. Olin	I26D2		
19	R. Porter	N30D3		
20	G. Rogers	I26D2		
21	R. Van Riper	I26D2		
22	L. Webster	I26D2		
23	B. Wiest	I26D2		
24-28	Dept. 5240	N30D3		
29	Library	2I25B4		
30-34	Spares (DW)	DWP		

1. Report No. NAS CR-174832	2. Government Accession No.	3. Recipient's Catalog no.	
4. Title and Subtitle Multi-Hundred Kilowatt Roll Ring Assembly Final Report		5. Report Date March 1985	
		6. Performing Org. Code	
7. Author(s) Peter E. Jacobson		8. Perf. Org. Report No.	
9. Performing Organization Name and Address Sperry - Aerospace & Marine Space Systems Division Phoenix, Az. 85027		10. Work Unit No.	
		11. Contract or Grant No. NAS3-24264	
12. Sponsoring Agency Name and Address NASA-Lewis Research Center 21000 Brookpark Road Cleveland, Ohio 44135		13. Type of Report & Per.	
		14. Sponsoring Agency Cd.	
15. Supplementary Notes			
16. Abstract <p>A program was completed to develop an evaluation unit of a high power rotary transfer device for potential application in a space environment. This device was configured around a Roll Ring concept which performs the same function as a slip ring/brush assembly with a rolling instead of sliding interface. An eight circuit Evaluation Unit (EU) and a portable Test Fixture (TF) were designed and fabricated. The EU was designed to transfer currents to 200 amperes at a potential of as high as 500 volts for an ultimate 100KW/ circuit transfer capability. The EU was evaluated in vacuum at DC transfer currents of 50 to 200 amperes at voltages to 10 volts and at 500 volts at 2 amperes. Power transfer to levels of 2KW through each of the eight circuits was completed. Power transfer in vacuum at levels and efficiencies not previously achieved was demonstrated. The terminal-to-terminal resistance was measured to be <0.42 milliohms which translates to an efficiency at 100KW of 99.98 percent.</p> <p>The EU and TF have been delivered to the Lewis Research Center and are being prepared for testing at increased power levels and for life testing. This testing will include both DC and AC power.</p>			
17. Key Words (Suggested by Author(s)) Rotary power transfer High power transfer High current/high voltage transfer Power/signal transfer		18. Distribution Statement	
19. Security Class(this rep) Unclassified	20. Security Class(this pg) Unclassified	21.No. pgs 0	22.Price*